CALIBRATION AND APPLICATION OF LIPID H ISOTOPIC RATIOS FOR QUANTITATIVE RECONSTRUCTION OF NEW ENGLAND CLIMATE VARIABILITY OVER THE PAST 15 KYR

BY

JUZHI HOU

B.A., CHINA UNIVERSITY OF GEOSCIENCES, 1998

PH.D., CHINESE ACADEMY OF SCIENCES, 2003

SC.M., BROWN UNIVERSITY, 2006

A DISSERTATION SUBMITTED IN PARTIAL FULFILLMENT OF THE REQUIREMENS FOR THE DEGREE OF DOCTOR OF PHILOSOPHY IN THE DEPARTMENT OF GEOLOGICAL SCIENCES AT BROWN UNIVERSITY

PROVIDENCE, RHODE ISLAND

MAY, 2009

This dissertation by Juzhi Hou is accepted in its present form by the Department of Geological Sciences as satisfying the dissertation requirements of the degree of Doctor of Philosophy

Date_____

Dr. Yongsong Huang (Advisor)

Recommended to Graduate Council

Date_____

Dr. Timothy Herbert (Reader)

Date_____

Dr. James Russell (Reader)

Date_____

Dr. Alberto Saal (Reader)

Date_____

Dr. Julie Brigham-Grette (Reader)

Approved by the Graduate School and Research

Date_____

Dr. Sheila Bonde
Dean of the Graduate School

VITA

JUZHI HOU was born in Xingtai, Hebei Province, China on November 29, 1975. He attended China University of Geosciences, Wuhan, from 1994-1998. Prior to his graduate studies at Brown University in 2003, Juzhi studied Quaternary Geology and Environment at Institute of Geology and Geophysics, Chinese Academy of Sciences, Beijing, from 1998 to 2003.

PREVIOUS EDUCATION:

Sc.M.	Geological Sciences, **Brown University,** May, 2006
Ph.D.	Institute of Geology and Geophysics,
	Chinese Academy of Sciences, June 2003
B.S.	College of Geosciences
	China University of Geosciences, Jun 1998

RESEARCH EXPERIENCE:

Brown University, Sep 2003 – July 2008.

Investigating the application of lipid H isotopic ratios climatic and environmental change and biogeochemical cycles in terrestrial ecosystems. Major specific activities include: Developing new proxies for precipitation isotopic ratios and surface air temperature, and investigating quantitative climate variability in northeastern North

America, Tibetan Plateau, East Africa; Investigating terrestrial biogeochemical dynamics by developing a novel method to organic matter; Investigating the influence of human activities on environment using carbon isotopic ratios of terrestrial biomarkers.

Chinese Academy of Sciences, Sep 1998 – June 2003.

Investigated variability of East Asian monsoon during late Holocene. Specific activities included: Examining optical characteristics of speleothem micro-bands in north and south China; Constructing speleothem micro-band chronology by comparing radiometric dates and micro-band counting; Investigating temperature variability at annual-scale, precipitation and atmospheric circulation associated with East Asian monsoon during late Holocene.

TEACHING EXPERIENCE:

Teaching Assistant, Brown University. Environmental Geochemistry, Limnology. Planed, organized field trips; Organized, prepared, and lead laboratories for 3 groups of 7-8 students each; Lectured at beginning of each laboratory; Supervised entire lab procedures and data production; Graded homework; Met with students one-on-one for tutoring and mentoring. Rated very good to excellent as a TA.

Supervisor, Brown University. Senior thesis, Luke Parsons (2005-2006); Corynn Brodsky (2007-present); Independent research by undergraduate students, Mena Ramos

(2004-2005), Sophie McCoy (2005-2006), Gideon Ng (2006-2007), Tsveta Krumova (2005-2007), Baird Langenbrunner (2006-present).

Teaching Assistant, Chinese Academy of Sciences, Quaternary Environment. Rated excellent as a TA.

PEER REVIEWED PAPERS:

1. **Hou J.**, D'Andrea W.J. and Huang Y. (2008) Can sedimentary leaf waxes record D/H ratios of continental precipitation? Field, model and experimental assessments. *Geochimica et Cosmochimica Acta*, 72, 3503-3517, doi:10.1016/j.gca.2008.04.030
2. **Hou J.,** Huang Y., Oswald W.W., Foster D.R. and Shuman B. (2007) Centennial-scale compound-specific hydrogen isotope record of Pleistocene - Holocene climate transition from southern New England. *Geophysical Research Letters*, 34, L19706, doi:10.1029/2007GL030303.
3. **Hou J.**, D'Andrea W. J., Macdonald D. and Huang Y. (2007) Evidence for water use efficiency as an important factor in determining the δD values of tree leaf waxes. *Organic Geochemistry*, doi: 10.1016/j.orggeochem.2007.03.011.
4. **Hou J.**, D'Andrea W. J., Macdonald D. and Huang Y. (2007). Hydrogen isotopic variability in leaf waxes among terrestrial and aquatic plants around Blood Pond, Massachusetts (USA). *Organic Geochemistry*, doi:10.1016/j.orggeochem.2006.12.009.

5. Lindbladh M., Oswald W. W., Foster D. R., Faison E., **Hou J.** and Huang Y. (2007) A late-glacial transition from *Picea glauca* to *Picea Mariana* in southern New England. *Quaternary Research*, 67, 502-508.
6. **Hou J.**, Huang Y., Wang Y., Shuman B., Oswald W.W., Faison E. and Foster D.R. (2006) Postglacial climate reconstruction based on compound-specific D/H ratios of fatty acids from Blood Pond, New England. *Geochemistry Geophysics Geosystems*, 7, doi:10.1029/2005GC001076.
7. Cai B., Cheng H., **Hou J.**, Liu H., Wang G. and Liu T.S. (2005) The impact of soil erosion on the formation of Yunnan Stone Forest: Evidence from Stalagmite and field observations. *Quaternary Sciences (in Chinese with English Abstract)*, 25, 170-176.
8. Tan M., **Hou J.** and Liu T.S. (2004) Sun-coupled climate connection between eastern Asia and northern Atlantic. *Geophysical Research Letters* , 31, doi:10.1029/2003GL019085.
9. **Hou J.** and Tan M. (2003) Image characteristics of annual layers in very young Chinese stalagmites. *Supplementi di Geografia Fisica e Dinamica Quaternaria*, 65-69.
10. **Hou J.**, Tan M., Liu T.S. and Cheng H. (2003) Stable isotope records of plant cover change and monsoon variation in the past 2200 years: evidence from laminated stalagmites. *Boreas*, 32, 304-313.
11. Tan M., Liu T.S., **Hou J.**, Qin X., Zhang H. and Li T. (2003) Cyclic rapid warming on centennial-scale revealed by a 2650-year stalagmite record of warm season temperature. *Geophysical Research Letters*, 30, doi:10.1029/2003GL017352.
12. **Hou J.**, Tan M. and Liu T.S. (2002) Counting chronology and climate records with

about 1000 annual layers of a Holocene stalagmite from the Water Cave in Liaoning, China. *Science in China*, 45(5), 385-391.

13. Tan M., **Hou J.** and Cheng H. (2002) Methodology of quaternary reconstructing paleoclimate from annually laminated stalagmites. *Quaternary Sciences (in Chinese with English Abstract)*, 22(3), 209-219.
14. **Hou J.**, Tan M., Cheng H. and Liu T.S. (2001) Preliminary research on Layer counting chronology of young stalagmite from Water Cave, Benxi. *Science in China (Series D, Earth Sciences, in Chinese)*, 31(5), 387-392
15. **Hou J.** (2001) Image characteristics of annual micro-bands in stalagmites. *Quaternary Sciences (in Chinese)*, 21(3), 278
16. Tan M., Cheng H., Edwards R.L., **Hou J.** and Liu T.S. (2000) TIMS-^{230}Th dating for very young annual laminated stalagmites. *Quaternary Sciences (in Chinese)*, 20, 391.

PRESENTATIONS:

1. **Hou J.**, Russell J.M. and Huang Y. Penetration of Atlantic Walker circulation into easternmost Africa during Early-mid Holocene: Hydrogen isotopic evidence from Sacred Lake. Oral presentation at American Geophysical Union Fall Meeting, 2007.
2. Majumdar S., Feng X., **Hou J.**, Faiia A.M. and Huang Y. Relationship between Leaf Water and Leaf Waxes in Growing Pine Needles. Poster presentation at American Geophysical Union Fall Meeting, 2007.
3. **Hou J.**, D'Andrea W.D., Toney J. and Huang Y. Factor controlling hydrogen isotope ratios of sedimentary leaf waxes: Implications for interpreting δD records of

paleoclimate (PP41A-1178). Poster presentation at American Geophysical Union Fall Meeting, 2006.

4. **Hou J.**, Parsons L., Huang Y., Shuman B. and Donnelly J. High resolution hydrogen isotope records of climate change during the early Holocene from two adjacent lakes in northeastern North America (PP43A-1227). Poster presentation at American Geophysical Union Fall Meeting, 2006.
5. Toney J., **Hou J.** and Huang Y. H-isotope fractionation during biosynthesis of leaf waxes in C_3 plants: trees vs. grasses (PP41A-1177). Poster presentation at American Geophysical Union Fall Meeting, 2006.
6. **Hou J.**, Huang Y., Shuman B., Oswald W.W., Faison E. and Foster D.R. Postglacial climate reconstruction based on D/H ratios of fatty acids from Blood Pond, New England. Oral presentation at American Geophysical Union Fall Meeting, 2005.
7. **Hou J.**, Huang Y., Tan M., Edwards R.L. and Smith E. Carbon isotopic ratios of lignin moieties in stalagmites as a novel indicator of past C3/C4 plant variation (PP43-0607). Poster presentation at American Geophysical Union Fall Meeting, 2004.
8. **Hou J.**, Tan M. and Liu T.S. Layer chronology of stalagmite from northeast China. Oral presentation at The 5th International Conference on Geomorphology, Tokyo, 2001.
9. **Hou J.**, Tan M., Liu T.S. and Cheng H. Stable isotope records of plant cover change and monsoon variation in the past 2200 years: evidence from laminated stalagmites. Oral presentation at The 5th International Conference on Geomorphology, Tokyo, 2001.
10. **Hou J.** and Tan M. Optical characteristics of speleothem micro-bands and their

climatic implications. Oral presentation at Annual of High-resolution Committee in Chinese Association of Quaternary Research, Guangzhou, 2001.

PROFESSIONAL SOCIETY MEMBERSHIPS:

Member, American Geophysical Union

Member, Geological Society of America

Member, International Paleolimnology Association

Member, Rhode Island Natural History Survey

AWARDS AND GRANTS:

National Ocean Sciences Accelerator Mass Spectrometry, Woods Hole Oceanographic Institution, Graduate Student Internship, Jan 2008 - Jul 2008.

Brown University, University Fellowship, Sep 2003 – Jun 2004.

Chinese Academy of Sciences, Peng Yin-Gang Scholarship, 2001.

Chinese Academy of Sciences, Institute of Geology and Geophysics, 2003, Award to excellent publications.

PREFACE

INTRODUCTION

The late Pleistocene – early Holocene transition is characterized by abrupt climatic fluctuations around North Atlantic Ocean (e.g., Stuiver et al., 1995; Hughen et al., 1996). However, the spatial variations in the timing, amplitude, and phasing of the abrupt events are less understood on the adjacent continents. This is particularly true for the northeastern North America where the driving forces for climate were particularly complex, comprising a combination of changes in North Atlantic surface temperature, Laurentide ice sheet (LIS) extent, atmospheric composition, and insolation (e.g., Webb et al., 1993). Centennial-scale quantitative records from the northeastern North America are thus extremely important for better understanding marine-terrestrial-atmosphere-cryosphere connections and regional climatic responses.

Existing paleoclimate records from the northeastern North America are mainly based on paleoecological and stratigraphic approaches, such as assemblages of pollen (e.g., Peteet et al., 1990; Webb et al., 1993; Shuman et al., 2002), Chironomidae (midge, e.g., Cwynar and Spear, 2001; Walker et al., 1997) and lake level (Shuman et al., 2001; Newby et al., 2000) from lake sediments. However, the possibility of transient vegetation responses to short-term, small-magnitude climate variations (e.g., Davis and Botkin, 1985), and the non-analogue conditions for Chironomidae (e.g., Kurek et al., 2002) could increase the difficulty of using pollen and Chironomidae data to assess abrupt

(<centennial-scale) climate variability. The lake level records usually reveal millennial-scale variations, which can hardly resolve abrupt climate reversals.

Compound-specific hydrogen isotope analyses of aquatic lipids in sediments (e.g., Sauer et al., 2001; Huang et al., 2002; 2004; Dawson et al., 2004) offer a new way to quantify past climate variability. The technique is especially useful for regions like northeastern North America where the lake sediments lack carbonate deposit. Organic compounds produced by algae and macrophytes track lake water isotopic variations (e.g., Huang et al., 2002; 2004; Hou et al., 2006; Sauer et al., 2001; Zhang and Sachs, 2007) and mean annual surface air temperature (Hou et al., 2007; Hou et al., in preparation). The lake water in regions of high precipitation-evaporation (P-E) ratio mimic precipitation isotopic variations. For example, the palmitic acid (C_{16} *n*-alkanoic acid) from both solvent extractable and sediment fractions track lake water at nearly constant hydrogen isotopic fractionation along transects in eastern North America (Huang et al., 2002, 2004).

This thesis contains two important parts: 1) Clibration of proxies for temperature and precipitation. I demonstrate that D/H ratios of C_{22} and C_{16} n-acids are reliable proxy for lake water and mean annual surface air temperature. I also investigate the sedimentary leaf wax δD values as a proxy for precipitation isotopic composition. 2) High-resolution, quantitative temperature records from lakes in northeastern North America. I present temperature records of centennial and decadal scale from two lakes during the late Pleistocene to early Holocene.

SUMMARY

In Chapter 1, I use transects of modern lake surface sediment in eastern North America to demonstrate that the D/H ratios of C_{22} *n*-alkanoic acid (δD_{BA}), mainly produced by aquatic macrophytes, effectively capture lake water isotopic composition. Downcore variations in δD_{BA} values and pollen taxa are highly consistent with the known climate change history of New England. D/H fractionations of long chain even numbered fatty acids (C_{24}-C_{30} *n*-acids) relative to lake water provide independent estimates of relative humidity during the growing season. Combined analyses of D/H of short and long chain fatty acids from lake sediment cores thus allow reconstructions of both past temperature and effective moisture conditions.

In Chapter 2, I investigate the variability of δD values of leaf waxes produced by various terrestrial plants in order to understand the controlling factors of leaf wax δD values. Paleoclimate interpretation of the hydrogen isotope values of plant leaf waxes extracted from sediments requires a thorough understanding of the factors controlling the isotopic ratios. I studied on D/H ratios of leaf waxes from 48 species in 7 types of terrestrial and aquatic C3 plants around Blood Pond, Dudley, Massachusetts. The δD values of leaf waxes differ by as much as 70 ‰ for different plant types, with those from trees and ferns having the highest values and those from grasses having the lowest values. The large isotopic variation indicates that the apparent hydrogen isotopic fractionation between leaf waxes and precipitation is not constant for different plants. The results

indicate that inferring precipitation D/H ratios based on sedimentary leaf waxes are only viable when significant vegetation change is absent or can be accounted for isotopically. In addition, the negative correlation between leaf wax δD and $\delta^{13}C$ values of various trees suggest that plant water-use efficiency exerts an important control on the leaf wax δD variation among different tree species.

In Chapter 3, the D/H ratios of leaf waxes (δD_{wax}) derived from terrestrial plants and preserved in lake sediments have been shown as a reliable proxy for precipitation isotopic variation, especially in relative dry regions. I used a transect of 32 lake surface sediments across large gradients of precipitation, relative humidity, and vegetation in the southwestern United States to study the natural factors affecting sedimentary δD_{wax}. δD values of C_{28} *n*-alkanoic acids show significant correlation with δD_P values ($R^2 = 0.76$) with an apparent isotopic enrichment of ~ 99 ± 8 ‰, indicating that sedimentary δD_{wax} values track overall δD_P variation along the entire transect. Leaf waxes produced by plants grown under controlled conditions (RH = 80, 60, 40%) show a small increase in D/H ratios as RH decreases, consistent with prediction from the Craig-Gordon model. However, the isotopic effect of RH on δD_{wax} along the entire transect is partially countered by the opposing influence of vegetation changes. The correlation between δD_{wax} and δD_P values is significantly higher ($R^2 = 0.84$) in the drier portions of the transect than in the wetter regions ($R^2 = 0.64$). This study suggests that D/H ratios of sedimentary leaf waxes can be used as a proxy for precipitation δD variations, with particularly high fidelity in dry regions, although more studies in other regions will be important to further test this proxy.

In Chapter 4, I present a centennial-scale record of climate change during the transition based on D/H ratios of C_{22} *n*-alkanoic acid (δD_{BA}) from a sediment core in Blood Pond, Massachusetts, based on the correlation between δD_{BA} and mean annual surface air temperature along a transect of 19 lakes in eastern North America. The temperature proxy is validated by the relationship between precipitation δD value and temperature in Global Network of Isotopes in Precipitation (GNIP) stations. The abrupt climate events observed in Blood Pond records show remarkable similarity with Greenland ice core $\delta^{18}O$ records during the Pleistocene. During the early Holocene, the northeastern North America δD_{BA} record was more variable than Greenland, possibly due to the close proximity of the Laurentide ice sheet, and impact of freshwater outbursts as the ice sheet rapidly retreated.

In Chapter 5, I present decadal-scale temperature records from Blood Pond, Massachusetts during the early Holocene which revealed two abrupt climate reversals. The isotopic records infer a cooling of 3~4 °C between 9.3 and 9.1 ka against the millennial scale climate background, mainly induced by changes in precipitation seasonality. In comparison, the 8.2 ka event displays smaller amplitude of temperature cooling of 1~2 °C at our southern New England site. The observed climatic reversal at ~ 9.2 ka as representing increased proportion of winter precipitation in conjunction with a drier and cooler summer, triggered by slowdown in thermohaline circulation as a result of freshwater release from the proglacial lakes. The difference in climate response at 8.2 ka and 9.2 ka events could be attributed to the configuration of LIS, with 9.2 ka LIS having

a much stronger blocking effect on the moisture from the Gulf of Mexico during the summer. The results suggest that the seasonality of the precipitation at the southern New England was highly sensitive to meltwater releases, especially prior to the final collapse of the LIS.

In Chapter 6, I present decadal to centennial resolution temperature records from two lakes in the northeastern North America to investigate the relationship between solar activity and temperature changes during the late Pleistocene to early Holocene. Sensitivity of the Earth's climate to the solar activity has profound implications for modeling future climate changes, but is a subject of intense scientific debate. GCM modeling considering solar forcing can successfully simulate climatic variations in the past millennia such as the Little Ice Age (LIA), but volcanic forcing during the same time period can also yield similar climatic effect and confound interpretations. The temperature reconstructions from the two lakes of 100 km apart in New England are highly consistent with each other and agree well with established general climatic scenarios. More importantly, our records contain centennial-scale cyclicities related to the solar cycles (88 and 232 yr), indicating strong links between the pronounced 1 to 2^{o}C temperature oscillations and solar activity during the late Pleistocene. The results strongly support the presence of an internal amplification mechanism for the solar forcing that is capable of causing disproportionally large climatic responses with relative small changes in the incoming solar radiation.

REFERENCE

Cwynar L.C. and Spear R.W. (2001) Late glacial climate change in the White Mountains of New Hampshire. *Quaternary Science Reviews* 20, 1265-1274.

Davis M.B. and Botkin D.B. (1985) Sensitivity of cool-temperate forests and their fossil pollen record to rapid temperature-change. *Quaternary Research* 23, 327-340.

Hou J., Huang Y., Wang Y., Shuman B., Oswald W.W., Faison E. and Foster D.R. (2006) Postglacial climate reconstruction based on compound-specific D/H ratios of fatty acids from Blood Pond, New England, *Geochemistry Geophysics Geosystems* 7, doi:10.1029/2005GC001076.

Hou J., Huang Y., Oswald W.W., Foster D.R. and Shuman B. (2007) Centennial-scale compound-specific hydrogen isotope record of Pleistocene-Holocene climate transition from southern New England. *Geophysical Research Letters* 34, doi:10.1029/2007GL030303.

Hou J. and Huang Y. Solar activity induced pronounced temperature oscillations during the late Pleistocene to early Holocene in the northeastern North America. In preparation.

Huang Y., Shuman B., Wang Y. and Webb T.III. (2002) Hydrogen isotope ratios of palmitic acid in lacustrine sediments record late Quaternary climate variations, *Geology* 30, 1103-1106.

Huang Y., Shuman B., Wang Y. and Webb T., III. (2004) Hydrogen isotope ratios of individual lipids in lake sediments as novel tracers of climatic and environmental change: a surface sediment test. *Journal of Paleolimnology* 31, 363-375.

Hughen K.A., Overpeck J.T., Peterson L.C. and Trumbore S. (1996) Rapid climate changes in the tropical Atlantic region during the last deglaciation. *Nature* 380, 51-54.

Kurek J., Cwynar L.C. and Spear R.W. (2004) The 8200 cal yr BP cooling event in eastern North America and the utility of midge analysis for Holocene temperature reconstructions. *Quaternary Science Reviews* 23, 627-639.

Newby P.E., Killoran P., Waldorf M.R., Shuman B., Webb R.S., Webb T.III. (2000) 14,000 years of sediment, vegetation, and water-level changes at the Makepeace Cedar Swamp, Southeastern Massachusetts. *Quaternary Research* 53, 352-368.

Peteet D.M., Vogel J.S., Nelson D.E., Southon J.R., Nickmann R.J. and Heusser L.E (1990) Younger Dryas Climatic Reversal in Northeastern USA - AMS Ages for an Old Problem. *Quaternary Research*, 33 219-230.

Shuman B., Bartlein P.J., Logar N., Newby P. and Webb T.III. (2002) Parallel climate and vegetation responses to the early Holocene collapse of the Laurentide Ice Sheet. *Quaternary Science Reviews* 21, 1793-1805.

Shuman B., Bravo L., Kaye J., Lynch J.A., Newby P. and Webb T.III. (2001) Late Quaternary water-level variations and vegetation history at Crooked Pond, Southeastern Massachusetts. *Quaternary Research* 56, 401-410.

Sauer P.E., Eglinton T.I., Hayes, J.M., Schimmelmann, A. and Sessions, A.L. (2001) Compound-specific D/H ratios of lipid biomarkers from sediments as a proxy for environmental and climatic conditions. *Geochimica et Cosmochimica Acta* 65, 213-222.

Stuiver M., Grootes P.M. and Braziunas T.F. (1995) The GISP2 $\delta^{18}O$ climate record of the

past 16,500 years and the role of sun, ocean, and volcanoes. *Quaternary Research* 44, 341-354.

Walker I.R., Levesque A.J., Cwynar L.C. and Lotter A.F. (1997) An expanded surface-water palaeotemperature inference model for use with fossil midges from eastern Canada. *Journal of Paleolimnology* 18, 165-178.

Webb T.III., Bartlein P.J., Harrison S.P. and Spaulding W.G. (1993) Vegetation, lake levels, and climate in Eastern North America for the past 18,000 years, in *Global Climates since the Last Glacial Maximum*, edited by H.E. Wright Jr, J. E. Kutzbach, T. Webb, III, W. F. Ruddiman, F. A. Street-Perrot, and P. J. Bartlein, University of Minnesota Press, Minneapolis, 415-467.

Zhang Z. and Sachs J.P. (2007) Hydrogen isotope fractionation in freshwater algae: I. Variations among lipids and species. *Organic Geochemistry* 38, 582-608, doi:10.1016/j.orggeochem.2006.12.004.

ACKNOWLEDGEMENTS

I owe much to the many people who helped me throughout my graduate career. First and many thanks go to my advisor, Dr. Yongsong Huang, who has given me a rich perspective. Yongsong guided me to the wonderful world of organic geochemistry, which I had no any experience before I came to Brown. His funding through an NSF grant supported research in this thesis.

Thanks also to other members of my committee, who shaped my experience at Brown in a positive way: Tim Herbert, Jeff Donnelly, Alberto Saal and Jim Russell. I have enjoyed our many discussions. In addition to my committee, I have also gained a great deal of insight from some of my colleagues from other institutions, Bryan Shuman at University of Wyoming, David Foster at Harvard Forest, and Wyatt Oswald at Emerson College. I also thank Dave Murray, Joe Orchardo and Dana MacDonald who helped so much on the lab work. Thanks all the members in the Geological Science main office, who helped me go through the past five years.

I have also enjoyed and benefited from interacting with my graduate student peers and recent Ph.D.s from Brown, including Zhonghui Liu, Kira Lawrence, Billy D'Andrea (my 5-yr officemate), Jon Nichols, Jaime Toney, Li Gao, Susie Theroux, Paige Newby, Jess Tieney, Caitlin Chatzen, Lora Cleverland, Emily Pohlman, Yun Wang and Qinglan Peng. Many undergraduate students have been deeply involved in the lab as well. In particular, Luke Parsons, Corynn Brodsky, Mena Ramos, Sophie McCoy, Gideon Ng, Tsveta Krumova and Baird Langenbrunner.

Similarly, the Huang Lab has been a great team, with great individuals. Marcelo Alexander, the always-available technician, organized the lab, ran all the instruments smoothly, and helped me to run a lot of samples (which I owed tons of beers I can not afford now). Our former technician, Frankie Yi Wang (currently at Princeton University), also helped me when I began to work in the organic geochemistry lab.

My parents were also an endless source of support. They are traditional Chinese, who do not like their kids be far away from them, but they always supported my choices from Wuhan, to Beijing, to Providence, RI. I would never have done this without their effort and love. I owe so much to my wife, Lei and my daughter, Cathy that I cannot even express in words.

TABLE OF CONTENTS

LIST OF TABLES

LIST OF ILLUSTRATIONS

CHAPTER 1:

CHAPTER 2:

CHAPTER 3:

precipitation in this region. The lakes are divided into two groups according to the geographic division and mean annual precipitation: Plains (including lakes from Texas); Basin and range (including lakes from New Mexico and Arizona).

Figure 2. Hydrogen isotope data for the SW transect: δD_{wax}= measured D/H ratios of sedimentary leaf waxes; δD_P= D/H ratios of precipitation calculated from OIPC; δD_{lake}= measured D/H ratios of lake water; δD_{model}= modeled D/H ratios of lake water; 95% CF (δD_P)= 95% confidence interval for δD_P; 95% CF (δD_{wax})= 95% confidence interval for δD_{wax}.

Figure 3. Correlation between δD_{wax} and δD_P for the lake surface sediment samples along the SW transect. (A) Correlation for the entire data set showing both linear and polynomial regressions. (B) Correlation for data from distinct geographical provinces (Basin and Range, and Plains). 95% confidence intervals are shown.

Figure 4. Differences in the apparent isotopic enrichment of leaf waxes for plants grown in growth chamber at three humidity levels. The left-hand plots depict changes in enrichment factor ($\varepsilon_{wax\text{-}water}$) as RH changes from 80% to 40% (A: RH = 80%; B: RH = 60%; C: RH = 40%). The vertical dashed line represents the average $\varepsilon_{wax\text{-}water}$ value at RH = 80%. The righthand plots show hydrogen isotopic differences (D values) between different RH levels. (D = $\Delta D_{80\text{-}60\%}$; E = $\Delta D_{60\text{-}40\%}$; F = $\Delta D_{80\text{-}40\%}$).

Figure 5. The correlation between RH and apparent isotopic enrichment of sedimentary leaf waxes relative to (A) precipitation ($\varepsilon_{wax\text{-}p}$), (B) modeled soil water ($\varepsilon_{wax\text{-}soil\ water}$) assuming *f*e = 15%, (C) modeled soil water ($\varepsilon_{wax\text{-}soil\ water}$) assuming a linear east to west gradient of *f*e from 15% to 25% for our study sites. $\varepsilon_{wax\text{-}soil\ water}$ =

$[(D/H)_{wax}/(D/H)_{soil\ water} - 1] \times 1000$ ‰. Three of the lakes, AD (Animas Ditch), UGL (Upper Glacial Lake) and SRL (Santa Rosa Lake) show different $\varepsilon_{wax\text{-}p}$ values (see text for discussion).

Figure 6. Modeled D/H ratios of soil water and leaf water for plants (A) in the growth chamber and (B) in the field. To facilitate the comparison between the plants from the growth chamber and the field, the D/H ratio of precipitation is set to the δD value of irrigation water in the growth chamber (-49 ‰).

Figure 7. (A) Models showing the opposing effects of RH and vegetation on the sedimentary δD_{wax}. The data for RH effect (circles) are obtained by assuming the production percentage of tree leaf waxes is 100%, whereas the data for vegetation effect (triangles) are obtained by assuming RH is 100% for all lakes. The average of the RH effect and vegetation effect for all sites ($\delta D_{wax(model)}$, dashed line) is then compared with measured D/H ratios of leaf waxes from the lake sediments ($\delta D_{wax,}$ black line). To facilitate comparison, second order polynomial regressions are shown for all four datasets. (B) and (C) Sensitivity tests for the model combining RH and vegetation effects. As the percentage of tree cover increases from 0.7RH (B) to 1.2RH (C), the modeled dD_{wax} vs. dD_p relationship does not change significantly.

Figure 8. The schematic variation of D/H ratios for low RH and/or warm regions (left panel), and high RH and/or cool regions (right panel; This panel is adapted from Sachse et al. (2006)). ε_1, ε_2, ε'_1, ε'_2 represent the evaporation effect from precipitation to soil water, then to leaf water; ε_{bio} and ε'_{bio} are the hydrogen isotopic enrichment during biosynthesis. ε_{aq} is the biosynthesis effect for aquatic

plants. $\varepsilon_{wax\text{-}p}$ and $\varepsilon'_{wax\text{-}p}$ are the apparent hydrogen isotopic enrichment from precipitation to leaf waxes. E is the isotopic enrichment between precipitation and lake water due to evaporation.

CHAPTER 4:

Figure 1. Map showing the location of Blood Pond (star), the GNIP stations (solid circles) and lakes along north-south transect (solid triangles).

Figure 2. Correlation between (a) D/H ratios of behenic acid (C_{22} *n*-acid) or δD_{BA} and surface air temperature (T) along the north-south transect in eastern North America, (b) mean annual δD of precipitation (δD_P) and surface air temperature (T) in eastern North America (1961-1987, data from Rozanski et al., 1993).

Figure 3. δD_{BA} record and pollen-inferred temperature from Blood Pond during the transition from late Pleistocene to Holocene in comparison with $\delta^{18}O$ data from Greenland Ice Sheet Project 2 (GISP2), and carbonate $\delta^{18}O$ from Crawford Lake. The dashed lines indicate the corresponding cold periods, OD1: Oldest Dryas; OD2: Older Dryas, IACP: Intra-Allerød cold period; YD: Younger Dryas; PBO: Pre-Boreal oscillation; B: Bølling; A: Allerød. The arrows besides of δD_{BA} curve indicate the freshwater outburst from proglacial lakes. Calibrated ages from accelerator mass spectrometry radiocarbon (AMS ^{14}C) dating with errors are shown.

CHAPTER 5:

alkanoic acid; (C) Blood Pond C_{22} *n*-alkanoic acid. The Y-axes at the left side are of hydrogen isotopic scale, the Y-axes at the right side are of temperature scale which were calculated based on the correlation between δD_{BA}, δD_{PA} and mean annual surface air temperature (T) ($\delta D_{BA} = 4.3T - 208.4‰$, $\delta D_{PA} = 3.3\ T - 202$). The GISP2 $\delta^{18}O$ records are also shown for comparison (D).

Figure 3. Spectral components of the temperature records from lakes in northeastern North America, (bottom to top), Rocky Pond C_{16}, Rocky Pond C_{22}, and Blood Pond C_{22}. The sunspot number records from Solanki et al. (2004) is also shown for comparison. All spectral analyses were performed by Singular Spectrum Analysis - MultiTaper Method (SSA-MTM) Toolkit.

Figure 4. Band pass of two prominent solar cycles (232 and 88 years) of the Blood Pond C_{22}, Rocky Pond C_{16}, C_{22} and radiocarbon data (Stuiver et al., 1998). The hydrogen isotope data (orange curves) are also plotted to show the corresponding cyclicities.

CHAPTER 1

Postglacial climate reconstruction based on compound-specific D/H ratios of fatty acids from Blood Pond, New England

Co-authors: Yongsong Huang, Yi Wang, Bryan Shuman, W. Wyatt Oswald, Edward Faison, David R. Foster,

Published in ***Geochemistry Geophysics Geosystems***, 2006, v. 7,

doi:10.1029/2005GC001076

ABSTRACT

We determined hydrogen isotope ratios of individual fatty acids in a sediment core from Blood Pond, Massachusetts, USA, in order to reconstruct climate changes during the past 15 ka. In addition to palmitic acid (C_{16} *n*-acid) which has been shown to record lake water D/H ratios, our surface sediments and downcore data indicate that behenic acid (C_{22} *n*-acid), produced mainly by aquatic macrophytes, is also effective for capturing past environmental change. Calibration using surface sediments from two transects across eastern North America indicates that behenic acid records δD variation of lake water. Downcore variations in δD values of behenic acid and pollen taxa are highly consistent with the known climate change history of New England. D/H fractionations of long chain even numbered fatty acids (C_{24}-C_{30} *n*-acids) relative to lake water provide independent estimates of relative humidity during the growing season. Combined analyses of D/H of short and long chain fatty acids from lake sediment cores thus allow reconstructions of both past temperature and effective moisture conditions. Comparison of δD records from two lakes in New England provides critical information on regional climate variation and abrupt climate change, such as the 8.2 ka event.

INTRODUCTION

Organic matter preserved in lacustrine sediments contains important paleoenvironmental information (Meyers, 2003). For example, compositions of lipid biomarkers provide information on changes in biological inputs (e.g., Coolen et al., 2004; D'Andrea and Huang, 2005), and carbon, hydrogen and oxygen isotopic ratios of organic matter allow reconstruction of lake biogeochemistry and paleoclimatic conditions (Meyers and Ishiwatari, 1993; Edwards, 1993; Krishnamurthy et al., 1995; Lamb et al., 2004). Important progress has been made in the past decade on compound-specific isotope analysis which allows the determination of carbon and hydrogen isotope ratios of individual organic compounds (Hayes et al., 1990; Burgoyne and Hayes, 1998; Anderson et al., 1997; Huang et al., 1999, 2001, 2002, 2004; Sauer et al., 2001; Sessions et al., 2002). Because organic substances in lake sediments are often derived from multiple sources including aquatic and terrestrial plants, as well as microbes (Cranwell, 1982; Huang et al., 1999; Meyers and Ishiwatari, 1993), measuring isotope ratios of individual lipid compounds minimizes the complications due to multiple sources of organic matter and the effect of selective diagenesis.

Compounds of aquatic sources are of particular interest for compound-specific hydrogen isotope analysis because of their potential to record lake water D/H ratios which respond strongly to climatic changes (e.g., temperature change). However, lipid compounds exclusively biosynthesized by aquatic organisms are rare in lake sediments.

In order to validate the ability of a lipid compound to record lake water D/H ratios, one of the most effective tests is to study modern lake water and surface sediments (Huang et al., 2002, 2004; Sauer et al., 2001). For example, hydrogen isotope ratios of C_{27} and C_{28} sterols from surface sediment of lakes and oceans have been shown to record those of lake and ocean water (Sauer et al., 2001). Huang et al. (2002) demonstrated that hydrogen isotope ratios of palmitic acid (PA, C_{16} *n*-acid) isolated from lake sediments captured the lake water composition, and recorded the late Quaternary climate changes. Ester-bound palmitic acid has been shown to better record hydrogen isotope ratios of lake water than free palmitic acid (Huang et al., 2004). Although none of these lipid compounds is an exclusive biomarker of aquatic organisms, they faithfully record lake water D/H ratios because contributions from other organisms with different isotopic fractionation factors are small in lake sediments. In addition to lipids attributable to aquatic sources, lake sediments also contain compounds derived from terrestrial plants, such as long chain leaf waxes (Huang et al., 1999; Meyers, 2003). Organic matter of terrestrial plants becomes enriched in D/H ratios under conditions of lower effective moisture due to combined soil evaporation and transpiration effects (Yapp and Epstein, 1982). Higher plant biomarkers, such as long chain C_{26} to C_{30} fatty acids, may thus be used to reconstruct of past changes in precipitation/evaporation ratios (P/E). Therefore, a combined study of D/H ratios of both aquatic and terrestrial lipids may provide important paleotemperature and paleoprecipitation information.

Among various lipids in lake sediments, fatty acids have advantages over other compounds particularly for paleoclimate study. Fatty acids 1) are abundant in lake sediments, 2) are relatively easy to isolate and purify, thus minimizing coelution in GC and 3) contain compounds from both aquatic and terrestrial sources. Because fatty acids of different chain length appear in the same fraction during sample preparation, isotopic analyses on these compounds can often be performed simultaneously, reducing the time for sample processing and isotopic analyses. The possibility of multiple source organisms for short-chain fatty acids may add isotopic heterogeneities, but the overall impact on the hydrogen isotopic records from lake sediments appears to be small based on our surface sediment calibrations (Huang et al., 2002, 2004).

The objectives of the present study are: 1) to further test the utility of various fatty acids as paleoclimate proxies. We are particularly interested in the δD values of a middle chain fatty acid, behenic acid (BA, C_{22} *n*-acid), which has not been discussed in our previous papers (Huang et al., 2002; 2004). Ficken et al. (2000) have shown that the middle chain (C_{20} to C_{24}) *n*-alkyl lipids have exceptionally high abundance in submerged and emergent aquatic macrophytes relative to terrestrial higher plants. This compound hence has the potential to record the D/H ratio of lake water; 2) to reconstruct paleoclimate changes for the past 15 ka from Blood Pond, New England by combined isotope and pollen stratigraphy; and 3) to compare this record with our previous published data on Crooked Pond, to better understand the influence of hydrology on δD

records of fatty acids. Moreover, the records provide new insights on the range and intensity of abrupt climate events such as the Younger Dryas and 8.2 ka events.

SAMPLE AND METHODS

Sample collection

Samples for surface calibration have been described in previous papers (*Huang et al.*, 2002, 2004). Briefly, lake water and surface sediment samples were collected from sites across eastern North America along two transects 1) from Ontario to Florida, and 2) from South Dakota to Wisconsin (Figure 1). Water samples were collected from lake centers, at approximately 50 cm below the surface. Surface sediments (0-2 cm) were collected using an Ekman dredge or a short gravity corer. Sediment samples were kept at 0°C immediately after sampling, and frozen once returned to Brown University.

Blood Pond (42.081^{o}N, 71.961^{o}W, 212.1 m a.s.l.) is a kettle pond located in the south-central Massachusetts town of Dudley. The lake surface area is about 0.08 km^2, with a 0.96 km^2 watershed. The water depth was 3.6 m when coring took place in 2001. There is an outlet drains to the south, flowing into the Quinebaug River. Plants in the watershed include oak, clethra, white pine, and red maple, with alder and highbush blueberry in a swampy area on the pond edge. We used a 7-cm diameter plastic tube fitted with a piston to collect the upper sediments (180 cm) and a 4.5-cm diameter modified Livingstone sampler to collect lower sediments in 1-m-long drive lengths. The lower drives were extruded horizontally in the field, and the sediment cores were wrapped in

plastic wrap and aluminum foil. The upper core was extruded vertically in the laboratory at 1-cm intervals. The lower drives were sliced into 2-cm intervals. Pollen has been studied in detail throughout the core (Oswald et al., unpublished). Samples for isotope analyses were selected at 6 cm interval between two neighboring samples.

Chronology

Chronological control for samples from Blood Pond is provided by 1) radiocarbon dating of fifteen samples of bulk organic matter (Figure 2); and 2) pollen evidence (i.e., European settlement at 236 cal yr B.P. is evidenced by the increase in weedy taxa at 72 cm) verified via Pb-210 dating (Oswald et al., unpublished). The ^{14}C dates were converted to calendar years before present (cal yr B.P.) using OxCal 3.9 (Bronk Ramsey, 2001).

Laboratory analyses

Sediment samples were freeze dried. Free lipids were extracted using an Accelerated Solvent Extractor ASE 200 (Dionex). Carboxylic acid fraction was isolated from the total extracts using solid phase extraction (Aminopropyl Bond Elute®) and then methylated using anhydrous 2% HCL in methanol. Hydroxyl acids were removed using silica gel column chromatography (DCM as solvent), in order to further purify the fatty

acid methyl esters and avoid chromatographic coelution.

Quantification and identification of compounds were carried out using GC and GC-MS, respectively. An HP 6890 GC interfaced to a Finnigan Delta+ XL stable isotope spectrometer through a high-temperature pyrolysis reactor was used for hydrogen isotopic analysis (Huang et al., 2002, 2004). The precision (1σ) of triplicate analyses was kept <±2‰. The accuracy was routinely checked by an injection of laboratory isotopic standards between every six measurements. δD values obtained from individual acids (as methyl esters) were corrected by mathematically removing the isotopic contributions from added groups before reporting. The δD value of the added methyl group was determined by acidifying and then methylating (along with the samples) the disodium salt of succinic acid with a predetermined δD value (using TC/EA-IRMS) (*Huang et al.*, 2002).

RESULTS AND DISCUSSION

Surface sediment calibration for behenic acid (BA, C_{22} n-acid).

Previous studies have demonstrated that surface sediment calibration is an effective approach to test a paleoclimate proxy (Bartlein et al., 1984; Huang et al., 2002, 2004; Sauer et al., 2001). We have further examined behenic acid (i.e., C_{22} *n*-acid) using the same approach and the same set of samples as used in Huang et al. (2002), because middle chain n-alkyl lipids are particularly abundant in aquatic macrophytes (Ficken et al., 2000). Figure 3a shows comparison between δD values of behenic acid from surface sediment and lake water from our two transects. The δD_{BA} values (δD values of behenic acid) correlate highly with the δD_{water} values in all 33 lakes,

$$\delta D_{BA} = 0.8185 \times \delta D_{water} - 140.01,\ R = 0.898;\ p < 0.05 \qquad (1)$$

If only lakes from the south-north transect are used (Figure 3b), the regression becomes:

$$\delta D_{BA} = 0.8681 \times \delta D_{water} - 136.40,\ R = 0.938;\ p < 0.05 \qquad (2)$$

Sessions and Hayes (2005) derived the exact equations to calculate fractionation

factors for hydrogen isotope without approximations commonly used for carbon and oxygen isotopes. Lake water is the only source for aquatic plants to biosynthesize behenic acid, so a single component isotope fractionation ($\delta D_{Product} = \alpha \times \delta D_{Source} + \varepsilon$) can be applied (where $\varepsilon = (\alpha - 1) \times 1000$). Using this equation (1), we obtain a fractionation factor (α) of 0.8185 from the slope, and of 0.8599 from the intercept. From equation (2), we obtain a fractionation factor (α) of 0.8681 from the slope, and of 0.8636 from the intercept.

Theoretically, the fractionation factor calculated from slope and from intercept should be equivalent. However, in practice, small difference is inevitable. The potential causes for the difference may be: 1) the lipid compounds are not completely derived from a simple group of organisms; 2) the isotopic fractionation factor is slightly different for the various organisms that are sources of behenic acid. When only the north-south transect of samples is used, the regression is better than using samples from both transects, and fractionation factors derived from the slope and intercept are virtually identical. Our north-south transect is located a region with high precipitation/evaporation ratio (P/E), whereas the east-west transect encompasses large regional differences in P/E. Since our surface sediment samples probably represent deposition in the last 10s of years, the lake water from our east-west transect may be more susceptible to short–term changes, resulting in more variable D/H ratios and lower correlation with δD_{BA}.

The maximum discrepancy in the fractionation factor for behenic acid between α_{slope} (0.8185) and $\alpha_{intercept}$ (0.8599) is only 0.0414 in our transects of 33 lake samples. This is very small when compared with previously published data. For example, bulk aquatic plant lipids had a difference of 0.313 (α_{slope} 0.546 vs. $\alpha_{intercept}$ 0.859) (Sternberg, 1988), phytoplantonic sterols differed by 0.053 (0.748 vs. 0.801) (Sauer et al., 2001), and free palmitic acid had a difference of 0.106 (0.939 vs. 0.833) (Huang et al., 2002). Our result is close to that for ester-bound palmitic acid, which differed by 0.026 (0.850 vs. 0.824) (Huang et al., 2004). We therefore conclude that δD_{BA} is also an excellent biomarker to record lake water D/H ratios. In particular, for lakes with abundant submerged and emergent aquatic macrophytes (such as Blood Pond, which is surrounded by a large swampy area), δD_{BA} may be especially suitable for paleoclimate reconstructions.

Comparison of hydrogen isotope records of behenic acid and palmitic acid with pollen stratigraphy

The δD_{BA} and δD_{PA} values show similar downcore variations (Figure 4). However, absolute values and ranges of variation of δD of behenic acid are somewhat different from those of palmitic acid. δD_{PA} ranges from -194 to -159‰, while δD_{BA} ranges from -165 to -140‰. Average hydrogen isotope ratios of palmitic acid are more depleted than those of behenic acid. The differences in absolute δD values result from different isotopic

fractionation effects during biosynthesis of their producers.

δD records of both palmitic and behenic acid suggest a gradual temperature increase from 15 000 to 13 000 cal yr B.P. The warming was accompanied by increasing pollen percentages of spruce (*Picea*) and subsequently pine (*Pinus*). Changes in fossil chironomid assemblages from lakes in maritime Canada and northern New England also indicate that summer lake-water temperature rose until about 13 000 cal yr B.P. (Cwynar and Levesque, 1995).

The Younger Dryas chronozone (YDC) (Shuman et al., 2002a; Stuiver et al., 1995), which appears between ~13 000 and 11 700 cal yr B.P. according to our age model, was the coldest period since 15 000 cal yr B.P. (Figure 4). Both Greenland isotope records (Stuiver et al., 1995) and chironomid records from maritime Canada and northern New England (Cwynar and Levesque, 1995) recorded the YDC as the coldest postglacial period. At Crooked Pond (Huang et al., 2002), hydrogen isotope ratios decline by 20‰ at 12 900 cal yr B.P., indicating that conditions during the YDC were > 5°C cooler than before (based on the global relationship between surface air temperature and δD for mean annual precipitation, –5.6‰/°C (Dansgaard, 1964)). At Blood Pond, the temperature change at the YDC derived from hydrogen isotope records of palmitic acid and behenic acid ranges from 3 to 5 °C (the small difference between the two compounds may be due to mixing the contributions of organisms with small fractionation differences). The

temperature estimates are close to the temperature variation estimated from nitrogen and argon isotopes from the Greenland ice core (Severinghaus et al., 1998). This cold period was accompanied by increased abundance of boreal taxa such as *Picea*, *Alnus* and *Betula*, and lower abundance of *Pinus* and *Quercus* around Blood Pond (Figure 4). At the end of the YDC, the isotopic records indicate rapid warming (Figure 4), which is consistent with the isotopic records from Crooked Pond (Huang et al., 2002; Shuman et al., 2002b), and the Greenland ice core isotopic records (Stuiver et al., 1995). Moreover, the YDC in our study site was not a uniformly cold period. There were some fluctuations, including a warm (~2°C) and wet reversal occurred during the later part of the YDC. Pollen data (and to some extent, Greenland ice core data) also appear to record corresponding variations.

From the end of the YDC to 9000 cal yr B.P., temperature variations derived from the hydrogen isotopic records at Blood Pond show different patterns from the Greenland ice core isotopic records. Greenland ice core isotopic records show a gradual warming with small variability until 9000 cal yr B.P. However, two relative cool periods are indicated by the temperature records from Blood Pond and Crooked Pond (Huang et al., 2002). The first cool period is coincident with high percentages of *Tsuga* pollen, while the second coincides with an *Alnus* pollen peak around 9800 cal yr B.P.

The 8.2 ka event was a major, abrupt climate change event in the early Holocene (Alley and Agustsdottir, 2005; Alley et al., 1997). It is believed that the strongest

evidence of this cooler, drier and perhaps windier event should be recovered in eastern North America. However, so far evidence for a strong 8.2 ka event in eastern North America has been sparse. For example, Yu and Eicher (1998) found an oxygen isotope shift in carbonate toward colder values in a lake in southern Ontario, Canada. A lake in central Nova Scotia, Canada showed a short-lived shift to more minerogenic conditions at the time of the event, indicating ecological change in the lake (Spooner et al., 2002). In New England, a sharp drop in loss-on-ignition was detected in two lakes from New Hampshire (Kurek et al., 2004). Shuman et al. (2004) showed that pollen data from North Pond (western Massachusetts) contain a reversal that may be attributed to the 8.2 ka event.

There is no clear response of pollen record from Blood Pond to the 8.2 ka cold event. In contrast, δD records of palmitic acid and behenic acid clearly record this cold event (~9000 – 8000 cal yr B.P.). The estimated temperature variation based on our data is 1.7 to 2.8 °C. This cooling is less than suggested by the Greenland ice core (5-7°C) (Alley and Agustsdottir, 2005; Severinghaus et al., 1998), but is consistent with the variation in a lake in southern Ontario, Canada (Yu and Eicher, 1998). The 8.2 ka event at Blood Pond appears to have started earlier and lasted longer than at the Greenland summit. Similar longer-duration cold events have been reported in North America (Spooner et al., 2002) and Europe (Ariztegui et al., 2001; Heiri et al., 2003). However, our dating control is based on linear interpolation between only a few ^{14}C dates, and

hence we cannot accurately determine the duration of the event without further detailed radiocarbon dating.

A relatively cool period between 7000 and 5000 cal yr B.P. was revealed by the δD records from Blood Pond. $\delta^{18}O$ records from the Greenland ice core also show slight cooling during the same period (Stuiver et al., 1995). Temperatures remained high from 5000 to 3000 cal yr B.P., and then declined. After ~3000 cal yr B.P., declines in the δD values of behenic acid and *Carya* pollen percentages suggest a cooling trend. This trend is consistent with pollen and hydrogen isotope records from Crooked Pond (Huang et al., 2002; Shuman et al., 2004). Overall, our compound-specific D/H data provide a new paleoclimate proxy that is particularly sensitive to relatively short-term events, such as the 8.2 ka event

δD records of long chain fatty acids and implication for effective moisture balance changes

Long chain normal fatty acids (C_{24} to C_{32} *n*-acids) originate from the waxy coating of terrestrial plants which can be transported to lake sediments by wind and streams (Meyers, 2003). Higher plants use soil water as their source water for biosynthesis. As a result, the isotopic compositions of organic compounds derived from higher plants are affected by precipitation-evaporation ratios and plant evapotranspiration.

We estimated the lake δD values for the past 15 ka in Blood Pond using δD_{BA}, based on the regression established from surface sediments calibration. We then calculated the fractionation factor of long chain fatty acids relative to lake water. The assumption here is that lake water δD values are the same as those used by terrestrial plants, which is the best we can do since we have no other means to reconstruct soil water δD values. Biosynthesis of leaf waxes from leaf water involves many biochemical steps with the possibility of hydrogen isotope fractionation (Buddenbaum and Shiner, 1997). However, it is the overall fractionation rather than the fractionation associated with any one step that is of interest of us. We therefore calculated the overall hydrogen isotope fractionation using the following equations:

$$\alpha = (1000+\delta D_{\text{long chain acid}})/(1000+\delta D_{\text{lake water}}) \qquad (3)$$

An empirical relationship ($\alpha = -0.124h + 1.089$) between net hydrogen isotope fractionation factor and growing season relative humidity has been obtained from tree ring cellulose (Yapp and Epstein, 1982), indicating higher value of fractionation factor (α) under lower relative humidity. A quantitative relationship between hydrogen isotope fractionation of leaf waxes and relative humidity has not been established. However, study of a loess profile spanning the past 130 ka by Liu and Huang (2005) has demonstrated that δD values of long chain leaf waxes during dry periods are 40 to 50 ‰

higher than during wet periods in the Chinese Loess Plateau. Therefore, the impact of relative humidity on hydrogen isotopic fractionation must be in the same direction for both tree ring cellulose and leaf waxes.

The variations of growing season relative humidity estimated from isotope fractionation factor can be compared with the Blood Pond pollen record and well-established climate scenarios (Figure 4). Growing season relative humidity increased in parallel with *Picea* and *Pinus* pollen percentages from 15 000 to 13 000 cal yr B.P. Subsequently, the D/H fractionation factor increases during the YDC, indicating lower growing season relative humidity (Figure 4). This finding is inconsistent with lake-level reconstructions for Crooked Pond and Makepeace Cedar Swamp in eastern Massachusetts, which show a rise during the YDC (Newby et al., 2000; Shuman et al., 2001). Our estimates of the growing season relative humidity are related to precipitation during the growing season of plants (spring and summer in New England). In contrast, lakes in New England were recharged mainly by winter precipitation (Shuman et al., 2001). It is possible that a P/E increase in winter and a P/E reduction in spring and summer occurred during the YDC, resulting in the observed discrepancy in isotope and lake level data.

From the end of YDC to 9000 cal yr B.P., the isotope data suggest that growing season relative humidity changed from relatively low to high values (Figure 4). This

change coincides with an interval of high *Pinus* and *Tsuga* pollen percentages, and a subsequent increase in *Quercus* abundance. The cool event around 8.2 ka also appears to have lower relative humidity based on the fractionation factor of the long chain acids, a finding which is consistent with climate conditions in other regions (Alley and Agustsdottir, 2005). However, the pollen data did not show clear evidence for the 8.2 ka event (Figure 4), perhaps indicating that isotope ratios are a more sensitive proxy for detecting short climate events. After 8000 cal yr B.P., growing season relative humidity remained relatively high, with minor fluctuations around 5000 and 3000 cal yr B.P. This pattern is inconsistent with the lake-level reconstruction from Crooked Pond (Shuman et al., 2004), which suggests decreased effective moisture during that interval.

Comparison with δD records of palmitic acid from Crooked Pond

Our previously published hydrogen isotope record from Crooked Pond, Massachusetts (Huang et al., 2002) shows a similar general trend of climate variations to that from Blood Pond, particularly the clear climate cooling during the YDC (Figure 5). The mid-Holocene warm period and relatively cool late Holocene were also observed in our isotope data in both lakes, although the Blood Pond data show more variability. Downcore variations of δD_{BA} and δD_{PA} from Blood Pond are very similar to those of δD_{PA} from Crooked Pond. However, there are a few differences between the records from the two lakes. First, δD_{PA} from Crooked Pond did not reveal a clear response to the cool

event around 8200 cal yr B.P. Secondly, the full range of δD_{PA} variation (-245.1 to -157.1‰, ~88 ‰) from Crooked Pond is larger than that of δD_{BA} (-167.3 to -140.7 ‰, ~ 27 ‰) and δD_{PA} (-200.7 to -162.0‰, ~38 ‰) from Blood Pond. The differences are likely due to 1) different sampling resolution for the two records; 2) different hydrological conditions at Crooked and Blood Ponds. Blood Pond is surrounded by a large area of shallow-water swamp, which is not present at Crooked Pond. There is intermittent inflow and a continuous outlet at Blood Pond, whereas Crooked Pond is hydrologically closed.

CONCLUSIONS

Surface calibration using 33 lakes in eastern North America demonstrated that behenic acid (BA, C_{22} *n*-acid) captures lake water isotope ratios effectively. Correlation between lake water δD and δD_{BA} is significant ($\delta D_{BA} = 0.8185 \times \delta D_{lake\ water} - 140.01$, R= 0.898). Consistent fractionation factors derived from the slope and intercept of the equation suggests that behenic acid is mainly produced by submerged and emergent macrophytes. Downcore comparisons show that δD_{BA} is consistent with pollen record from the same sediment core. In Blood Pond, the downcore variations in δD_{BA} and δD_{PA} are similar and appear to reflect primarily temperature changes for the last 15 ka. In contrast, the isotopic fractionation factor variations of terrestrial plant leaf waxes (long chain acids) reflect growing season relative humidity.

Our isotope data are highly sensitive to abrupt climate changes, such as the YDC and the 8.2 ka event. Based on our data, the duration of 8.2 ka event in New England may be longer than on the Greenland ice sheet, although higher resolution radiocarbon dating of Blood Pond sediments is needed to further constrain its exact duration. Hydrogen isotope ratios of long chain fatty acids also allowed us to estimate moisture balance changes during the YDC and the 8.2 ka event. Current pollen records from Blood Pond do not show the relatively short-term climate events such as 8.2 ka event. This suggests that our isotope approach is promising for high resolution reconstruction of Holocene

climate change in New England.

Fatty acids are a particularly promising class of compounds for paleoclimatic and paleoenvironmental reconstructions because of the possibility of simultaneous reconstruction of both temperature and moisture balance changes. Fatty acids are relatively easy to isolate and purify during sampling preparation, minimizing coelution during gas chromatography – isotope ratio mass spectrometry analyses. Although palmitic and behenic acid are not exclusive biomarkers for aquatic plants, our surface sediment calibrations demonstrate that they do capture modern lake water conditions, and our downcore studies suggest their D/H values record paleoclimatic changes.

ACKNOWLEDGEMENTS

This work was supported by grants from the National Science Foundation (NSF 0318050, 0318123, 0402383) to Y, Huang. We thank Alex Sessions and an anonymous reviewer for critical reviews on the manuscript and helpful discussions with Dana McDonald.

REFERENCES

Alley R.B. and Agustsdottir A.M. (2005) The 8k event: cause and consequences of a major Holocene abrupt climate change. *Quaternary Science Reviews 24*, 1123-1149.

Alley R.B., Mayewski P.A., Sowers T., Stuiver M., Taylor K.C. and Clark P. U. (1997) Holocene climatic instablity: A prominent, widespread event 8200 yr ago. *Geology 25*, 483-486.

Anderson W.T., Mullins H.T. and Ito E. (1997) Stable isotope record from Seneca Lake, New York: Evidence for a cold paleoclimate following the Younger Dryas. *Geology 25*, 135-138.

Ariztegui D., Chondrogianni C., Lami A., Guilizzoni P. and Lafargue E. (2001) Lacustrine organic matter and the Holocene paleoenvironmental record of Lake Albano (central Italy). *Journal of Paleolimnology 26*, 283-292.

Bartlein P.J., Webb T. III. and Fleri E. C. (1984) Holocene climate change in the northern Midewest: Pollen-derived estimates. *Quaternary Research 22*, 361-374.

Bronk Ramsey C. (2001) Development of the radiocarbon program OxCal. *Radiocarbon 43*, 355-363.

Buddenbaum W.E. and Shiner V.J.J. (1977) Computation of isotope effects on equilibria and rates, in *Isotope effects on Enzyme-catalyzed reactions*, edited by W. Cleland et al., University Park Press, Baltimore.

Burgoyne T.W. and Hayes J.M. (1998) Quantitative production of H2 by pyrolysis of gas

chromatographic effluents. *Analytical Chemistry*, 70, 5136-514.

Coolen M.J.L., Muyzer G., Rijpstra W.I.C., Schouten S., Volkman J.K. and Damste J.S.S. (2004) Combined DNA and lipid analyses of sediments reveal changes in Holocene haptophyte and diatom populations in an Antarctic lake. *Earth and Planatary Science Letters 223*, 225-239.

Cranwell P.A. (1982) Lipids of aquatic sediments and sedimenting particulates. *Progress in Lipid Research 21*, 271-308.

Cwynar L.C. and Levesque A.J. (1995) Chironomid evidence for late-Glacial climatic reversals in Maine. *Quaternary Research 43*, 403-415.

D'Andrea W.J. and Huang Y. (2005) Long chain alkenones in Greenland lake sediments: Low $\delta^{13}C$ values and exceptional abundance. *Organic Geochemistry 36*, 1234-1241.

Dansgaard W. (1964) Stable isotopes in precipitation. *Tellus 16*, 436-468.

Edwards T.W.D. (1993) Interpreting past climate from stable isotofpes in continental organic matter, in *Climatic change in continental isotopic records: American Geophysical Union Geophysical Monograph*, edited by P. K. Swart, pp. 333-341.

Ficken K.J., Li B., Swain D.L. and Eglinton G. (2000) An *n*-alkane proxy for the sedimentary input of submerged/floating freshwater aquatic macrophytes. *Organic Geochemistry 31*, 745-749.

Hayes J.M., Freeman K.H., Popp B.N. and Hoham C.N. (1990) Compound-specific isotope analyses: A novel tool for reconstruction of ancient biogeochemical

processes. *Organic Geochemistry 16*, 1115-1128.

Heiri O., Lotter A.F., Hausmann S. and Kienast F. (2003) A chironomid-based Holocene summer air temperature reconstruction from the Swiss Alps. *The Holocene 13*, 477-484.

Huang Y., Freeman K.H., Eglinton T.I. and Street-Perrott F.A. (1999) $\delta^{13}C$ analyses of individual lignin phenols in Quaternary lake sediments: A novel proxy for deciphering past terrestrial vegetation changes. *Geology 27*, 471-474.

Huang Y., Shuman B., Wang Y. and Webb T.III. (2002) Hydrogen isotope ratios of palmitic acid in lacustrine sediments record late Quaternary climate variations. *Geology 30*, 1103-1106.

Huang Y., Shuman B., Wang Y. and Webb T.III. (2004) Hydrogen isotope ratios of individual lipids in lake sediments as novel tracers of climatic and environmental change: a surface sediment test. *Journal of Paleolimnology 31*, 363-375.

Huang Y., Street-Perrott F.A., Metcalfe S.E., Brenner M., Moreland M. and Freeman K.H. (2001) Climate change as the dominant control on glacial-interglacial variations in C_3 and C_4 plant abundance. *Science 293*, 1467-1471.

Krishnamurthy R.V., Syrup K.A., Baskaran M. and Long A. (1995) Late glacial climate record of midwestern United States from the hydrogen isotope ratios of lake orgnaic matter. *Science 269*, 1565-1567.

Kurek J., Cwynar L.C. and Spear R.W. (2004) The 8200 cal yr BP cooling event in eastern North America and the utility of midge analysis for Holocene temperature

reconstructions. *Quaternary Science Reviews 23*, 627-639.

Lamb A.L., Leng M.J., Mohammed M.U. and Lamb H. F. (2004) Holocene climate and vegetation change in the Main Ethiopian Rift Valley, inferred from composition (C/N and $\delta^{13}C$) of lacustrine organic matter. *Quaternary Science Reviews 23*, 881-891.

Liu W. and Huang Y. (2005) Compound specific D/H ratios and molecular distributions of higher plant leaf waxes as novel paleoenvironmental indicators in the Chinese Loess Plateau. *Organic Geochemistry 36*, 851-860.

Meyers P. A. (2003) Applications of organic geochemistry to paleolimnological reconstructions: a summary of examples from the Laurentian Great Lakes. *Organic Geochemistry 34*, 261-289.

Meyers P. A. and Ishiwatari R. (1993) Lacustrine organic geochemistry - an overview of indicators of organic matter sources and diagenesis in lake sediments. *Organic Geochemistry 20*, 867-900.

Newby P.E., Killoran P., Waldorf M.R., Shuman B., Webb R.S. and Webb T.III. (2000) 14,000 years of sediment, vegetation, and water-level changes at the Makepeace Cedar Swamp, Southeastern Massachusetts. *Quaternary Research 53*, 352-368.

Sauer P.E., Eglinton T.I., Hayes J.M., Schimmelmann A. and Sessions A.L. (2001) Compound-specific D/H ratios of lipid biomarkers from sediments as a proxy for environmental and climatic conditions. *Geochimica et Cosmochimica Acta 65*, 213-222.

Sessions A.L. and Hayes J.M. (2005) Calculation of hydrogen isotopic fractionations in biogeochemical systems. *Geochimica et Cosmochimica Acta 69*, 593-597.

Sessions A.L., Jahnke L.L., Schimmelmann A. and Hayes J.M. (2002) Hydrogen isotope fractionation in lipids of the methane-oxidizing bacterium *Methylococcus capsulatus*. *Geochimica et Cosmochimica Acta 66*, 3955-3969.

Severinghaus J.P., Sowers T., Brook E.J., Alley R.B. and Bender M.L. (1998) Timing of abrupt climate change at the end of the Younger Dryas interval from thermally fractionated gases in polar ice. *Nature 391*, 141-146.

Shuman B., Bartlein P.J., Logar N., Newby P. and Webb T.III. (2002a) Parallel climate and vegetation responses to the early Holocene collapse of the Laurentide Ice Sheet. *Quaternary Science Reviews 21*, 1793-1805.

Shuman B., Bravo J., Kaye J., Lynch J.A., Newby P. and Webb T.III. (2001) Late Quaternary water-level variations and vegetation history at Crooked Pond, Southeastern Massachusetts. *Quaternary Research 56*, 401-410.

Shuman B., Newby P., Huang Y. and Webb T.III. (2004) Evidence for the close climatic control of New England vegetation history. *Ecology 85*, 1297-1310.

Shuman B., Webb T.III., Bartlein P.J. and Williams J.W. (2002b) The Anatomy of a climatic oscillation: vegetation change in eastern North America during the Younger Dryas chronozone. *Quaternary Science Reviews 21*, 1777-1791.

Spooner I., Douglas M.S.V. and Terrusi L. (2002) Multiproxy evidence of an early Holocene (8.2 kyr) climate oscillation in central Nova Scotia, Canada. *Journal of*

Quaternary Science 17, 639-645.

Sternberg L.D.S.L. (1988) D/H ratios of environmental water recorded by D/H ratios of plant lipids. *Nature 333*, 59-61.

Stuiver M., Grootes P.M. and Braziunas T.F. (1995) The GISP2 $\delta^{18}O$ climate record of the past 16,500 years and the role of sun, ocean, and volcanoes. *Quaternary Research 44*, 341-354.

Yapp C.J. and Epstein S. (1982) A re-examination of cellulose carbon-bound hydrogen dD measurements and some factors affecting plant-water D/H relationships. *Geochimica et Cosmochimica Acta 46*, 955-965.

Yu Z. and Eicher U. (1998) Abrupt climate oscillations during the last deglaciation in central North America. *Science 282*, 2235-2238.

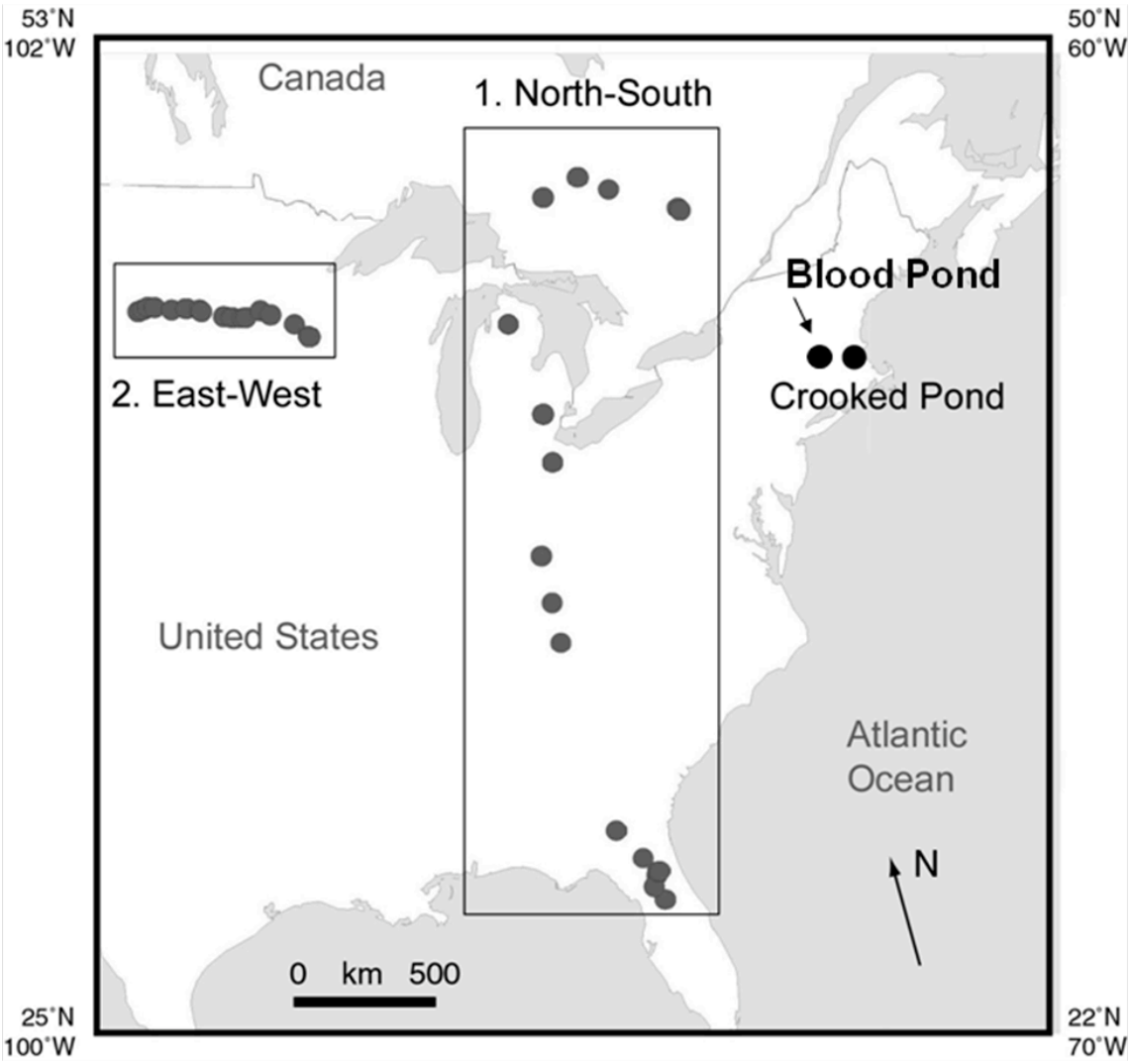

Figure 1. Sampling sites (n=33) for lake surface sediments along north-south and east-west transects, and the locations of Blood Pond and Crooked Pond, Massachusetts.

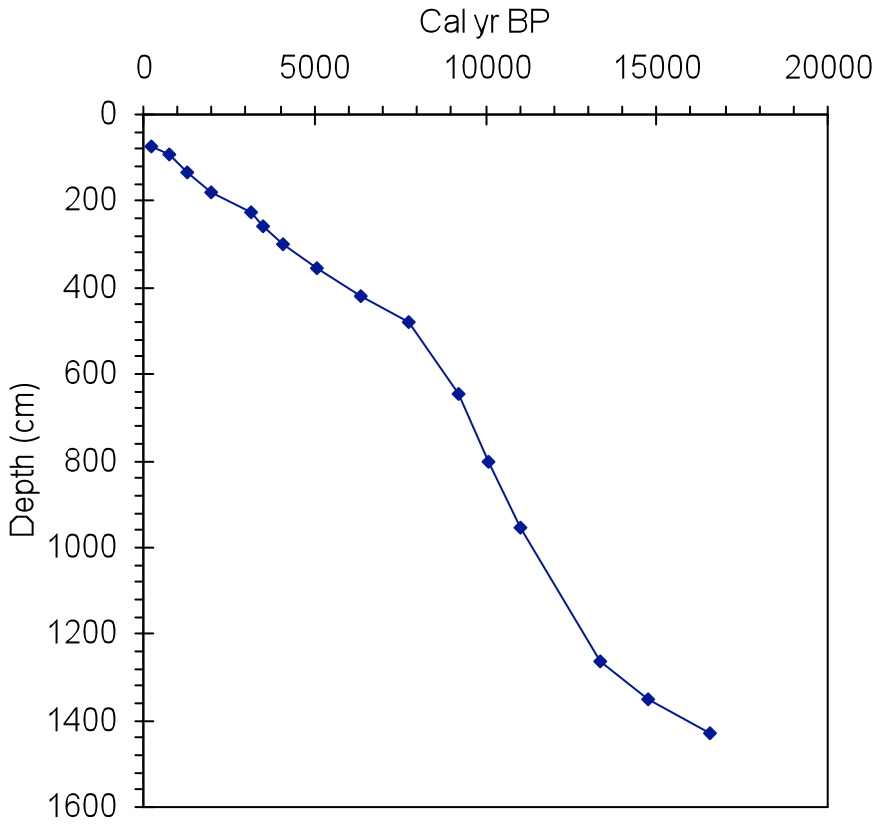

Figure 2. Age model for the sediment core from Blood Pond, Massachusetts. A total of twenty one ^{14}C dates were obtained, but six were excluded due to age inversions (^{14}C date of a sample is younger than a sample above it).

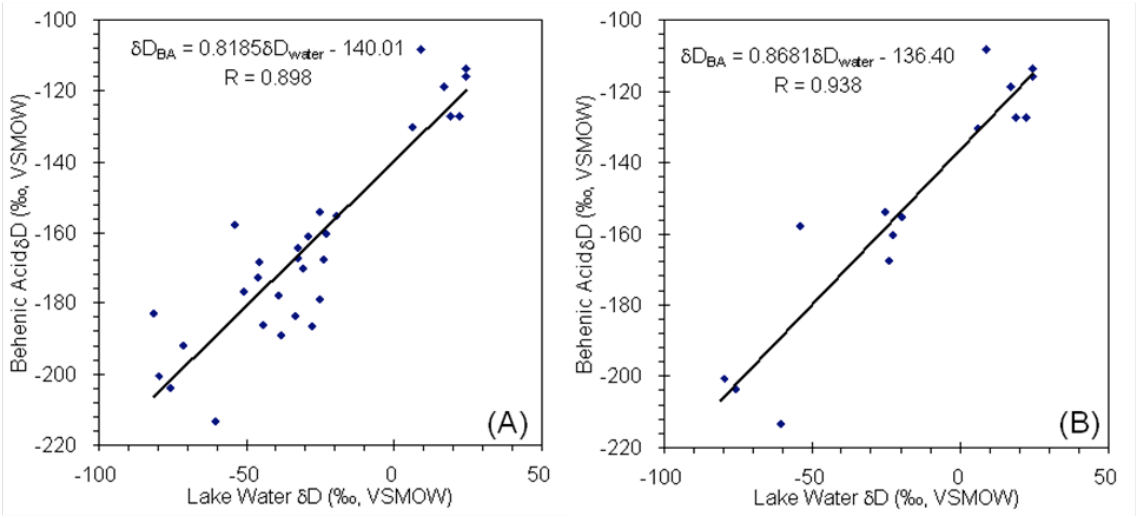

Figure 3. (A) Correlation between δD values of behenic acid (BA, C_{22} *n*-acid) from surface sediments and δD values of lake water (n=33; VSMOW is Vienna standard mean ocean water) of both transects; (B) Correlation between δD_{BA} and $\delta D_{lake\ water}$ of lakes in the north-south transect.

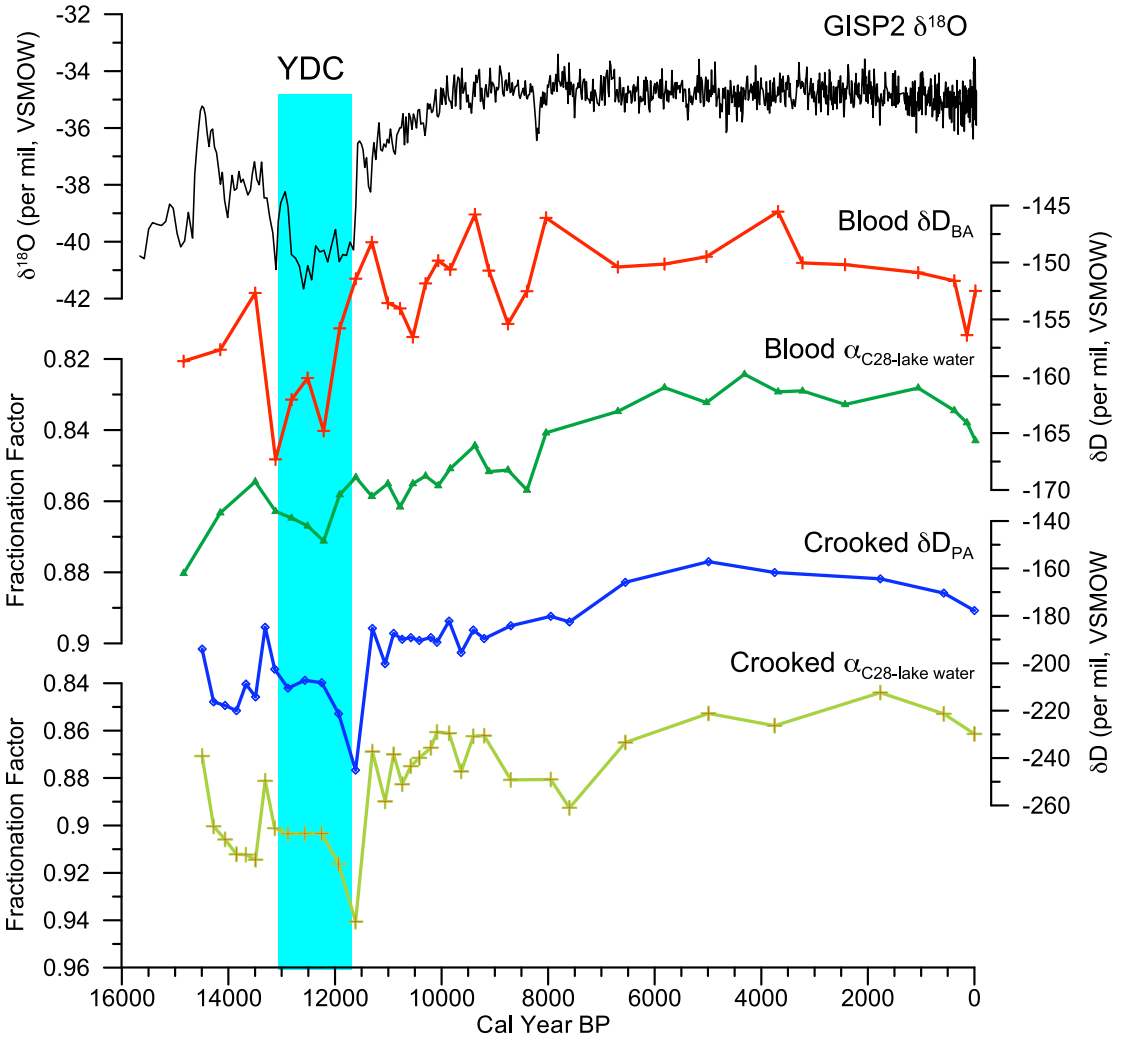

Figure 4. Hydrogen isotope records of behenic acid (δD_{BA}), palmitic acid (δD_{PA}), fractionation factor of C_{28} *n*-acid relative to lake water ($\alpha_{C28\text{-}lakewater}$) from Blood Pond, Massachusetts. The pollen records from the same sediment core provide vegetation information. The GISP2 $\delta^{18}O$ record is shown for comparison. Shaded columns indicate the Younger Dryas chronozone (YDC) and the 8.2 ka cool event.

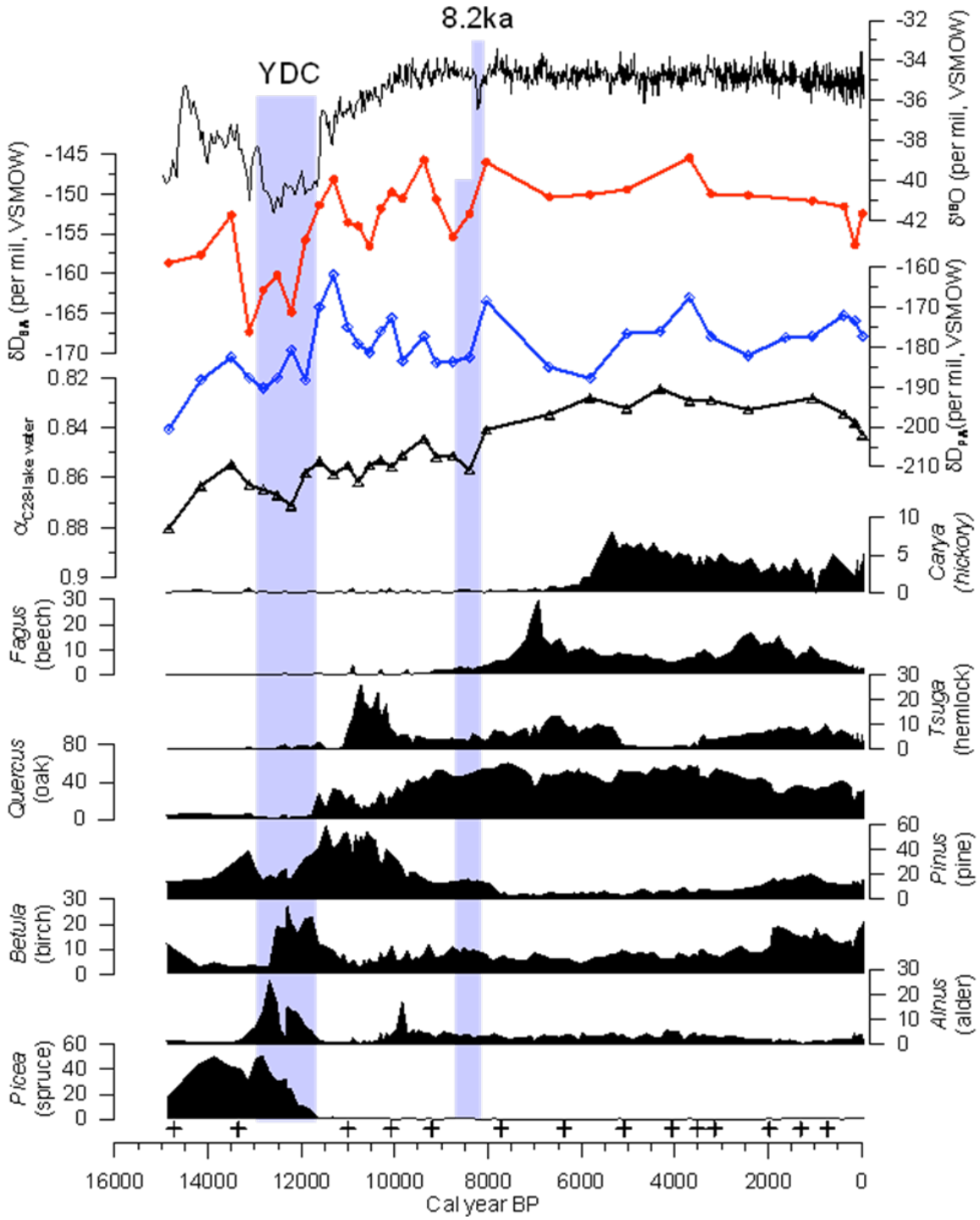

Figure 5. Comparison of isotope records from Blood Pond (Blood δD_{BA}, Blood $\alpha_{C28\text{-lake water}}$), Crooked Pond (Crooked δD_{PA}, Crooked $\alpha_{C28\text{-lake water}}$) and Greenland Ice Sheet isotope record (GISP2 $\delta^{18}O$). Blood Pond and Crooked Pond data show similar trends which slightly differ from the GISP2 record, probably suggesting climate differences between New England and the Greenland summit.

CHAPTER 2

Hydrogen isotopic variability in leaf waxes of plants

Part 1

Hydrogen isotopic variability in leaf waxes among terrestrial and aquatic plants around Blood Pond, Massachusetts

Co-authors: William J. D'Andrea, Dana MacDonald, Yongsong Huang

Published in ***Organic Geochemistry***, 2007, v. 38, p. 977-984,

doi:10.1016/j.orggeochem.2006.12.009

ABSTRACT

Paleoclimate interpretation of the hydrogen isotope values of plant leaf waxes extracted from sediments requires a thorough understanding of the factors controlling the isotopic ratios. Existing studies have found relatively small variability in hydrogen isotope fractionation among plants of different photosynthetic pathways (C_3, C_4 and CAM) and between gymnosperms and angiosperms. However, there has been no systematic study so far *at a single site* to determine how leaf wax hydrogen isotope (D/H) ratios differ in different plant types under the same precipitation and environmental regime. Such data are nevertheless crucial for understanding the impact of past vegetation changes on the sedimentary hydrogen isotope records of leaf waxes. Here we present a study on D/H ratios of leaf waxes from 48 species in 7 types of terrestrial and aquatic C_3 plants around Blood Pond, Dudley, Massachusetts. The δD values of leaf waxes differ by as much as 70 ‰ for different plant types, with those from trees and ferns having the highest values and those from grasses having the lowest values. The large isotopic variation indicates that the apparent hydrogen isotopic fractionation between leaf waxes and precipitation is not constant for different plants. Our results indicate that inferring precipitation D/H ratios based on sedimentary leaf waxes are only viable when significant vegetation change is absent or can be accounted for isotopically.

INTRODUCTION

Compound-specific hydrogen isotope (D/H) ratios of leaf waxes from lake surface sediments across large climatic gradients have been shown to track the D/H ratios of environmental water (Huang et al., 2004; Liu and Huang, 2005) or precipitation (e.g., Sachse et al., 2004, 2006; Shuman et al., in press). Long chain *n*-alkanes from different sites have been suggested to track D/H ratios of precipitation at nearly constant apparent isotopic fractionation (Saches et al., 2004; 2006). Based on hydrogen isotopic analyses of both aquatic and terrestrial compounds, Hou et al. (2006) and Shuman et al. (in press) have constructed late-glacial to Holocene climate reconstructions that are consistent with existing climate data (Huang et al., 2002; Shuman et al., 2004). However, despite these corroborated paleoclimate reconstructions, the reliability with which D/H ratios of sedimentary leaf waxes record ancient precipitation depends on an important premise: the natural hydrogen isotopic variability among different plants *at a given site* is relatively small. If, on the other hand, different plants at a given site produce leaf waxes with large hydrogen isotopic differences, vegetation changes through time could confound or even overpower the precipitation δD signal believed to be recorded by sedimentary leaf waxes.

D/H ratios of leaf waxes in plants that use different photosynthetic pathways, and in several plant types (gymnosperms, angiosperms, ferns, aquatic plants), have been studied

(e.g., Chikaraishi et al., 2003, 2004; Bi et al., 2005; Smith and Freeman, 2006). In contrast to the large carbon isotopic differences observed between C_3 and C_4 plants (Farquhar et al., 1989), hydrogen isotopic differences between C_3 and C_4 plants are relatively small (Chikaraishi et al., 2003; Bi et al., 2005). If only grasses are considered, C_4 *grasses* are enriched in deuterium by ~ 20‰ relative to C_3 *grasses* collected from the same site (Smith and Freeman, 2006). The plant samples studied by Chikaraishi et al. (2003) were collected from a wide range of ecosystems, locations, and climate zones making it difficult to ascertain the D/H ratios of plant source waters and to distinguish the effect of plant types from the effect of source water and environmental conditions (e.g., nutrients, soil types, evaporation, relative humidity, sun light etc.) on the hydrogen isotopic fractionations. At different locations, plants may utilize soil water derived from precipitation falling during different seasons, and may incorporate different amounts of ground water for photosynthesis (White et al., 1985). Therefore, determining plant apparent hydrogen isotopic fractionation relative to either mean annual or summer precipitation may introduce significant uncertainty, especially when comparing sites with large climatic, hydrological and micro-environmental differences.

Here we present a systematic study of 48 species of terrestrial and aquatic plants (all are C_3 plants) around Blood Pond, MA (Hou et al., 2006) to examine the difference in their leaf wax δD values. By collecting plant samples within the close vicinity (within 50

m) of Blood Pond, we minimize the impact of various hydrological and environmental factors on leaf wax D/H ratios. We aim to 1) systematically study the δD values of leaf waxes produced by different terrestrial and aquatic plants under the same hydrological and environmental system; 2) evaluate the influence of plant composition on the application of leaf waxes to climate reconstruction; 3) determine the biosynthetic hydrogen isotopic fractionation between δD values of long chain normal acids and alkanes.

SAMPLES AND METHODS

Samples

Blood Pond (42.08°N, 71.96°W, 212.1 m a.s.l.) is a kettle pond located in the south-central Massachusetts town of Dudley (Hou et al., 2006). We collected 74 samples of plant leaves, representing 48 species of terrestrial and aquatic plants around Blood Pond on Aug 11, 2005 (Table 1). There are 11 tree species (35 leaf samples), 9 shrub species (11 leaf samples), 3 vine species (3 leaf samples), 9 herb species (9 leaf samples), 7 grass species (7 samples), 4 fern species (4 leaf samples) and 5 species of aquatic macrophytes (5 leaf samples). All plants in this study are C_3 plants. Multiple samples from different heights (6m, 4.5m, 3 m) of individual trees or shrubs (Table 1) were also collected to determine the hydrogen isotopic variability within the same plant.

Methods

All leaf samples were freeze-dried and then ultrasonically extracted with dichloromethane three times for 15 minutes. The extract was separated into neutral and acid fractions using solid phase extraction (Aminopropyl Bond Elute®). The acid fraction was then methylated using anhydrous 2% HCL in methanol. Hydroxyl acids were

removed using silica gel column chromatography (DCM as solvent), in order to further purify the fatty acid methyl esters and avoid chromatographic coelution. The neutral fraction was further separated into hydrocarbon, ketone/aldehyde, and alcohol fractions using hexane, DCM, and a mixed solvent (ethyl acetate:hexane=1:3), respectively.

Quantification and identification of compounds were carried out using GC and GC-MS. An HP 6890 GC interfaced to a Finnigan Delta+ XL stable isotope mass spectrometer through a high-temperature pyrolysis reactor was used for hydrogen isotopic analysis (Huang et al., 2002, 2004). The H_3^+ factor was determined daily prior to sample analysis (average values 2.0 during this study). The precision (1σ) of triplicate analyses was <±2‰. The accuracy was routinely checked by an injection of laboratory isotopic standards between every six measurements. δD values obtained from individual acids (as methyl esters) were corrected by mathematically removing the isotopic contributions from added groups before reporting. The δD value of the added methyl group was determined by acidifying and then methylating (along with the samples) the disodium salt of succinic acid with a predetermined δD value (using TC/EA-IRMS) (Huang et al., 2002). There is no kinetic isotopic fractionation and hydrogen exchange during the methylation (Yang and Huang, 2003).

RESULTS AND DISCUSSION

Hydrogen isotopic variation among plant types

Hydrogen isotopic values of C_{27}, C_{29}, C_{31} *n*-alkanes and C_{26}, C_{28} and C_{30} *n*-acids of all plant samples are listed in Table 1. Because δD values are strongly correlated for C_{27}, C_{29} and C_{31} *n*-alkanes (Figure 1A, Table 2) and for C_{26}, C_{28}, C_{30} *n*-acids (Figure 1B, Table 2), our subsequent discussions will focus on C_{29} *n*-alkane and C_{30} *n*-acid. To facilitate comparison, we also group plants into 7 types: trees, shrubs, vines, herbs, grasses, ferns and aquatic macrophytes based on their growth habits (Raven et al., 2003; Figure 2). The definitions of growth habits and their acronyms (e.g., BEPO for *Betula populifolia* Marsh.) used in Table 1 are obtained from the PLANTS database on the United States Department of Agriculture website (USDA, 2006).

δD values of leaf waxes from the different plant types sampled at Blood Pond vary significantly (Table 1; Figure 2). Long chain *n*-acids and *n*-alkanes from trees and ferns have the highest average δD values, whereas grasses have the lowest. The hydrogen isotopic difference between ferns/trees and grasses is as large as 60 to 70‰. Shrubs, vines, herbs, and macrophytes have intermediate δD values. Within each plant type, the δD values vary among different species of plants. Trees, grasses and herbs show larger

isotopic variability than the other types. For example, among the trees, δD values of C_{30} *n*-acid range from -190 ‰ (CARYA-2, *Carya sp.* Nutt) to -121 ‰ (FRAM2(a), *Fraxinus americana* L., Table.1). The δD values of C_{30} *n*-acid in grasses range from -227 ‰ (PHPR3, *Phleum pratense* L.) to -182‰ (DAGL, *Dactylis glomerata* L. and JUTE, *Juncus tenuis* Willd.). The large variability observed for trees and grasses may partially reflect the relatively large number of samples taken from trees and grasses in this study.

Factors leading to D/H variability in different plants

A number of factors may affect the D/H ratios of leaf waxes. The source water used by plants may differ, even though the regional precipitation is the same. Different trees root to different depths, and may have access to water with different D/H ratios. In general, shallow soil water should have higher D/H ratios due to evaporation (Barnes and Turner, 1998). Trees, having more extensive root systems, may tap into deeper ground water than grasses and herbs. Our data do not, however, suggest that this is an important mechanism controlling the D/H ratios of leaf waxes from trees, grasses, and herbs, since grasses and herbs have on average 60 to 70 ‰ lower δD values than trees, opposite to what would be expected if source water depth exerted a primary control.

The higher δD values in trees relative to grasses and herbs may result from

differences in the microclimate around tree crown and grasses that lead to different degrees of evapotranspiration. Grasses and herbs are more likely to be shaded by trees and shrubs in the forest. In contrast, most trees receive direct sun light and experience more windy conditions (which also facilitate more evapotranspiration). The temperature at the surface of tree leaves should be higher than that experienced by grasses due to the direct sun light on tree leaves and shading effect on grasses. The deep roots of trees also enhance transpiration (Raven et al., 2003). The relative humidity around tree leaves may also be lower than that around grasses because of the moisture from soil water evaporation. Lower humidity would act to increase the kinetic isotopic effect for trees relative to grasses. The evapotranspiration effect, which enriches deuterium in the leaf water, could thus be smaller for the grasses than for trees. The differences in evapotranspiration rate may therefore be an important factor leading to higher hydrogen isotopic ratios of the leaf waxes of trees relative to grasses. In addition, the difference in leaf morphology affects the isotopic composition of leaf water (Grice et al., 2005), which then may also contribute the δD values of leaf waxes for different plants. It is also possible that differences in plant physiology and biochemistry could contribute to the hydrogen isotopic differences. However, we currently do not have data to support this possibility. Modified Craig-Gordon isotopic models on leaf water (Roden and Ehleringer, 1999) for different plants may help to explain the isotopic difference amongst the plants.

Leaf samples collected from different heights of individual plants do not show significant variation (Table 1). The leaves of BELE-2, PIST, NYSY show little change in *n*-acid δD values with height of the sample. There is a slightly increasing trend (~9 ‰) of δD values with height for BEPO-1 and FRAM2, but the trend is reversed for BEPO-2 (same plant species). Within individual plant types, the variation of δD values of *n*-acids and *n*-alkanes may also result from evapotranspiration differences among different species, but further work is needed to test this hypothesis.

Implication for reconstructing past precipitation D/H ratios

The mean annual δD value of precipitation at Blood Pond (Dudley, MA) is calculated to be -63 ‰, while summer δD is -40 ‰, using the online precipitation isotope calculator (Bowen and Revenaugh, 2003). Since all our samples were collected within 50 m of Blood Pond, all plants from this study have received the same precipitation. Thus, the difference in δD values of the leaf samples (Table 1 and Figure 2) are equivalent to the differences in the *apparent* hydrogen isotopic fractionation relative to precipitation. The apparent hydrogen isotopic fractionation between leaf waxes and precipitation must be known in order to reconstruct past precipitation D/H ratios from leaf waxes preserved in lake sediment. Based on our data, the apparent H isotopic enrichment relative to summer precipitation for trees ranges from -156 to -85‰ for *n*-acids (mean = -117‰),

and -180 to -115‰ for *n*-alkanes (mean = -150‰). Grasses show much larger apparent isotopic fractionation, with *n*-acids ranging from -195 to -148‰ (mean = -171‰), and *n*-alkanes ranging from -206 to -154 ‰ (mean = -183‰). Lower average δD values for grasses and herbs relative to trees may help explain the low δD values of *n*-alkanes from lake sediments relative to *n*-alkanes from surrounding tree leaves reported by Sachse et al. (2006).

Sachse et al. (2004) suggest that D/H ratios of leaf wax *n*-alkanes in surface sediments fractionate relative to precipitation by approximately 130 ‰. However, the results from this study suggest large differences in hydrogen isotopic fractionation of different types of plants at a single site. Leaf waxes are transported into lake sediment primarily by wind. Sedimentary leaf waxes thus integrate those produced by all terrestrial and aquatic plants. Our data indicate the apparent H isotopic enrichment can differ by as much as 60 to 70 ‰ between trees and grasses. Therefore, it is inappropriate to assume constant fractionation between sedimentary leaf waxes and precipitation over intervals where there have been significant changes in vegetation. Naturally, vegetation is often sensitive to climate change. Hence, paleoclimate interpretations based on leaf wax δD values must first consider the isotopic variation induced by changing vegetation types. In regions where vegetation is less variable, such as arid grasslands, it is possible that a relatively invariable H isotopic fractionation could be applied to sedimentary leaf wax

records to obtain precipitation D/H ratios. In addition, *n*-alkanes from sphagna may resemble the environmental water hydrogen isotopes (Xie et al., 2004), which can be used to reconstruct past precipitation variation.

H isotopic difference between n-acids and n-alkanes

C_{30} *n*-acid is the biosynthetic precursor of C_{29} *n*-alkane in plants. There is biosynthetic isotopic fractionation during the decarboxylation process. This fractionation for various plants has not been reported in literature. Our data (Table 1, Fig 1C, Fig 2) show that C_{29} *n*-alkanes are depleted in D by up to 30 ‰ relative to C_{30} n-acids. This indicates that decarboxylation discriminates against D, as expected. Grasses and herbs appear to show smaller D depletion of C_{29} *n*-alkane relative to C_{30} *n*-acid (<13 ‰) than trees, although we cannot exclude the possibility that such difference is a result of sampling bias at this time. C_{28} *n*-acid and C_{27} *n*-alkane from the same plants show similar difference in their δD values (Table 1, Fig 1D). Chikaraishi et al (2004) reported much larger hydrogen isotopic effect (up to 100 ‰) during enzymatic desaturation of fatty acids, which is apparently larger than δD change during decarboxylation.

CONCLUSIONS

We systematically studied the hydrogen isotopes of leaf waxes from 48 species of 7 types of terrestrial and aquatic C_3 plants around Blood Pond, Massachusetts. The δD values of leaf waxes show large differences among plant types. The difference between average δD values of ferns, trees and grasses is as large as 70‰. We attribute the hydrogen isotopic difference to different degrees of evapotranspiration as a result of microenvironmental differences for different plants, such as sun light exposure, temperature, humidity and turbulence (wind). Differences in plant physiology and biochemical fractionation may also be important, but we currently do not have data to demonstrate their impact on hydrogen isotopic fraction of leaf waxes. Our data indicate that caution must be taken when attempting to use sediment leaf wax D/H ratios to reconstruct past precipitation isotopic ratios. Variable fractionation among different plants must be considered to minimize the effect of vegetation changes under different climate conditions. It is possible that combining isotopic and pollen stratigraphy will allow more accurate paleoclimate interpretations based on leaf wax δD values in sediments. In regions with more monotonic plant types (e.g., arid regions, Liu and Huang, 2005), hydrogen isotopic ratios of sedimentary leaf waxes may more faithfully track precipitation D/H ratios.

ACKNOWLEDGEMENTS

We would like to thank Koebke Farm (Dudley, MA) for access to Blood Pond. This work was supported by grants from the National Science Foundation (NSF 0318050, 0318123, 0402383) to Y. Huang.

REFERENCES

Barnes C.J. and Turner J.V. (1998) Isotopic exchange in soil water. In: C. Kendall, J.J. McDonnell (Eds.), Isotope tracers in catchment hydrology (Ed. by C. Kendall, J.J. McDonnell), pp. 137-163. Elsevier.

Bi X., Sheng G., Liu X., Li C. and Fu J. (2005) Molecular and carbon and hydrogen isotopic composition of n-alkanes in plant leaf waxes. *Organic Geochemistry* 36, 1405-1417.

Bowen G. J. and Revenaugh J. (2003) Interpolating the isotopic composition of modern meteoric precipitation. *Water Resources Research* 39, 1299, doi:10.129/2003WR002086.

Chikaraishi Y. and Naraoka H. (2003) Compound-specific dD-d13C analyses of n-alkanes extracted from terrestrial and aquatic plants. *Phytochemistry* 63, 361-371.

Chikaraishi Y., Naraoka H. and Poulson S.R. (2004) Hydrogen and carbon isotopic fractionations of lipid biosynthesis among terrestrial (C_3, C_4 and CAM) and aquatic plants. *Phytochemistry* 65, 1369-1381.

Farquhar G.D., Ehleringer J.R. and Hubick K.T. (1989) Carbon Isotope Discrimination and Photosynthesis. *Annual Review of Plant Physiology and Plant Molecular Biology* 40, 503-537.

Grice K., Zhou Y., Stuart-Williams H., Wong S.C., Schouten S., Wang S.X. and Farquhar G.D. (2005) D/H of water, lipids and carbohydrates from modern plants grown under controlled conditions (Temperature, light intensity, CO2 concentration and water availability). *Organic Geochemistry*: Challenges for the 21st Century, 22nd IMOG, Serille, Spain., 734-735.

Hou J., Huang Y., Wang Y., Shuman B., Oswald W.W., Faison E. and Foster D.R. (2006) Postglacial climate reconstruction based on compound-specific D/H ratios of fatty acids from Blood Pond, New England, *Geochemistry Geophysics Geosystem* 7, Q03008, doi:10.1029/2005GC001076.

Huang Y., Shuman B., Wang Y. and Webb T.III. (2002) Hydrogen isotope ratios of palmitic acid in lacustrine sediments record late Quaternary climate variations. *Geology* 30, 1103-1106.

Huang Y., Shuman B., Wang Y. and Webb T.III. (2004) Hydrogen isotope ratios of individual lipids in lake sediments as novel tracers of climatic and environmental

change: a surface sediment test. *Journal of Paleolimnology* 31, 363-375.

Killops S. and Killops V. (2005) Introduction to Organic Geochemistry. Blackwell Publishing Company.

Liu W. and Huang Y. (2005) Compound specific D/H ratios and molecular distributions of higher plant leaf waxes as novel paleoenvironmental indicators in the Chinese Loess Plateau. *Organic Geochemistry* 36, 851-860.

Raven P.H., Evert R.F. and Eichhorn S.E. (2003) Biology of Plants. W.H. Freeman and Company, New York, pp. 466-494.

Roden J.S. and Ehleringer J.R. (1999) Observations of hydrogen and oxygen isotopes in leaf water confirm the Craig-Gordon model under wide-ranging environmental conditions. *Plant Physiology* 120(4), 1165-1173.

Sachse D., Radke J. and Gleixner G. (2004) Hydrogen isotope ratios of recent lacustrine sedimentary n-alkanes record modern climate variability. *Geochimica et Cosmochimica Acta*, 68, 4877-4889.

Sachse D., Radke J. and Gleixner G. (2006) δD values of individual n-alkanes from terrestrial plants along a climatic gradient - Implications for the sedimentary biomarker record. *Organic Geochemistry* 37, 469-483.

Shuman B., Huang Y., Newby P. and Wang Y. (2006) Compound-specific isotopic analyses track changes in the seasonality of precipitation in the Northeastern United States at ca. 8200 cal yr BP. *Quaternary Science Reviews* 25, 2992-3002.

Shuman B., Newby P., Huang Y. and Webb T.III. (2004) Evidence for the close climatic control of New England vegetation history. *Ecology* 85, 1297-1310.

Smith F.A. and Freeman K.H. (2006) Influence of physiology and climate on δD of leaf wax n-alkanes from C3 and C4 grasses. *Geochimica et Cosmochimica Acta* 70, 1172-1187.

USDA NRCS. (2006) *The PLANTS Database*, 6 March 2006 (http://plants.usda.gov). National Plant Data Center, Baton Rouge, LA 70874-4490 USA.

White J.W.C., Cook E.R., Lawrence J.R. and Broecker W.S. (1985) The D/H Ratios of Sap in Trees - Implications for Water Sources and Tree-Ring D/H Ratios. *Geochimica Et Cosmochimica Acta* 49, 237-246.

Xie S.C., Nott C.J., Avsejs L.A., Maddy D., Chambers F.M. and Evershed R.P. (2004) Molecular and isotopic stratigraphy in an ombrotrophic mire for paleoclimate reconstruction. *Geochimica Et Cosmochimica Acta* 68, 2849-2862.

Yang H. and Huang Y. (2003) Preservation of lipid hydrogen isotope ratios in Miocene lacustrine sediments and plant fossils at Clarkia, northern Idaho, USA. *Organic Geochemistry* 34, 413-423.

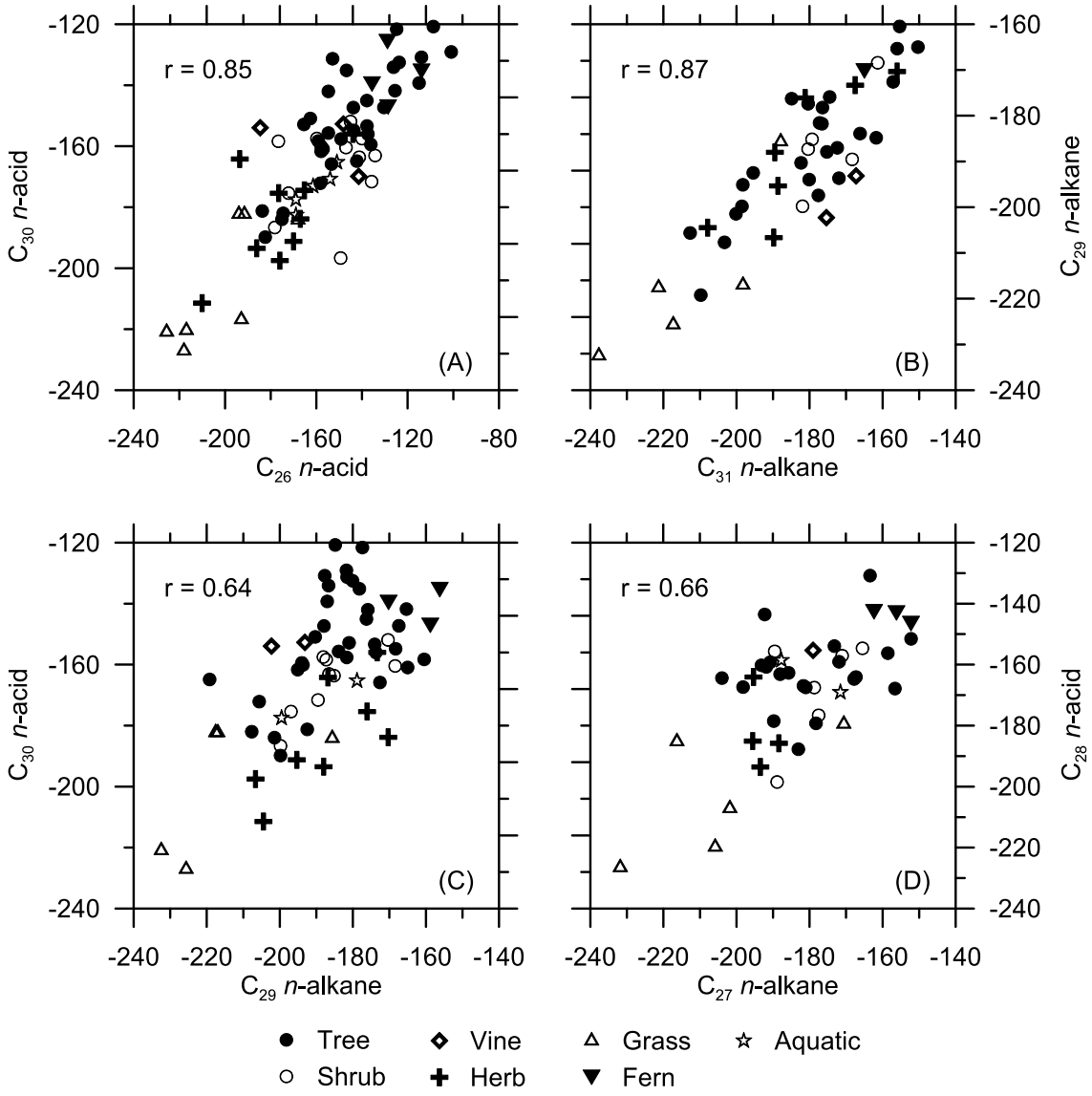

Figure 1. Correlations between δD values of leaf wax compounds.

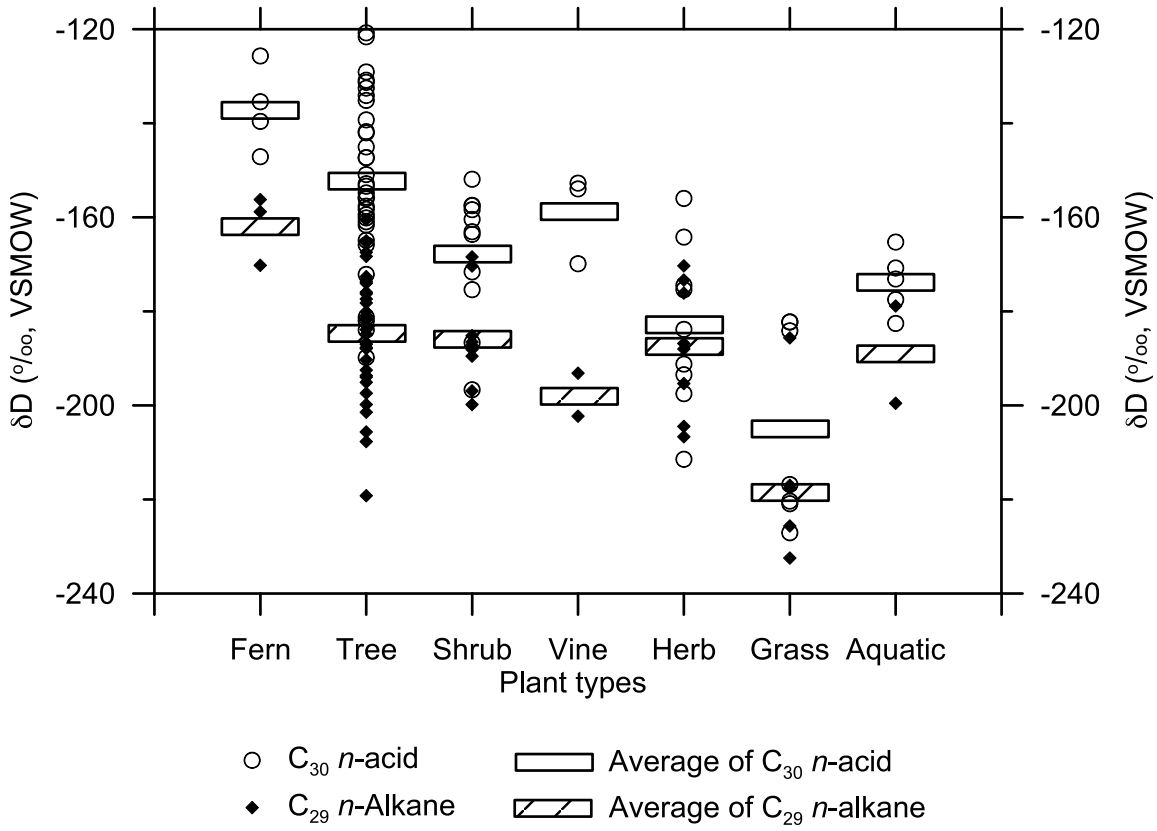

Figure 2. Hydrogen isotope ratios of leaf waxes collected around Blood Pond. δD values of C_{29} *n*-alkanes (diamonds) and C_{30} *n*-acids (circles) for each plant are shown, and the respective average values are depicted as horizontal bars. FE - Ferns, TR - Trees, SH - Shrubs, VI - Vines, HB - Herbs, GR - Grasses, AQ - Aquatic Macrophytes.

Table 1. δD values of leaf wax compounds extracted from leaf samples

Type	Symbol	Scientific Name	*n*-Alkanes			*n*-Acids		
			C_{27}	C_{29}	C_{31}	C_{26}	C_{28}	C_{30}
TR	BEPO-1(a)	*Betula populifolia* Marsh.	-191	-182	-177	-153	-159	-131
TR	BEPO-1(b)	*Betula populifolia* Marsh.	-186	-176	-174	-155	-163	-142
TR	BEPO-1(c)	*Betula populifolia* Marsh.	-198	-190	-182	-163	-167	-151
TR	BEPO-2(a)	*Betula populifolia* Marsh.	-192	-178	-176	-147	-161	-135
TR	BEPO-2(b)	*Betula populifolia* Marsh.	-192	-177	-180	-125	-144	-122
TR	QUVE	*Quercus velutina* Lam.	-152	-167		-130	-152	-147
TR	ACRU-1	*Acer rubrum* L.	-172	-194	-180	-136	-159	-159
TR	ACRU-2	*Acer rubrum* L.	-157	-195	-198	-158	-168	-162
TR	ACRU-3(a)	*Acer rubrum* L.		-206	-213	-158	-173	-172
TR	ACRU-3(b)	*Acer rubrum* L.		-219	-210	-142	-171	-165
TR	BELE-1(a)	*Betula lenta* L.	-182	-182		-149	-167	-158
TR	BELE-1(b)	*Betula lenta* L.		-197	-178			
TR	BELE-1(c)	*Betula lenta* L.	-181	-181		-165	-167	-153
TR	BELE-2(a)	*Betula lenta* L.	-188	-168		-144	-163	-155
TR	BELE-2(b)	*Betula lenta* L.	-193	-174		-137	-160	-156
TR	BELE-2(c)	*Betula lenta* L.	-204	-174		-138	-164	-153
TR	CARYA-1(a)	*Carya sp.* Nutt.		-194	-172	-158	-162	-160
TR	CARYA-1(b)	*Carya sp.* Nutt.		-188	-175	-144	-152	-147
TR	CARYA-1(c)	*Carya sp.* Nutt.		-176	-185	-138	-144	-145
TR	CARYA-2	*Carya sp.* Nutt.	-190	-208	-203	-175	-179	-182
TR	PIST (a)	*Pinus strobus* L.	-183	-192	-195	-184	-188	-181
TR	PIST(b)	*Pinus strobus* L.	-173	-201	-200	-175	-154	-184
TR	PIST(c)	*Pinus strobus* L.	-178	-200	-199	-182	-179	-190
TR	PRSE(a)	*Prunus serotina* Ehrh.		-184	-166	-155	-153	-156
TR	PRSE(b)	*Prunus serotina* Ehrh.	-201	-173				
TR	QURU(a)	*Quercus rubra* L.	-167	-165	-150	-157	-164	-161
TR	QURU(c)	*Quercus rubra* L.	-168	-173	-157	-153	-165	-166
TR	FRAM2(a)	*Fraxinus americana* L.		-185	-162	-109	-124	-121
TR	FRAM2(b)	*Fraxinus americana* L.		-182	-177	-101	-122	-129
TR	FRAM2(c)	*Fraxinus americana* L.		-187	-172	-115	-125	-139
TR	TSCA(b)	*Tsuga canadensis* L.	-159	-160	-155	-159	-156	-158
TR	TSCA(c)	*Tsuga canadensis* L.	-163	-165	-156	-126	-131	-142
TR	NYSY(a)	*Nyssa sylvatica* Marsh.		-180		-124	-126	-133
TR	NYSY(b)	*Nyssa sylvatica* Marsh.		-187		-126	-130	-134
TR	NYSY(c)	*Nyssa sylvatica* Marsh.		-188		-114	-125	-131
SH	HAVI4-1	*Hamamelis virginiana* L.	-166	-188		-140	-155	-158
SH	HAVI4-2	*Hamamelis virginiana* L.	-179	-170		-145	-168	-152
SH	HAVI4-3	*Hamamelis virginiana* L.	-171	-168	-161	-147	-157	-160

SH	LOTA	*Lonicera tatarica* L.		-185	-179	-141	-151	-164
SH	RUAL	*Rubus allegheniensis*	-178	-187	-180	-177	-177	-158
SH	VIAC	*Viburnum acerifolium* L.		-187		-134	-145	-163
SH	CLAL3	*Clethra alnifolia* L.		-197		-172	-176	-175
SH	LIBE3	*Lindera benzoin* (L.)	-189	-200	-182	-178	-198	-187
SH	DEVE	*Decodon verticillatus* (L.) Elliot				-149	-179	-197
SH	ILVE	*Ilex verticillata* (L.) Gray				-160	-163	-157
SH	RHODO	*Rhododendron sp.* L.	-190	-190	-168	-136	-156	-172
VI	SMHE	*Smilax herbacea* L.				-141	-175	-170
VI	SMRO	*Smilax rotundifolia* L.		-202	-175	-185	-172	-154
VI	VIAE	*Vitis aestivalis* Michx.	-179	-193	-167	-148	-155	-153
HB	ASDI	*Aster Divaricatus* L.		-176	-181	-176	-177	-175
HB	DACA6	*Daucus carota* L.	-188	-170	-156	-167	-186	-184
HB	PLMA2	*Plantago majo*r L.		-204	-208	-210	-213	-211
HB	TRPR2	*Trifolium pratense* L.	-196	-207	-190	-176	-185	-198
HB	UNKN1	Unknown				-165	-181	-174
HB	UNKN2	Unknown		-188	-190	-186	-162	-193
HB	IMCA	*Impatiens capensis*	-193	-187		-194	-194	-164
HB	MIRI	*Mimulus ringens* L.		-173	-168	-144	-155	-156
HB	TYLA	*Typha latifolia* L.	-195	-195	-189	-170	-164	-191
GR	CAPE6	*Carex pensylvanica* Lam.				-193	-210	-217
GR	AGRO	*Agropyron* sp.	-175	-231	-228	-217	-220	-220
GR	DAGL	*Dactylis glomerata* L.	-202	-218	-221	-194	-207	-182
GR	JUTE	*Juncus tenuis* Willd.	-216	-217	-198	-192	-185	-182
GR	PHPR3	*Phleum pratense* L.	-232	-226	-217	-218	-226	-227
GR	POAC	*Poaceae*	-206	-232	-238	-226	-220	-221
GR	ALOPE	*Alopecurus sp*. L.	-171	-186	-188	-168	-179	-184
FE	DEPU2	*Dennstaedtia punctilobula*				-129	-123	-126
FE	POAC4	*Polystichum acrostichoides*	-162	-170	-165	-136	-143	-140
FE	OSCI	*Osmunda cinnamomea* L.	-152	-159		-129	-147	-147
FE	ONSE	*Onoclea sensibilis* L.	-156	-156		-114	-143	-135
AQ	BRSC	*Brasenia schreberi* J. F. Gmel				-154	-162	-171
AQ	LEMNA	*Lemna sp.* L.	-172	-200		-169	-169	-178
AQ	NYMPH	*Nymphaea* L.				-161	-165	-173
AQ	NYMPH	*Nymphaea* L.				-169	-173	-183
AQ	POCO14	*Pontederia cordata* L.	-188	-179		-151	-159	-165

*Type of plants: TR-Tree, SH-Shrub, VI-Vine, HB-Herb, GR-Grass, FE-Fern, AQ-Aquatic macrophytes;
** Symbols are obtained from USDA PLANTS database (http://plants.usda.gov/). The number following the symbol indicates individual plants. The letters, (a), (b), (c) indicate the height of the leaf samples above the ground (a = 6 m, b = 4.5 m, c = 3 m). For example, BEPO-1(a) indicates the leaf sample was taken from the first *Betula populifolia* at 6 m above the ground.

Part 2

Evidence for water use efficiency as an important factor in determining the δD values of tree leaf waxes

Co-authors: William J. D'Andrea, Dana MacDonald, Yongsong Huang

Published in ***Organic Geochemistry***, 2007, v. 38, p. 1251-1255,

doi:10.1016/j.orggeochem.2007.03.011

ABSTRACT

D/H ratios of sedimentary leaf waxes can provide useful information about past climate changes. However, factors controlling δD values of higher plant leaf waxes (δD_{wax}) are poorly understood. Here we show that δD_{wax} are negatively correlated with $\delta^{13}C$ values of leaf waxes ($\delta^{13}C_{wax}$) based on study of 35 leaf samples of 11 tree species around Blood Pond, Massachusetts. Our data suggest that plant water-use efficiency exerts an important control on the δD_{wax} variation among different tree species.

INTRODUCTION

Hydrogen isotope ratios of plant leaf waxes (δD_{wax}) from lake and ocean sediments track δD of environmental waters and have potential for paleoclimate reconstructions (e.g., Schefuβ et al., 2005; Liu and Huang, 2005; Sachse et al., 2004; Shuman et al., 2006; Pagani et al., 2006). However, values of δD_{wax} show considerable variation among different plants from a single site receiving the same precipitation (Hou et al., 2007). While existing data suggest plant water-use strategies may affect δD values of plant leaf waxes (Smith and Freeman, 2006; Sachse et al., 2006; Hou et al., 2007), there have been no data directly linking plant water-use efficiency to hydrogen isotope ratios of leaf waxes. Carbon isotope ratios are well-established indicators of plant water-use efficiency, which is defined as the ratio of carbon assimilation, *A*, to the transpiration water loss of the plants, *E* (Farquhar et al., 1989; Bacon, 2004),

$$WUE = \frac{A}{E} = \frac{(1-\phi)p_a}{1.6v(b-a)}(b-\Delta^{13}C) = k'(b-\Delta^{13}C) \qquad (1)$$

where ϕ is the respired proportion of assimilated carbon; p_a is the atmospheric CO_2 pressure; v is the difference between intercellular and atmospheric water vapor pressure; the factor 1.6 is the ratio of diffusivities of water vapor and CO_2 in air; a is the

fractionation occurring due to diffusion in air and *b* is the net fractionation caused by carboxylation; $\Delta^{13}C$ is the carbon isotopic discrimination of plant material relative to ambient CO_2; $\Delta^{13}C$ is defined as $(\delta^{13}C_a - \delta^{13}C_p)/(1 + \delta^{13}C_a)$, where $\delta^{13}C_a$ and $\delta^{13}C_p$ represent the $\delta^{13}C$ values of atmospheric CO_2 and plant materials, respectively (Farquhar et al., 1989). Carbon isotope discrimination ($\Delta^{13}C$) is relevant to WUE via the extent of stomatal conductance and capacity of CO_2 fixation during photosynthesis. Smaller stomatal conductance causes smaller $\Delta^{13}C$ and larger WUE, while greater stomatal conductance causes larger $\Delta^{13}C$ and smaller WUE. WUE is a function of plant type and also depends on environmental factors such as humidity, sunlight exposure, and temperature. Here we compare carbon and hydrogen isotope ratios of tree leaf waxes to assess the relationship between tree water-use efficiency and δD_{wax}.

SAMPLES AND METHODS

35 leaf samples from 11 tree species were collected near the shoreline of Blood Pond, Massachusetts in August 2005 (Table 1). All leaf samples were growing below the forest canopy, receiving dappled sunlight throughout the day. Hydrogen isotope ratios of the leaf waxes from these trees have been reported in Hou et al. (2007). Carbon isotope analyses of individual leaf wax compounds were performed using a gas chromatography – combustion – isotope ratio mass spectrometer (Thermo Finnigan). An HP 6890 GC was connected to a Finnigan MAT Delta^{+}-XL mass spectrometer via a combustion interface. Helium was used as the carrier gas, operating at constant flow mode with a rate of 1.1 mL min^{-1}. The oven programming was 40 ^{o}C – 200 ^{o}C @ 20^{o}C/min – 315 @ 5 ^{o}C/min and hold for 20 min. Compounds separated by GC column were converted to CO_2 and H_2O through a combustion furnace operated at 940 ^{o}C and loaded with CuO and Pt wires as oxidant and catalyst, respectively. A small stream of 1% O_2 in helium was added right in front of reactor to maintain the oxidation capacity of CuO. Six pulses of CO_2 reference gas with known $\delta^{13}C$ values were injected via interface to the isotope ratio mass spectrometer for the computation of $\delta^{13}C$ values of sample compounds. Samples were analyzed in duplicate, with standard deviation smaller than ± 0.2 ‰. $\delta^{13}C$ values obtained from individual acids (as methyl esters) were corrected by mathematically removing the isotopic contributions from added groups. The $\delta^{13}C$ values are reported relative to the VPDB standard.

RESULTS AND DISCUSSION

δD and $\delta^{13}C$ variation in tree leaf waxes

δD values of three long chain *n*-acids (C_{26}, C_{28}, C_{30}) from different trees show an overall range of 60 to 70 ‰ variation (Table 1). C_{30} *n*-acids range from -190 to -120 ‰, C_{28} *n*-acids from -179 to -116 ‰, and C_{26} *n*-acids from -184 to -101 ‰. The leaf waxes from evergreen trees appear to have lower δD values than those from deciduous trees (e.g., the δD_{wax} values of the evergreen *Pinus strobus* L. (~ -180 to -190 ‰) are 20 to 50 ‰ lower than δD_{wax} values of deciduous trees [Table 1]).

$\delta^{13}C$ values of the long chain *n*-acids ($\delta^{13}C_{wax}$) range from -39.7 to -32.9‰ and show strong inter-correlation among the three *n*-acids (r = 0.85 for C_{30} and C_{28} *n*-acids, 0.79 for C_{28} and C_{26} *n*-acids, and 0.55 for C_{30} and C_{26} *n*-acids, respectively). The variation in $\delta^{13}C$ values is not a result of different biosynthetic pathways as all trees are C_3 plants. $\delta^{13}C_{wax}$ values of different leaf samples from individual trees also show some variability. However, there is no clear correlation between $\delta^{13}C_{wax}$ and the height of leaf samples in this study.

Hydrogen and carbon isotope ratios show significant negative correlation for the

three individual *n*-acids (Figure 3). The correlation coefficients between δD_{wax} and $\delta^{13}C_{wax}$ are $R^2 = 0.55$ for C_{30} *n*-acids ($n = 27$, $p<0.001$), 0.40 for C_{28} *n*-acids ($n = 31$, $p<0.001$), and 0.34 for C_{26} *n*-acids ($n = 26$, $p<0.005$), respectively.

WUE and $\delta^{13}C$ values of leaf waxes

Published data have shown that there is a strong negative correlation between $\Delta^{13}C$ and WUE in field samples. For example, Hubick et al. (1986) demonstrate such a correlation for peanuts grown under wet and dry conditions. Ismail and Hall (1992) show a strong linear relationship between WUE and $\Delta^{13}C$ for different cowpea genotypes. This relationship is also observed among different tree species. For example, higher WUE for evergreen tree species is accompanied by higher $\delta^{13}C$ values (or smaller $\Delta^{13}C$) relative to deciduous trees (Garten and Taylor, 1992). The difference in WUE and $\delta^{13}C$ values between evergreen and deciduous trees was modeled by Marshall and Zhang, 1994. Their results suggest that $\Delta^{13}C$ can be used as an estimate of WUE for plants from a given region where environmental variables (e.g., soil type, temperature, humidity) are relatively constant.

As discussed in the introduction, WUE and $\Delta^{13}C$ are negatively correlated, with $\Delta^{13}C$ is negatively correlated with $\delta^{13}C_{wax}$ values. Therefore, $\delta^{13}C_{wax}$ values show positive

correlation with WUE, i.e. higher $\delta^{13}C_{wax}$ values should correspond to higher water use efficiency in trees. For example, the $\delta^{13}C$ values of leaf waxes from *Pinus strobus* L. are higher than those from *Betula lenta* L. and *Nyssa sylvatica* Marsh, suggesting that *Pinus strobus* L. has a higher water-use efficiency than *Betula lenta* L. and *Nyssa sylvatica* Marsh. Leaf waxes of evergreen trees have been shown to have higher $\delta^{13}C$ values than deciduous trees (Chikaraishi and Naraoka, 2003; Huang et al., 2006). These data are consistent with the previous observation that evergreen species tend to have higher water-use efficiency than co-occurring deciduous species (e.g., DeLucia et al., 1988; Gower and Richards, 1990; DeLucia and Schlesinger, 1991; Garten and Taylor, 1992).

WUE and δD_{wax}

The significant negative correlation between $\delta^{13}C_{wax}$ and δD_{wax} (Figure 1) in the leaf samples of this study indicate that tree WUE is likely an important control on hydrogen isotope ratios of leaf waxes. D/H ratios of plant leaf waxes are influenced by WUE in addition to δD values of precipitation. Other factors, such as temperature, relative humidity, and photosynthetic pathways may also affect δD_{wax} (Smith and Freeman, 2006; Sachse et al., 2006). However, since all our samples were collected within 50 m of Blood Pond's shoreline, precipitation, temperature, humidity, soil, and source water should be very similar for all trees. The observed hydrogen isotopic

variation among different trees is therefore likely related to the WUE of the different trees.

In this study, trees with higher WUE (as inferred from higher $\delta^{13}C_{wax}$ values) were found to have lower δD_{wax} values. This is readily understandable. Plants with higher WUE require transpiration of less water to produce the same amount of leaf waxes as plants with lower WUE. As water evaporates from the sub-stomatal cavity, the remaining leaf water becomes enriched in deuterium (Farquhar et al., 1989). Smaller transpiration rates result in less hydrogen-isotopic enrichment of leaf water, resulting in the subsequent synthesis of leaf waxes with lower δD values. For example, δD values of C_{30} *n*-acid from *Betula lenta* L. and *Nyssa sylvatica* Marsh. are -155‰ and -133‰, respectively. The δD of C_{30} *n*-acid from *Pinus strobus* L. is around -185‰. The higher δD values indicate that *Betula* and *Nyssa* have lower WUE than *Pinus*, consistent with higher $\delta^{13}C$ values observed in *Pinus*.

Chikaraishi and Naraoka (2006) measured both δD and $\delta^{13}C$ of plant leaf waxes, but did not observe the relationship we report here. The samples used in Chikaraishi and Naraoka (2006), however, were collected from multiple sites in Japan and in Thailand. Environmental factors such as temperature, humidity, and soil type, at the different sites may affect the carbon and hydrogen isotope ratios of leaf waxes in complex ways,

thereby complicating comparisons between δD_{wax} and $\delta^{13}C_{wax}$. Contrary to our findings, Bi et al. (2005) show a positive correlation between weighted mean δD_{wax} and $\delta^{13}C_{wax}$ values for 9 tree samples from a well maintained botanic garden in China. However, the relationship is defined by one data point relative to a cluster of 8 points. Plants in the botanic garden are grown under varying degrees of artificial irrigation, fertilization and other soil treatment (e.g., adjustment of pH), which could also complicate the relationship between δD_{wax} and $\delta^{13}C_{wax}$.

CONCLUSIONS

$\delta^{13}C$ and δD values of leaf waxes from 35 leaf samples of 11 tree species from Blood Pond, MA show a statistically significant negative correlation, suggesting that water-use efficiency exerts an important control on δD values of leaf waxes in trees. Plants with higher WUE display lower δD_{wax} values. The correlation is not perfect, reflecting the fact that other independent factors also affect δD_{wax}. Nevertheless, our study represents the first step to decipher the complex mechanisms controlling the variations of leaf wax δD values in terrestrial plants.

ACKNOWLEDGEMENTS

We would like to thank Koebke Family (Koebke Farm, Dudley, MA) for access to Blood Pond. We thank Jonathan Nichols for field assistance. We are grateful to Dr. Stefan Schouten and Dr. Enno Schefuss for their constructive comments. This work was supported by grants from the National Science Foundation (NSF 0318050, 0318123, 0402383) to Y. Huang.

REFERENCES

Bacon M.A. (2004) Water-use efficiency in plant biology. In: M.A. Bacon (Ed.), Water-use efficiency in plant biology. Blackwell, pp. 1-26.

Bi X., Sheng G., Liu X., Li C. and Fu J. (2005) Molecular and carbon and hydrogen isotopic composition of *n*-alkanes in plant leaf waxes. *Organic Geochemistry* 36, 1405-1417.

Chikaraishi Y. and Naraoka H. (2003) Compound-specific δD-δ^{13}C analyses of n-alkanes extracted from terrestrial and aquatic plants. *Phytochemistry* 63, 361-371.

Chikaraishi K. and Naraoka H. (2006) δ^{13}C and δD relationships among the three n-alkyl compound classes (n-alkanoic acid, *n*-alkane and n-alkanol) of terrestrial higher plants, *Organic Geochemistry*, doi:10.1016ij.orggeochem.2006.10.003.

Collister J.W., Rieley G., Stern B., Eglinton G. and Fry B. (1994) Compound-Specific δ^{13}C Analyses of Leaf Lipids from Plants with Differing Carbon-Dioxide Metabolisms. *Organic Geochemistry* 21(6-7), 619-627.

DeLucia E.H., Schlesinger W.H. (1991) Resource-use efficiency and drought tolerance in adjacent great basin and Sierran plants. *Ecology* 72, 51-58.

DeLucia E.H., Schlesinger W.H. and Billings W.D. (1988) Water relations and the maintenance of sierran conifers on hydrothermally altered rock. Ecology 69, 303-311.

Farquhar G.D., Hubick K.T., Condon A.G. and Richards R.A. (1989) Carbon isotope fractionation and plant water-use efficiency. In: Rundel P.W., Ehleringer J.R., Nagy K.A. (Eds.), Stable isotopes in ecological research. Springer-Verlag, New York, pp. 21-40.

Garten C.T. and Taylor G.E. (1992) Foliar delta C-13 within a temperature decisuous forest – spatial, temporal, and species sources of variation. *Oecologia* 90, 1-7.

Gower S.T. and Richards J.H. (1990) Larches: deciduous conifers in an evergreen world. *BioScience* 40, 818-826.

Hou J., D'Andrea W., MacDonald D. and Huang Y. (2007) Hydrogen isotopic variability in leaf waxes among terrestrial and aquatic plants around Blood Pond, Massachusetts (USA). *Organic Geochemistry* 38, 977-984 doi:10.1016/j.orggeochem.2006.12.009.

Huang Y., Shuman B., Wang Y., Webb T., Grimm E.C. and Jacobson G.L. (2006) Climatic and environmental controls on the variation of C_3 and C_4 plant abundances in central Florida for the past 62,000 years. *Palaeogeography, Palaeoclimatology, Palaecology* 237, 428-435.

Liu W. and Huang Y. (2005) Compound specific D/H ratios and molecular distributions of higher plant leaf waxes as novel paleoenvironmental indicators in the Chinese Loess Plateau. *Organic Geochemistry* 36, 851-860.

Pagani M., Pedentchouk N., Huber M., Sluijs A., Schouten S., Brinkhuis H., Damste

J.S.S., Dickens G.R. and Scientists E. (2006) Arctic hydrology during global warming at the Palaeocene/Eocene thermal maximum. *Nature* 442, 671-675.

Sachse D., Radke J. and Gleixner G. (2006) δD values of individual n-alkanes from terrestrial plants along a climatic gradient - Implications for the sedimentary biomarker record. *Organic Geochemistry* 37, 469-483.

Saurer M., Siegwolf R.T.W. and Schweingruber F.H. (2004) Carbon isotope discrimination indicates improving water-use efficiency of trees in northern Eurasia over the last 100 years. *Global Change Biology* 10, 2109-2120.

Shuman B., Huang Y., Newby P. and Wang, Y. (2006) Compound-Specific Isotopic Analyses Track Changes in the Seasonality of Precipitation in the Northeastern United States at ca. 8200 cal yr BP. *Quaternary Science Reviews* 25, 2992-3002.

Smith F.A. and Freeman K.H. (2006) Influence of physiology and climate on δD of leaf wax n-alkanes from C_3 and C_4 grasses. *Geochimica et Cosmochimica Acta* 70, 1172-1187.

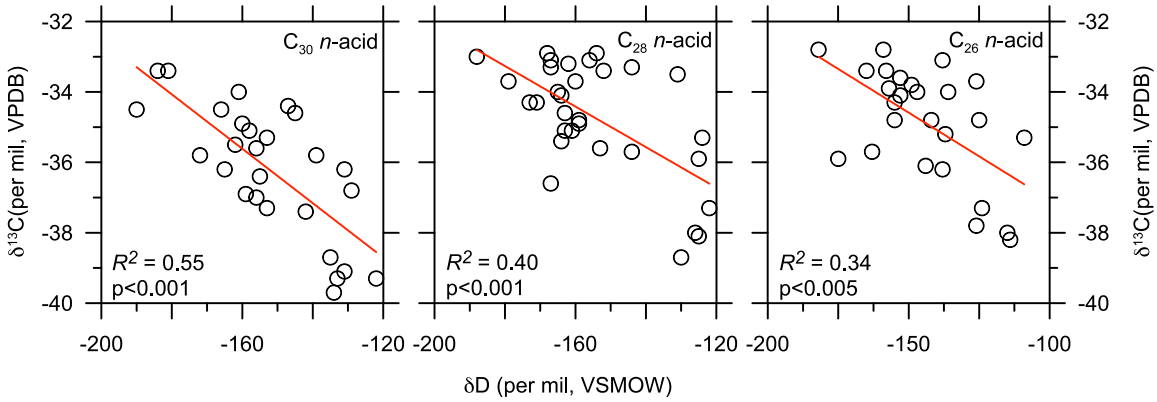

Figure 3. Correlations between $\delta^{13}C$ and δD values of leaf wax compounds (C_{30}, C_{28}, and C_{26} *n*-acids) from natural trees around Blood Pond, Massachusetts.

Table 1. $\delta^{13}C$ and δD of leaf wax compounds (*n*-acids) from trees around Blood Pond, Massachusetts

Scientific Name	Height (m)	δD* (‰, VSMOW)			$\delta^{13}C$ (‰, VPDB)		
		C_{26}	C_{28}	C_{30}	C_{26}	C_{28}	C_{30}
Betula populifolia Marsh. (1)	6	-153	-159	-131	-33.6	-34.9	-36.2
Betula populifolia Marsh. (1)	4.5	-155	-163	-142	-34.3	-35.1	-37.4
Betula populifolia Marsh. (1)	3	-163	-167	-151	-35.7	-36.6	
Betula populifolia Marsh. (2)	6	-147	-161	-135	-34.0	-35.1	-38.7
Betula populifolia Marsh. (2)	4.5	-125	-144	-122	-34.8	-35.7	-39.3
Betula lenta L. (1)	6	-144	-163	-155	-36.1	-34.6	-36.4
Betula lenta L. (1)	4.5	-137	-160	-156	-35.2	-33.7	-35.6
Betula lenta L. (1)	3	-138	-164	-153	-36.2	-35.4	-37.3
Betula lenta L. (2)	6	-149	-167	-158	-33.8	-33.1	-35.1
Betula lenta L. (2)	4.5				-34.2	-33.7	-34.4
Betula lenta L. (2)	3	-165	-167	-153	-33.4	-33.3	-35.3
Quercus velutina Lam.	3	-130	-152	-147			
Quercus rubra L. (1)	6	-157	-164	-161	-33.9	-34.1	-34.0
Quercus rubra L. (1)	4.5	-153	-165	-166	-34.1	-34.0	-34.5
Acer rubrum L. (1)	3	-136	-159	-159	-34.0	-34.8	-36.9
Acer rubrum L. (2)	3	-148	-168	-162		-32.9	-35.5
Acer rubrum L. (3)	6	-158	-173	-172	-33.4	-34.3	-35.8
Acer rubrum L. (3)	4.5	-142	-171	-165	-34.8	-34.3	-36.2
Carya sp. Nutt. (1)	6	-158	-162	-160		-33.2	-34.9
Carya sp. Nutt. (1)	4.5	-144	-152	-147		-33.4	-34.4
Carya sp. Nutt. (1)	3	-138	-144	-145	-33.1	-33.3	-34.6
Carya sp. Nutt. (2)	3	-175	-179	-182			
Pinus strobus L. (1)	6	-184	-188	-181		-33.0	-33.4
Pinus strobus L. (1)	4.5	-175	-154	-184	-35.9	-32.9	-33.4
Pinus strobus L. (1)	3	-182	-179	-190	-32.8	-33.7	-34.5
Prunus serotina Ehrh. (1)	6				-34.4	-35.2	-36.8
Prunus serotina Ehrh. (1)	4.5	-155	-153	-156	-34.8	-35.6	-37.0
Fraxinus americana L. (1)	6	-109	-124	-121	-35.3	-35.3	
Fraxinus americana L. (1)	4.5	-101	-122	-129		-37.3	-36.8
Fraxinus americana L. (1)	3	-115	-125	-139	-38.0	-35.9	-35.8
Tsuga canadensis L. (1)	4.5	-159	-156	-158	-32.8	-33.1	

Tsuga canadensis L. (1)	3	-126	-131	-142	-33.7	-33.5	
Nyssa sylvatica Marsh. (1)	6	-124	-126	-133	-37.3	-38.0	-39.3
Nyssa sylvatica Marsh. (1)	4.5	-126	-130	-134	-37.8	-38.7	-39.7
Nyssa sylvatica Marsh. (1)	3	-114	-125	-131	-38.2	-38.1	-39.1

*δD data first published in Hou *et al*. (2007)

Table 2. The correlation coefficients between δD values of individual leaf waxes

Compounds	C_{26} *n*-acid	C_{28} *n*-acid	C_{30} *n*-acid	C_{27} *n*-alkane	C_{29} *n*-alkane	C_{31} *n*-alkane
C_{26} *n*-acid	1					
C_{28} *n*-acid	0.91	1				
C_{30} *n*-acid	0.85	0.86	1			
C_{27} *n*-alkane	0.54	0.66	0.43	1		
C_{29} *n*-alkane	0.63	0.60	0.64	0.61	1	
C_{31} *n*-alkane	0.64	0.67	0.64	0.60	0.87	1

CHAPTER 3

Can Sedimentary Leaf Waxes record D/H ratios of Continental Precipitation? Field, Model, and Experimental Assessments

Co-authors: William D'Andrea, Yongsong Huang

Published in ***Geochimica et Cosmochimica Acta***, 2008, v. 72, p. 3503-3517

doi:10.1016/j.gca.2008.04.030

ABSTRACT

D/H ratios of leaf waxes (δD_{wax}) derived from terrestrial plants and preserved in lake sediments can provide important information on past continental hydrology. Ideally, δD_{wax} can be used to reconstruct precipitation D/H ratios (δD_P) which is a well-established paleoclimate proxy. However, many other factors, such as vegetation and relative humidity (RH), also affect δD_{wax} variation. How the combination of these factors affects sedimentary δD_{wax} is unclear. Here, we use a transect of 32 lake surface sediments across large gradients of precipitation, relative humidity, and vegetation in the southwestern United States to study the natural factors affecting sedimentary δD_{wax}. δD values of C_{28} *n*-alkanoic acids show significant correlation with δD_P values ($R^2 = 0.76$) with an apparent isotopic enrichment of ~ 99 ± 8 ‰, indicating that sedimentary δD_{wax} values track overall δD_P variation along the entire transect. Leaf waxes produced by plants grown under controlled conditions (RH = 80, 60, 40%) show a small increase in D/H ratios as RH decreases, consistent with prediction from the Craig-Gordon model. However, the isotopic effect of RH on δD_{wax} along the entire transect is partially countered by the opposing influence of vegetation changes. The correlation between δD_{wax} and δD_P values is significantly higher ($R^2 = 0.84$) in the drier portions of the transect than in the wetter regions ($R^2 = 0.64$). This study suggests that D/H ratios of sedimentary

leaf waxes can be used as a proxy for precipitation δD variations, with particularly high fidelity in dry regions, although more studies in other regions will be important to further test this proxy.

INTRODUCTION

Hydrogen and oxygen isotope ratios (D/H and $^{18}O/^{16}O$) of precipitation are among the most effective and quantitative proxies for past continental climate variability. Ice cores (e.g., Grootes et al., 1993; Petit et al., 1999) and speleothems (e.g., Wang et al., 2001; Yuan et al., 2004) are the most common archives for reconstructing precipitation isotopic ratios. While the fidelity of such reconstructions is exceptional, the global distribution of ice cores and speleothems is very limited; speleothems to regions with carbonate bedrock and adequate precipitation; and ice cores to polar and/or high altitude locations. Continental climate is characterized by large regional variability, requiring records from widely distributed sites to assess the underlying mechanisms of variation. The wide geographic distribution of lakes provides excellent opportunities to reconstruct the isotope ratios of past continental precipitation from sediment cores.

D/H ratios of aquatic lipids in lake sediments have been shown to track D/H ratios of lake water and precipitation in regions with high precipitation/evaporation (P/E) ratios (Sauer et al., 2001; Huang et al., 2002, 2004; Hou et al., 2006). However, in dry and warm regions, D/H ratios of lake water are strongly affected by evaporation, complicating climatic interpretation of δD records. Temporal variability in D/H ratios of leaf waxes (δD_{wax}) derived from terrestrial plants and preserved in sediments has been

attributed to past precipitation and hydrological changes (Liu and Huang, 2005; Schefuβ et al., 2005; Pagani et al., 2006; Shuman et al., 2006; Huang et al., 2007). However, in addition to δD of precipitation (δD_P), other factors, such as relative humidity (RH) and vegetation composition, may also affect sedimentary δD_{wax}. Without a full evaluation of these factors, the reliability and limitations of leaf wax δD as a paleohydrological proxy remains uncertain.

Sachse *et al*. (2004) showed that leaf wax D/H ratios (δD_{wax}) from lake surface sediments track δD_P variation along a 13-lake transect in Europe. However, the European sites used in the study have nearly constant relative humidity (RH = 75-85 %), and relatively invariable, forest-dominated vegetation, and therefore cannot be used to assess whether δD_{wax} tracks δD_P across relative humidity gradients and/or different biomes. While we know that RH has a significant effect on the hydrogen isotopic fractionation of water (Gonfiantini, 1986; Gat, 1996), the effect of RH on the δD values of leaf waxes has not been studied directly. Previous studies reported that the D/H ratios of cellulose increase dramatically as RH decreases (Yapp and Epstein, 1982; Edwards and Fritz, 1986), but other studies (Gray and Song, 1984; Ramesh et al., 1986; White et al., 1994; Terwilliger and DeNiro, 1995) contradict the claim. Most published studies (e.g., Sauer et al., 2001; Liu and Huang, 2005; Sachse et al. 2006; Pagani et al., 2006) have assumed that δD_{wax} values are also affected by RH in addition to hydrological factors. Furthermore,

recent studies have shown that hydrogen isotope enrichment between precipitation and leaf waxes ($\varepsilon_{wax\text{-}p}$) differs greatly among different types of higher plants (Liu and Huang, 2005; Liu et; 2006; Hou et al., 2007a; Liu and Huang, 2008), with grasses displaying ~40-50‰ lower δD values than trees. Therefore, in order to confidently reconstruct the variability of precipitation δD using leaf waxes, we must determine how RH and vegetation changes affect the relationship between δD_{wax} and δD_P values.

In this study, we aim to evaluate the degree to which δD_{wax} values in lake sediments reflect δD_P variation across large, natural environmental gradients of RH, precipitation and vegetation types. If it is to be used as a proxy for reconstructing past changes in δD_P, δD_{wax} must first be shown to track modern precipitation δD values across sites with highly variable RH and vegetation composition. To achieve this goal, we examined lake surface sediments from a 32-lake transect across large gradients in precipitation, RH, and vegetation cover (from Phoenix, AZ to Houston, TX). We also grew plants under controlled conditions to accurately assess the effects of RH and modeled the isotopic effects under both experimental and field conditions. Our integrated field, experimental, and modeling approaches allow us to objectively assess the fidelity of leaf wax δD values as a proxy for δD variation of past continental precipitation.

SAMPLES AND METHODS

The southwestern transect

Surface sediment and lake water samples were collected from 32 lakes spanning large precipitation and relative humidity gradients (extending from Phoenix, Arizona to Houston, Texas) in May 2004 (Figure 1; Table 1). For the purpose of this study (and based on our isotope data described below), the sampling sites along the transect are divided into two general groups according to their geographic setting and mean annual precipitation: 1) the Interior Plains (Texas and northeastern New Mexico, referred to hereafter as "the Plains"), eastward of 104.5 ^{o}W, with precipitation >400 mm, and 2) Southern Rocky Mountains and Basin and Range (Arizona and part of New Mexico, hereafter referred to as "Basin and Range") westward of 104.5 ^{o}W, with precipitation <400 mm. The lakes from the Plains are mostly naturally occurring, whereas the sampling sites from the Basin and Range represent reservoirs constructed by damming rivers and streams sourced from adjacent higher elevations.

There is a large mean annual precipitation gradient (120 to 1150 mm) and mean annual relative humidity gradient (36 to 82 %) along the transect from Phoenix to Houston (Figure 1A, 1B). Vegetation composition changes dramatically along the

transect, from shrubland to grassland to savanna to subtropical forest (Figure 1C). Mean annual temperature along the transect, excluding the highest elevation sites, ranges from 12 to 21^{o}C (Table 1). Three of the lakes (Upper Glacial Lake, Lake #1 and Mary's Lake) are at much higher elevation and have lower mean annual temperature (Table 1) than the rest.

Surface sediments (0-2 cm below the sediment-water interface) were collected from the deepest part of each lake (in reservoirs, deepest sites are typically near the dam site, far from river inlets) using an Ekman Dredge, and were kept cold and in the dark until being frozen at Brown University. Duplicate lake water samples for isotopic analysis were collected using 4 ml glass vials. The vials were filled to capacity and sealed to prevent evaporation.

Growth chamber experiments

We grew 15 trees (representing 6 species) and 11 grasses (representing 4 species) in an EGC® GC series temperature and humidity-controlled growth chamber. *Fraxinus americana* L. (white ash), *Carya glabra* (pignut hickory), *Acer rubrum* L. (red maple) and *Quercus rubra* L. (red oak) were collected from the watershed of Blood Pond, Massachusetts. Two coniferous tree species, *Thuja Occidentalis* (eastern white cedar) and

Picea Glauca (alberta spruce) were obtained from a local nursery. Tree seedlings were 30-50 cm in height before transplantation. The trees were transplanted into 8-inch pots using Canadian Growing Mix 2 (Fafard®). Grass seeds, including *Zea Mays* L. (corn), *Dactylis glomerata* L. (orchard grass), *Alopecurus spp*. (foxtail) and *Phleum pratense* L. (timothy weed), were obtained from a local grass seed distributor. The trees were kept in the greenhouse for 20 days and were irrigated with water of known isotopic composition twice daily before being moved into the growth chamber. The grasses were germinated and cultured in the greenhouse for 20 days before being moved to the growth chamber.

The temperature in the growth chamber was kept at 20 ^{o}C. RH was set to 80% during the first growing period (Jun 26 - Jul 27, 2006), 60% for the second growing period (Jul 28 - Sep 4, 2006), and 40% for the third growing period (Sep 5 - Oct 11, 2006). A dehumidifier was placed in the growth chamber for experiments with 60 % and 40 % RH settings, in order to assist the system to maintain stable RH levels. On the last day of each growing period, newly grown leaves from trees were collected for δD_{wax} analysis. There was no new leaf growth on the *Carya glabra* specimen during the experiment, so we collected preexisting leaves from *Carya glabra* on the last day of each growing period. For grass specimens, we collected whole leaves on the last day of each growing period. All plants were irrigated with 500 ml of water of known hydrogen isotopic ratio (δD = -49 ‰) every two days. The irrigation water was stored in Reliance

Fold-A-Carrier® collapsible containers at 4^{o}C prior to the experiment to ensure the isotope ratios remained constant.

Analyses of water δD values

D/H ratios of lake water samples and irrigation water were measured using Thermal Conversion/Elemental Analyzer-Isotopic Ratio monitoring Mass Spectrometry (TC/EA-IRMS). Nine 0.2 μl aliquots of each water sample were manually injected into the TC/EA. Standard Mean Ocean Water (SMOW, δD = 0 ‰), Greenland Ice Sheet Precipitation (GISP, δD = -190‰) and Standard Light Antarctic Precipitation (SLAP, δD = -428 ‰) were measured between every 10 sample analyses for isotope calibration (Huang et al., 2002). A regression line (R^2 = 1) was established between measured and actual δD values of the three isotope standards, and was used for instrument calibration. The standard deviation for water δD values was < ±1.5‰.

Analyses of sediment and plant samples

All sediment and leaf samples were freeze-dried. Sediment samples were extracted using an Accelerated Solvent Extractor (ASE200, Dionex) with dichloromethane:methanol (2:1 v/v) at 150^{o}C and 1200 psi for three 15-min cycles.

Approximately 5 g of each dry sample were extracted. Leaves were soaked in dichloromethane:methanol (2:1 v/v) and ultrasonicated for 15 minutes to extract lipids. This extraction procedure was repeated three times. The total lipid extract obtained from sediment and plant leaves was separated into neutral and acid fractions using Supelco® Supelclean™ LC-NH_2 SPE column and dichloromethane:isopropyl alcohol (2:1 v/v) and ether with 4% acetic acid (v/v), respectively, as eluents. Acid fractions were methylated with 5% anhydrous HCl in methanol at 60 ^{o}C for 12 hours. Hydroxyl acids were removed by eluting the methylated samples through silica gel columns with hexane, and the fatty acid methyl esters were collected by elution with dichloromethane.

Quantification and identification of compounds was performed by Gas Chromatography - Flame Ionization Detection (GC-FID) and Gas Chromatography-Mass Spectrometry (GC-MS) (HP 6890, Agilent). An HP 6890 GC interfaced to a Finnigan DeltaPlus XL stable isotope spectrometer through a high-temperature pyrolysis reactor was used for hydrogen isotopic analysis (Huang et al., 2004). The compounds separated by the GC were pyrolyzed to H_2 and CO at 1445^{o}C. A tank of ultra high purity hydrogen gas with known δD values was used as the isotope standard during the measurements. The H_3^+ factor was determined daily prior to sample analysis (average value was 2.5 ± 0.04 (1 sigma) during the course of this study). The accuracy for the instrument was routinely checked by an injection of laboratory isotopic standards (C_{16}, C_{18}, C_{22}, C_{24}

n-alkanoic acid methyl esters) between every six measurements. The precision (1σ) for the four laboratory standards were < ±2‰ throughout the entire process. The precision (1σ) for triplicate analyses of all samples was < ±2‰. δD values obtained from individual alkanoic acids (as methyl esters) were corrected by mathematically removing the isotopic contributions from added groups before reporting. The δD value of the added methyl group was determined by acidifying and then methylating (along with the samples) the disodium salt of succinic acid with a predetermined δD value (using TC/EA-IRMS) (Huang et al., 2002).

RESULTS

Precipitation and lake water δD

The D/H ratio of precipitation (δD_p, weighted average values based on monthly precipitation amount) at the location of each lake along the SW transect was calculated from the Online Isotopes in Precipitation Calculator (OIPC, Bowen and Revenaugh, 2003). The OIPC estimates the δD_P at a given site by combining an empirical model for isotopic trends related to latitude and altitude with detrended interpolation based on the isotope data from stations in Global Network of Isotopes in Precipitation (Bowen and Revenaugh, 2003). δD_P and lake water δD values (δD_{lake}) show similar variation along the transect (Figure 2; Table 1). Higher δD_P and δD_{lake} values occur in the eastern Plains and western Basin and Range. Lower δD_P and δD_{lake} values are found in the central part of the transect (Southern Rocky Mountains). Lake water samples from the Plains show greater deuterium enrichment relative to precipitation than the lakes from Basin and Range, which have δD_{lake} values that are very similar to that of precipitation (Figure 2).

δD of sedimentary leaf waxes

We focus on C_{26}, C_{28}, and C_{30} *n*-alkanoic acids, in the lake surface sediment

samples as representative compounds for modern leaf waxes. We avoided use of long chain *n*-alkanes as terrestrial plant biomarkers to minimize the possibility of contamination from fossil fuel products (most lakes in the region are heavily used by recreational boaters and likely receive atmospheric input of combustion products). The hydrogen isotope ratios of the C_{26}, C_{28}, and C_{30} *n*-alkanoic acids are strongly inter-correlated ($R^2 = 1.0$ for C_{28} and C_{30}, $R^2 = 0.82$ for C_{28} and C_{26}; $n = 32$, $p<0.001$). Therefore, in the following discussion δD values of C_{28} *n*-alkanoic acid (hereafter referred to as δD_{wax}) are taken as representative of integrated δD values of terrestrial leaf waxes from plants around the lakes.

Sedimentary δD_{wax} values show significant correlation with δD_P values along the entire transect ($R^2 = 0.76$, $y = 0.93x - 99.1$, $n = 32$, $p<0.001$, residual mean squares (RMS) = 122.3; Figure 2, Figure 3A). However, δD_{wax} and δD_p correlate much more strongly within the Basin and Range ($R^2 = 0.84$, $y = 1.69x - 42$, n = 18, $p<0.001$, RMS = 70.2) than they do for the entire transect ($R^2 = 0.76$) or the Great Plains lakes ($R^2 = 0.64$, $y = 0.67x - 109.7$, $n = 14$, $p<0.001$, RMS = 60.6; Figure 3B). Furthermore, a second-order polynomial regression through the entire transect provides an overall better fit for the δD_{wax} and δD_P data ($R^2 = 0.86$, $y = -0.02x^2 - 1.06x - 147.4$, $n = 32$, $p<0.001$, RMS = 73.0, Figure 3A) than does the linear regression. The correlation between δD_{wax} and δD_{lake} ($R^2 = 0.46$, $n = 32$, $p <0.001$, RMS = 280.3) is not as strong as that between δD_{wax} and δD_P.

Leaf wax δD for plants from growth chamber

δD values of C_{28} *n*-alkanoic acids are strongly correlated with C_{30} *n*-alkanoic acids for the growth chamber samples ($R^2 = 0.86$). As with the transect samples, δD values of C_{26} *n*-alkanoic acids show weaker correlation with C_{28} and C_{30} *n*-acids ($R^2 = 0.61$ and 0.44, respectively). This observation suggests that C_{28} or C_{30} *n*-alkanoic acids may be better choices for representative leaf wax compounds in sediment samples. It should also be noted that for certain growth chamber species, δD values of the three *n*-alkanoic acids show relatively large variation within and among specimens (Table 2), highlighting the natural variability of individual plants. The calculated leaf wax hydrogen isotopic enrichment from source water ($\varepsilon_{wax\text{-}water}$) for the growth chamber samples show an approximately normal distribution (Figure 4). The average $\varepsilon_{wax\text{-}water}$ values of all plants grown at 80%, 60% and 40% RH are -114 ‰, -111.5 ‰, and -107 ‰, respectively, depicting minor deuterium enrichment as RH decreases.

DISCUSSION

Controls on δD of precipitation and lake water

The patterns of δD_P variation along the transect in the southwestern United States result from differing water vapor sources and the continental isotope effect (Gat, 1996). The water vapor for precipitation in the Texas Plains mainly originates from the Gulf of Mexico, while the precipitation in the Basin and Range mainly derives from the eastern Pacific Ocean, off coastal Mexico (Figure 1A; Adams and Comrie, 1997). Due to Rayleigh distillation, as water vapor moves inland the heavier isotopes are preferentially precipitated, resulting in isotopically lighter precipitation with increasing distance from the source. This helps explain the observation that higher δD_P values are found at either end of the transect, and lower δD_P values are found in the central portion of the transect. The lowest δD_P values are found at Mary's Lake, ~ 105 ^{o}W (Figure 2). This site is the farthest from both vapor sources among all sites and at high elevation (2155 m) (Table 1).

The δD_{lake} values along the transect are controlled not only by δD_P, but also by the degree of evaporation and local hydrological conditions. Evaporation causes lake water to become isotopically enriched in D and ^{18}O, relative to precipitation (Gat, 1996). The evaporative effect explains the observation that δD_{lake} values are higher than δD_P values

within the Great Plains. However, the lake waters from the Basin and Range do not show isotopic enrichment with respect to precipitation (δD values of lakes fall within 95% confidence intervals of estimated δD values for local precipitation; Figure 2). This could be due to the fact that all Basin and Range lakes in this study are reservoirs, representing dammed rivers that originate in adjacent mountains (Table 1). The rivers are fed by precipitation within their catchments, including melt water from wintertime precipitation (e.g., snow) in the mountains. The water delivered to the reservoirs by river input is thus depleted in deuterium relative to precipitation falling directly onto the reservoirs (i.e., our estimated δD_P). Subsequent evaporative enrichment in the reservoirs might counter the influence of lower δD values of the winter snow precipitation, and help explain the similarity between δD_{lake} and the estimated δD_P in the Basin and Range (Figure 2).

As a further test of our explanation for lake water δD variations described above, we used the Craig-Gordon model to calculate the isotope ratios of lake water at steady state (Craig and Gordon, 1965; Gat, 1996), by assuming that all lake waters had the initial δD values of the precipitation prior to evaporative enrichment.

$$P = Q + E \qquad (1)$$

$$P\delta_P = Q\delta_Q + E\delta_E = Q\delta_L + E\delta_E \qquad (2)$$

where P, Q and E represent the amount of precipitation, outflow, and evaporation, respectively, and δ_P, δ_Q, and δ_E are their associated hydrogen isotope ratios. δ_L is the D/H ratio of lake water (note $\delta_L = \delta_Q$). We adopted the modified Craig-Gordon model described by Gibson and Edwards (2002),

$$\delta_E = \frac{\alpha^*\delta_L - RH \times \delta_A - (\varepsilon^* + \varepsilon_K)}{1 - RH + 10^{-3}\varepsilon_K} \qquad (3)$$

Where ε* is the equilibrium isotopic enrichment factor [$\varepsilon^* = 1158.8(T^3/10^9) - 1620.1(T^2/10^6) + 794.84(T/10^3) - 161.04 + 2.9992(10^9/T^3)$, T is temperature (K) (Gibson and Edwards, 2002)]. α* is the equilibrium isotopic fractionation factor, $\alpha^* = (1 + 10^{-3}\varepsilon^*)$. ε_K is the kinetic isotopic enrichment factor [$\varepsilon_K = 12.5 \times (1\text{-RH})$]. δ_A is the D/H ratio of atmospheric water vapor, estimated assuming equilibrium with flux-weighted precipitation ($\delta_A = \alpha^*\delta_P - \varepsilon^*$; Gibson and Edwards, 2002). RH is relative humidity, obtained from the NOAA Climate Diagnostic Center (http://www.cdc.noaa.gov/) for individual study sites. Mean annual precipitation and pan evaporation data are from the State Climatological Summaries (http://nndc.noaa.govgetsiteref) for each site (Table 1). Pan evaporation data for lakes in Texas were also obtained from Texas

Evaporation/Precipitation website (http://hyper20.twdb.state.tx.us/Evaporation/evap.html), and evaporation from lake surfaces has been estimated as 70% of that measured from evaporation pan (e.g., Gonfiantini, 1986; Gibson and Edwards, 1996; Gibson et al., 1998; Smith and Freeman, 2006).

Rearranging Eqs. (1), (2) and (3) yields

$$\delta_L = \left(\frac{P}{E}\delta_P + \frac{RH \times \delta_A + \varepsilon^* + \varepsilon_K}{A^*} \right) \Big/ \left(\frac{\alpha^*}{A^*} + \frac{P}{E} - 1 \right) \quad (4)$$

where, $A^* = 1 - RH + 10^{-3}\varepsilon_K$. We can obtain modeled D/H ratios of lake water ($\delta D_{model} = \delta_L$) from Eq.4. δD_{model} for all the lakes along the SW transect are plotted in Figure 2. For lakes in the Plains, the δD_{model} values are similar to the measured δD_{lake} values, consistent with our explanation that these lakes are largely recharged by local precipitation. However, for most lakes/reservoirs in Basin and Range, the δD_{model} values are markedly higher than the measured δD_{lake} values. The data are again consistent with our explanation that the Basin and Range reservoirs are mainly recharged by rivers rather than by local precipitation. The δD values of river water (sourced at colder temperatures and higher elevations than the reservoirs they recharge) are expected to be lower than the estimated

local δD_P, resulting in the correspondingly lower δD values for the observed lake waters than the modeled lake waters (the local δD_P is used to represent the initial or un-evaporated lake water in the model calculation) (Figure 2).

Sedimentary δD_{wax} as a proxy for δD_P: insights from the natural transect

Sedimentary δD_{wax} values are strongly correlated ($R^2 = 0.76$) with mean annual δD_P values along the entire transect (Figure 3A). Similar correlation ($R^2 = 0.77$) is observed between δD_{wax} values and mean summer (April-October) δD_P values calculated from OIPC. Water is the ultimate source for hydrogen in plant tissues, and organic matter derived from terrestrial plants should record the isotopic ratio of soil water, which is ultimately recharged by precipitation. The δD values of sedimentary leaf waxes could thus be expected to correlate with δD_P at a large scale. However, there are a number of other factors that could significantly impact the relative strength of this correlation. Two prominent factors are: 1) changes in evaporative isotopic enrichment at different RH due to evaporation from soil and leaf surfaces, and 2) variations in the apparent hydrogen fractionation among different vegetation types. Both factors could potentially impact δD_{wax} so strongly that reconstruction of δD_P from δD_{wax} would become too complicated and inaccurate for paleoclimate applications.

Surprisingly, however, even with the dramatic changes in RH and vegetation type along the lake surface sediment transect, the average apparent isotopic enrichments between local precipitation and sedimentary leaf waxes ($\varepsilon_{wax\text{-}p}$) do not differ significantly over the entire transect (-98.8 ± 7.8 ‰, Figure 5). This finding would suggest that the combined impact of environmental factors (e.g. vegetation cover, RH) is relatively small. Moreover, the stronger correlation between δD_{wax} and δD_P in dry regions ($R^2 = 0.84$) relative to the entire transect or the more humid regions (Figure 3B) may imply that δD_{wax} tracks δD_P variation with greater fidelity in dry regions. We will provide a detailed interpretation for this observation in Sections 4.3 and 4.4 after presenting data from growth chamber and model calculations.

Three lakes of the transect (Animas Ditch (AD), Upper Glacial Lake (UGL), and Santa Rosa Lake (SRL)) stand out as having significantly different $\varepsilon_{wax\text{-}p}$ (Figure 5). These exceptions can be understood in the context of their local geographical and hydrological settings. Animas Ditch is located adjacent to a major highway, within an extensive playa (dry lake bed). δD values measured for Animas Ditch (δD_{lake} = 4 ‰), a small remnant pond, are much higher than other lakes in Arizona (δD_{lake} ~ -40 to 110 ‰), indicating the influence of very strong evaporation. Therefore, exceptionally strong evaporation of soil water at Animas Ditch could explain the reduced $\varepsilon_{wax\text{-}p}$. Upper Glacial Lake receives water from nearby glaciers, and both precipitation and lake water show low

δD values (-96 and -94 ‰, respectively). Glacial melt water and snowmelt in the catchment of this high-elevation lake may represent a large proportion of the soil water recharge. Plants utilizing this soil water would produce leaf waxes with correspondingly low δD values. Santa Rosa Lake is a recently constructed man-made reservoir, completed in 1981. Disturbance associated with construction activities may complicate the δD_{wax} signal of surface sediment. Reservoirs are dammed rivers. It is therefore possible that a small fraction of the leaf waxes in sediments might have been contributed from fluvial input. However, we collected all of our sediment samples from the deepest part of the reservoirs (dammed side), minimizing the fluvial components. Therefore, the leaf waxes extracted from the lake sediments in this study should reflect primarily the local vegetation inputs.

The effect of RH on $\varepsilon_{wax\text{-}p}$

- *RH and $\varepsilon_{wax\text{-}p}$ variation along the transect*

The apparent isotopic enrichment between local precipitation and sedimentary leaf waxes ($\varepsilon_{wax\text{-}p}$) is plotted against RH in Figure 5A. There appears to be a small decrease in absolute $\varepsilon_{wax\text{-}p}$ values as RH decreases, although the correlation between RH and $\varepsilon_{wax\text{-}p}$ is relatively weak ($R^2 = 0.28$). To better understand whether soil evaporation or plant

transpiration causes the RH effect on $\varepsilon_{wax\text{-}p}$, we estimated the D/H ratios of soil water (δD_{soil}) at all sites using the modified Craig-Gordon model. We then took the fraction of evaporative water into consideration and adopted a binary isotope model (Smith and Freeman, 2006):

$$\delta D_{soil} = (1\text{-}f_e) \times \delta D_P + f_e \times \delta D_{model} \quad (5)$$

where δD_{model} (the modeled δD ratios of soil water subjected to evaporation) is calculated from Eq.4; f_e is the fraction of soil water subjected to evaporation in bulk soil water. Because accurate measurements for f_e are not available for all sites along the SW transect, f_e was set to 20 % according to Smith and Freeman (2006) who modeled soil evaporation over a similar relative humidity range. The estimated $\varepsilon_{wax\text{-}soil}$ shows no correlation to RH ($R^2 = 0.00$, Figure 5B). However, because the assumption of constant f_e along the SW transect might be too simplistic (f_e could be relatively higher in dry regions, such as in Basin and Range, than in wet regions, such as the Plains), we also modeled the soil water under the condition that f_e increases linearly from 15-25% for our sites from east to west along the transect. The new model results (shown in Figure 5C) still show no significant correlation between RH and $\varepsilon_{wax\text{-}soil}$ ($R^2 = 0.07$), suggesting that the small effect of RH on $\varepsilon_{wax\text{-}p}$ in our transect samples may be primarily due to soil evaporation rather than plant transpiration.

- *RH and $\varepsilon_{wax\text{-}p}$: growth chamber experiments*

Natural samples are inevitably influenced by many complicated environmental factors that may affect δD_{wax}, and varying levels of inaccuracy exist in estimates of precipitation δD. To examine the effect of RH on δD_{wax} while minimizing the complications inherent to natural systems, we conducted controlled plant growth experiments. The plants selected for the growth chamber experiments include broad leaf trees, conifers, C_3 grasses and C_4 grasses, and represent the typical plant types found in the catchments of lakes in the southwestern United States. The results of the growth experiments indicate that the effect of RH on the apparent hydrogen isotopic enrichment between irrigation water and leaf waxes ($\varepsilon_{wax\text{-}water}$) is very small (Figure 4). The average $\varepsilon_{wax\text{-}water}$ values for plants grown at 80, 60 and 40% RH are -114 ± 14, -111.5 ± 17, and -107 ± 15 ‰, respectively. Therefore, the $\varepsilon_{wax\text{-}water}$ values only increase by ~7 ‰ over a 40 % change in RH.

In order to quantify and to better understand the minor effect of RH on isotopic fractionation between plant leaf waxes and water, we modeled plant leaf water D/H ratios at different humidity levels using the modified Craig-Gordon model of Flanagan *et al*. (1991) and Roden *et al*. (2000), which considers the leaf boundary layer and diffusion

through stomata (equation 6). We also applied the same isotopic model to simulated plants around the lakes along the SW transect, to examine the RH effect on the isotopic composition of leaf waxes in the lake surface sediment.

$$R_{leaf} = \alpha * \left[\alpha_K R_{soil} \left(\frac{e_i - e_s}{e_i}\right) + \alpha_{KB} R_{soil} \left(\frac{e_s - e_a}{e_i}\right) + R_a \left(\frac{e_a}{e_i}\right) \right] \quad (6)$$

where R_{leaf}, R_{soil}, R_a refer to the D/H ratios of leaf water subject to evaporation, soil water, atmospheric water vapor, respectively. α^* is the equilibrium fractionation factor; α_K is kinetic fractionation associated with diffusion in air, and α_{KB} is the kinetic fractionation associated with diffusion through the boundary layer ($\alpha_{KB} = (\alpha_K)^{2/3}$; Roden et al., 2000). e_i, e_s, and e_a represent the vapor pressures of intercellular air spaces in the leaf, leaf surface, and the atmosphere, respectively. These vapor pressures were estimated using stomatal conductance and transpiration rate (Ball, 1987; Roden et al., 2000). Eq. 6 estimates the leaf water δD values at the site of evaporation. Because not all of the water within the leaf is subjected to evaporation, a correction is needed for bulk leaf water isotopic ratios (δ_{bulk}).

$$\delta_{bulk} = \delta_{leaf} f_l + \delta_{soil} (1 - f_l) \quad (7)$$

where f_l is the proportion of the leaf water subjected to evaporative enrichment and ranges from 13 - 33 % (Flanagan et al., 1991); because the accurate measurements of f_l are not available, f_l is set at 15 % for all sites in this study in order to provide the most conservative estimate.

The model results for growth chamber plants and field plants are plotted in Figure 6A and 6B, respectively. To facilitate comparison between the RH effect on the D/H ratios of soil water and leaf water, the precipitation for plants from the field is set to -49 ‰, the same as the irrigation water used in the growth chamber experiments. To be consistent with the plants in the growth chamber, the temperature in the field model was set to 20 ^{o}C. However, there are differences between the growth chamber model and the field model. δD_{soil} in the growth chamber experiments approximately equals δD of irrigation water because the plants were irrigated every two days, minimizing evaporative effects (note plant transpiration does not fractionate D/H ratios of the remaining water inside the growth chamber). Therefore, the RH effect on soil water in the growth chamber experiment is negligible. However, when modeling field conditions, soil evaporation must be considered. δD of soil water is estimated using Eq.4, where f_e is set to 20% according to Smith and Freeman (2006) and as discussed in Section 4.3.1. In other words, the field model takes into consideration both soil evaporation and plant transpiration, whereas the growth chamber model considers only plant transpiration. The modeled

$\delta D_{leaf\ water}$ value is -46 ‰ at RH = 80 %, $\delta D_{leaf\ water}$ = -43 ‰ at RH = 60 % and $\delta D_{leaf\ water}$ = -40 ‰ at RH = 40 % for the growth chamber plants. This 6‰ modeled increase in $\delta D_{leaf\ water}$ as RH decreases from 80-40% agrees well with the observed increases in δD_{wax} of 5.7‰ as RH in the growth chambers was lowered from 80-40% (Figure 4). The effect of RH on the D/H ratios of leaf water is small, as we observed in the transect samples (Figure 5). For the simulated field plants, modeled δD_{leaf} is slightly higher at corresponding humidity levels, -36, -27, -19 ‰, due to the additional isotope fractionation associated with soil water evaporation. $\delta D_{leaf\ water}$ increases by 17 ‰ when RH decreases from 80 to 40%. This modeled RH effect must represent an average value, as natural desert plants show large variability in their leaf water isotopic ratios (e.g., Gat et al., 2007). Inevitably, growth chamber results can never fully represent all the complex variables of natural settings.

The effect of vegetation types

Recent studies have shown that there is significant difference in δD_{wax} among different plant types. Our recent study at Blood Pond, MA shows that δD_{wax} values from trees are ~40 to 50 ‰ higher than those from grasses (Hou et al. 2007a). Because all plant samples at the Blood Pond site receive the same precipitation, our results suggest significantly larger apparent hydrogen isotopic fractionation during leaf wax synthesis in

grasses relative to trees. Similarly, Krull et al. (2006) found that leaf waxes from grasses and grassland soils are ~50 ‰ lower than those from trees and woodland soils. Discrepancy between the δD_{wax} of grasses and trees was also reported by Liu et al. (2006), although the precipitation δD values in their study were not well constrained. The vegetation change along the SW transect is dramatic, shifting from shrubland to savanna to temperate grassland to subtropical forest (Figure 1C). Relatively small $\varepsilon_{wax\text{-}p}$ would be expected in the eastern Texas Plains due to more extensive forest cover, while relatively large $\varepsilon_{wax\text{-}p}$ would be expected in the western part of the transect due to more extensive grassland, shrubland and CAM plants. However, these expectations are not observed and the large changes in vegetation cover are accompanied by a relatively small change in overall $\varepsilon_{wax\text{-}p}$. We hypothesize that the opposing hydrogen isotope fractionation effects of RH (as expressed in the above model and our growth experiments) and vegetation type offset one another and result in relatively constant $\varepsilon_{wax\text{-}p}$ across the transect.

In order to test our hypothesis, we modeled separately the effects of RH and vegetation cover on δD_{wax} ratios along the Southwestern US transect. First, we used the soil water model (Eq.5) and leaf water model (Eq.7) to estimate the effect of RH on δD_{wax} variation, while holding the vegetation constant (assuming 100% tree cover) (Figure 7A). We then calculated the effect of vegetation types on δD_{wax} values by holding RH constant (assuming RH = 100% for all sites). We used a binary isotopic model to estimate the

vegetation effect. Because we were unable to find accurate productivity data for different plant types (e.g., trees, grasses, shrubs, CAM plants) along the transect, we assumed that the relative proportion of trees vs. grasses-shrubs is linearly correlated to RH. CAM plant leaf waxes have mean enrichment factor $\varepsilon_{wax\text{-}p}$ values ~ -145‰ (Chikaraishi and Naraoka, 2003; Chikaraishi et al., 2004). Therefore, similar to an increase in grass-shrub cover, an increase in CAM plants relative to trees should also increase the $\varepsilon_{wax\text{-}p}$,justifying our use of a simple two end member model to simulate the vegetation effect along the SW transect.

The combined vegetation and RH effects are shown in Figure 7A. To simplify the plots, we show the polynomial regression for the measured and modeled D/H ratios of leaf wax ($\delta D_{wax(model)}$) values and δD_p values along the transect. The $\delta D_{wax(model)}$ - δD_p curve matches the measured $\delta D_{wax} - \delta D_p$ well (Figure 7A), supporting our hypothesis that the opposing RH and vegetation effects could regulate δD_{wax} values. Altering the modeled relationship between percent tree cover and RH (by varying the coefficient of the linear relationship from 0.7 to 1.2) only results in minor changes in the modeled δD_{wax} (Figure 7B, C). Of course, our model is a simplification of natural systems, and many other environmental factors may also play a part in determining the ultimate $\varepsilon_{wax\text{-}p}$ values at any given site. Moreover, there is very little published data showing that the vegetation effect extends to very arid regions. However, we are encouraged to see that

this simple model experiment closely matches our observations. It is likely that the RH and vegetation effects are not always perfectly canceled. For example, we observe two distinct relationships between δD_P and δD_{wax} in the transect data (one for the dry portion and one for the wet portion) (Figure 3B). In the Basin and Range, the dominance of grassland and shrubland may produce more leaf waxes with lower D/H ratios, resulting in a vegetation effect that overwhelms the RH effect. This would explain why sites from the Basin and Range show a greater slope in the relationship between δD_P and δD_{wax} than those from Texas Plains (Figure 3B).

Vegetation cover may also explain the much stronger correlation between δD_{wax} and δD_P observed in the dry portion of the transect (Figure 3B, $R^2 = 0.84$ for Basin and Range, $R^2 = 0.64$ for the Plains). Diverse types of vegetation, more variable seasonal δD_P values, groundwater versus summer precipitation input, and difference in plant growth seasons in the Plains may introduce greater variability to sedimentary δD_{wax} values, thereby introducing noise to the δD_{wax} - δD_P correlation over the more humid portion of the transect. In contrast, plants in dry regions might only grow in the rainy season, when soil water is available, reducing the variability in source water δD values used by plants during leaf wax biosynthesis.

IMPLICATIONS TO PALEOCLIMATE RECONSTRUCTIONS

Wet and/or cool regions with high P/E ratio

The δD values of aquatic lipids, biosynthesized using lake water, show strong correlation with δD values of lake water at a nearly constant isotopic fractionation (Sauer et al., 2001; Huang et al., 2002, 2004; Hou et al., 2006; Hou et al., 2007b). In cool and wet regions, such as northeastern North America (Huang et al., 2002) and western Europe (Sachse et al., 2004), lake water is mainly recharged by precipitation and/or ground water. Therefore, δD values of lake water more closely represent δD of mean annual precipitation (Figure 8, right panel). However, δD_{wax} values, especially those from low lying areas, are affected by multiple factors, including multiple water sources (direct precipitation, ground water), seasonality of precipitation, and diversity of vegetation cover. In addition to precipitation, plants can also use the shallow ground water for biosynthesis. The ground water in northeastern North America is mainly recharged in early spring, which adds isotopically-distinct (relative to direct summer precipitation) source water for plants. Diversity of plant types could also introduce significant uncertainties to the sedimentary δD_{wax} ratios, as different plant types at the same site have been shown to produce leaf waxes with quite different δD_{wax} values (Krull et al., 2006; Liu et al., 2006; Hou et al., 2007a; Liu and Huang, 2008). Therefore, δD_{wax} values from

higher RH and/or cool regions could, generally, show larger variability relative to δD of precipitation (Figure 8).

Dry and/or warm regions with low P/E ratios

In relatively dry and warm regions, such as the western part of the transect in this study, the evaporation effect on soil water and leaf water is enhanced due to the low RH (ε_1, ε_2 in Figure 8). The net biosynthetic H isotopic fractionation (ε_{bio} in Figure 8) also increases relative to wet regions because of the reduced input from trees (Liu et al., 2006; Hou et al., 2007a). In such regions, δD values of aquatic lipids (which record the isotopic composition of lake water) are isotopically enriched relative to precipitation due to strong evaporation. Therefore, in dry regions the δD values of terrestrial leaf waxes may prove to be better proxies for δD of precipitation. Since speleothems tend not to form in areas of insufficient precipitation, leaf waxes extracted from lake sediments may provide the best opportunity for reconstructing the δD of precipitation in arid regions. Saline lakes in arid regions, recharged by mountain glaciers (e.g., Mono Lake in the Western U.S.; Lake Qinghai in China), could represent excellent candidates for paleohydrological reconstruction using the δD of leaf waxes.

CONCLUSIONS

The hydrogen isotopic composition of higher plant leaf waxes represents an effective proxy for δD of past continental precipitation. The proxy may prove particularly useful in dry regions, such as those with annual precipitation lower than 400 mm shown in this study. It appears that plants grown in dry regions use direct precipitation as source water for biosynthesis, as a means to maximize their water use efficiency. If this is indeed the case, leaf waxes from these plants are likely to track precipitation δD values with high fidelity. While the relationship between and δD_P is also strong in wetter regions (such as those with annual precipitation exceeding 400 mm in this study), complicating factors such as multiple water sources (e.g., groundwater vs. summer precipitation), seasonality of precipitation and diversity of vegetation types could lead to reduced fidelity of δD_{wax} as a paleohydrologic proxy. However, because the sites in this study are restricted to the Southwestern United States, more research is needed to test whether our findings are also applicable to other regions around the world.

Our growth chamber experiments indicate that the effect of RH on δD_{wax} is small. Changing RH from 80 to 40 % led to a mere ~ 7 ‰ increase in hydrogen isotopic enrichment in $\varepsilon_{wax\text{-}water}$. The experimental results are consistent with output from the latest leaf water model. Based on model results using the natural transect data, soil evaporation

appears to make the largest contribution to the hydrogen isotopic variation induced by changes in relative humidity. However, the isotopic effect of relative humidity changes on plant leaf water and leaf waxes appears to be partially cancelled by the opposing isotopic effects of changing vegetation cover. We were able to reproduce the observed relationship between δD_{wax} and δD_P along our southwestern US transect using a simple model by combining the effects of RH with those of vegetation cover.

In arid settings, the combination of D/H ratios of terrestrial leaf waxes and aquatic lipids may provide important information concerning the past variability of the hydrologic cycle, including changes to both the isotopic composition of precipitation and lake water evaporation. In wet and/or cool regions, aquatic lipids from lakes in low lying areas are particularly useful for reconstructing past precipitation δD values. Leaf waxes in wet and/or cool regions may show greater variability relative to precipitation. However, if groundwater input could be minimized (e.g. lakes at topographic highs), leaf waxes could also provide valuable information on the δD values of growth season precipitation in wet and/or cool regions.

ACKNOWLEDGEMENTS

This work was supported by grants from the National Science Foundation (NSF 0318050, 0318123, 0402383) to Y. Huang. We would like to thank the Koebke Family (Dudley, MA) for access to Blood Pond. We thank Dana MacDonald for identifying and collecting the tree seedlings, Fred Jackson and Brian Leib for tending to plants in the greenhouse, David Murray and Joseph Orchardo for assistance during the growth chamber experiments, and Marcelo Alexandre for help during the sample analysis. We thank John Roden for providing the spreadsheet to model the leaf water D/H ratios.

REFERENCES

Adams D. K. and Comrie A. C. (1997) The North American monsoon. *Bulletin of the American Meteorological Society* 78, 2197-2213.

Ball J. T. (1987) Calculations related to leaf gas exchange. In: Zieger E., Farquhar G. D., and Cowan I. R. Eds.), Stomatal Function. Stanford University Press, Stanford, California.

Bowen G. J. and Revenaugh J. (2003) Interpolating the isotopic composition of modern meteoric precipitation. *Water Resources Research* 39, 1299,

doi:10.129/2003WR002086.

Chikaraishi Y. and Naraoka H. (2003) Compound-specific dD-d13C analyses of n-alkanes extracted from terrestrial and aquatic plants. *Phytochemistry* 63, 361-371.

Chikaraishi Y., Naraoka H. and Poulson S. R. (2004) Hydrogen and carbon isotopic fractionations of lipid biosynthesis among terrestrial (C_3, C_4 and CAM) and aquatic plants. *Phytochemistry* 65, 1369-1381.

Craig H. and Gordon L. I. (1965) Deuterium and oxygen 18 variations in the ocean and marine atmosphere. In *Stable Isotopes in Oceanographic studies and Paleotemperatures* (ed. E. Tongiorgi), pp. 9-130. Lab. Geologia Nucleare.

Edwards T. D. W. and Fritz P. (1986) Assessing meteoric water composition and relative from 18O and 2H in wood cellulose: Paleoclimatic implications for southern Ontario, Canada. *Applied Geochemistry* 1, 715-723.

Flanagan L. B., Comstock J. P. and Ehleringer J. R. (1991) Comparison of Modeled and Observed Environmental-Influences on the Stable Oxygen and Hydrogen Isotope Composition of Leaf Water in Phaseolus-Vulgaris L. *Plant Physiology* 96, 588-596.

Gat J. R. (1996) Oxygen and hydrogen isotopes in the hydrologic cycle. *Annual Review of Earth and Planetary Sciences* 24, 225-262.

Gat J. R., Yakir D., Goodfriend G., Fritz P., Trimborn P., Lipp J., Gev I., Adar E. and

Waisel Y. (2007) Stable isotope composition of water in desert plants. *Plant and Soil* 298, 31-45.

Gibson J. J. and Edwards W. T. (1996) Development and validation of an isotopic method for estimating lake evaporation. *Hydrological Processes* 10, 1369–1382.

Gibson J. J., Reid R. and Spence C. (1998) A six-year isotopic record of lake evaporation at a mine site in the Canadian subarctic: results and validation. *Hydrological Processes* 12, 1779–1792.

Gibson J. J. and Edwards T. W. D. (2002) Regional water balance trends and evaporation-transpiration partitioning from a stable isotope survey of lakes in northern Canada. *Global Biogeochemical Cycles* 16, doi: 10.1029/2001GB001839.

Gonfiantini R. (1986) Environmental isotopes in lake studies. In *Handbook of Environmental Isotope Geochemistry* (ed. P. Fritz and J. C. Fontes), pp. 113-168. Elsevier.

Gray J. and Song S. J. (1984) Climatic Implications of the Natural Variations of D/H Ratios in Tree-Ring Cellulose. *Earth and Planetary Science Letters* 70, 129-138.

Grootes P. M., Stuiver M., White J. W. C., Johnsen S. and Jouzel J. (1993) Comparison of Oxygen-Isotope Records from the GISP2 and GRIP Greenland Ice Cores. *Nature* 366, 552-554.

Hou J., Huang Y., Wang Y., Shuman B., Oswald W. W., Faison E. and Foster D. R. (2006)

Postglacial climate reconstruction based on compound-specific D/H ratios of fatty acids from Blood Pond, New England. *Geochemistry Geophysics Geosystems* 7, doi:10.1029/2005GC001076.

Hou J., D'Andrea W., MacDonald D. and Huang Y. (2007a) Hydrogen isotopic variability in leaf waxes among terrestrial and aquatic plants around Blood Pond, Massachusetts (USA). *Organic Geochemistry* 38, 977-984 doi:10.1016/j.orggeochem.2006.12.009.

Hou J., Huang Y., Oswald W.W., Foster D.R. and Shuman B. (2007b). Centennial-scale compound-specific hydrogen isotope record of Pleistocene - Holocene climate transition from southern New England. Geophysical Research Letters, 34, L19706, doi:10.1029/2007GL030303.

Huang Y., Shuman B., Wang Y. and Webb T. III. (2002) Hydrogen isotope ratios of palmitic acid in lacustrine sediments record late Quaternary climate variations. *Geology* 30, 1103-1106.

Huang Y., Shuman B., Wang Y. and Webb T., III. (2004) Hydrogen isotope ratios of individual lipids in lake sediments as novel tracers of climatic and environmental change: a surface sediment test. *Journal of Paleolimnology* 31, 363-375.

Huang Y., Clemens S.C., Liu W., Wang Y. and Prell W.L. (2007) Large scale hydrological change drove the late Miocene C_4 plant expansion in the Himalayan foreland and Arabian Peninsula. *Geology* 35, 531-534.

Krull E., Sachse D., Mugler I., Thiele A. and Gleixner G. (2006) Compound-specific $\delta^{13}C$ and $\delta^{2}H$ analyses of plant and soil organic matter: A preliminary assessment of the effects of vegetation change on ecosystem hydrology. *Soil Biology & Biochemistry* 38, 3211-3221.

Liu W. and Huang Y. (2005) Compound specific D/H ratios and molecular distributions of higher plant leaf waxes as novel paleoenvironmental indicators in the Chinese Loess Plateau. *Organic Geochemistry* 36, 851-860.

Liu Z. and Huang Y. (2008) Hydrogen isotopic compositions of plant leaf lipids are unaffected by a twofold pCO_2 change in growth chambers. *Organic Geochemistry*, doi: 10.1016/j.orggeochem.2008.01.020

Liu W., Yang H. and Li L.W. (2006) Hydrogen isotopic compositions of n-alkanes from terrestrial plants correlate with their ecological life forms. *Oecologia* 150, 330-338.

Pagani M., Pedentchouk N., Huber M., Sluijs A., Schouten S., Brinkhuis H., Damste J. S. S., Dickens G. R. and Scientists E. (2006) Arctic hydrology during global warming at the Palaeocene/Eocene thermal maximum. *Nature* 442, 671-675.

Petit J. R., Jouzel J., Raynaud D., Barkov N. I., Barnola J. M., Basile I., Bender M., Chappellaz J., Davis M., Delaygue G., Delmotte M., Kotlyakov V. M., Legrand M., Lipenkov V. Y., Lorius C., Pepin L., Ritz C., Saltzman E. and Stievenard M. (1999) Climate and atmospheric history of the past 420,000 years from the Vostok

ice core, Antarctica. *Nature* 399, 429-436.

Roden J. S., Lin G. and Ehleringer J. R. (2000) A mechanistic model for interpretation of hydrogen and oxygen isotope ratios in tree-ring cellulose. *Geochimica Et Cosmochimica Acta* 64, 21-35.

Sachse D., Radke J. and Gleixner G. (2004) Hydrogen isotope ratios of recent lacustrine sedimentary n-alkanes record modern climate variability. *Geochimica et Cosmochimica Acta* 68, 4877-4889.

Sachse D., Radke J. and Gleixner G. (2006) δD values of individual *n*-alkanes from terrestrial plants along a climatic gradient - Implications for the sedimentary biomarker record. *Organic Geochemistry* 37, 469-483.

Sauer P.E., Eglinton T.I., Hayes J.M., Schimmelmann A. and Sessions A.L. (2001) Compound-specific D/H ratios of lipid biomarkers from sediments as a proxy for environmental and climatic conditions. *Geochimica et Cosmochimica Acta* 65, 213-222.

Schefuβ E., Schouten S. and Schneider R. R. (2005) Climatic controls on central African hydrology during the past 20,000 years. *Nature* 437, 1003-1006.

Shuman B., Huang Y., Newby P. and Wang Y. (2006) Compound-specific isotopic analyses track changes in the seasonality of precipitation in the Northeastern United States at ca. 8200 cal yr BP. *Quaternary Science Reviews* 25, 2992-3002.

Smith F.A. and Freeman K.H. (2006) Influence of physiology and climate on dD of leaf

wax n-alkanes from C_3 and C_4 grasses. *Geochimica et Cosmochimica Acta* 70, 1172-1187.

Terwilliger V.J. and DeNiro M.J. (1995) Hydrogen isotope fractionation in wood-producing avocado seedlings: Biological constraints to paleoclimatic interpretations of delta D values in tree ring cellulose. *Geochimica et Cosmochimica Acta* 59, 5199-5207.

Wang Y.J., Cheng H., Edwards R.L., An Z.S., Wu J.Y., Shen C.C. and Dorale J. A. (2001) A high-resolution absolute-dated late Pleistocene monsoon record from Hulu Cave, China. *Science* 294, 2345-2348.

White J.W.C. (1989) Stable isotope ratios in plants: A review of current theory and some potential applications. In *Stable Isotopes in Ecological Research* (ed. P. W. Rundel et al.), pp. 142-162. Springer-verlag.

White J.W.C., Lawrence J.R. and Broecker W. S. (1994) Modeling and Interpreting D/H Ratios in Tree-Rings - a Test-Case of White-Pine in the Northeastern United-States. *Geochimica et Cosmochimica Acta* 58, 851-862.

Yapp C.J. and Epstein S. (1982) A re-examination of cellulose carbon-bound hydrogen dD measurements and some factors affecting plant-water D/H relationships. *Geochimica et Cosmochimica Acta* 46, 955-965.

Yuan D.X., Cheng H., Edwards R.L., Dykoski C.A., Kelly M.J., Zhang M., Qing J., Lin Y., Wang Y., Wu J., Dorale J.A., An Z.S. and Cai Y. (2004) Timing, during, and

transitions of last interglacial Asian monsoon. *Science* 304, 575-578.

Table 1. Geographical lake data and measured hydrogen isotopic ratios of lake water and sedimentary leaf waxes.

name	State	Lat (^{o})	Long(^{o})	Elv (m)	RH	P (mm)	E (mm)	T (^{o}C)	δD_P	δD_{Lake}	δD_{C26}	δD_{C28}	δD_{C30}
Horseshoe Lake*	AZ	33.99	-111.72	613	45.0	368	1615	16.2	-67	-73	-173	-161	-162
Bartelett Lake*	AZ	33.84	-111.64	527	44.0	500	1637	13.5	-65	-70	-164	-154	-155
Saguaro Lake*	AZ	33.57	-111.54	472	41.0	487	1717	13.2	-64	-49	-151	-150	-151
Apache Lake*	AZ	33.57	-111.26	567	41.0	304	1731	21.7	-65	-52	-154	-147	-147
Roosevolt Lake*	AZ	33.68	-111.10	655	43.0	234	1711	12.3	-67	-67	-164	-156	-157
San Carlos Reservoir*	AZ	33.17	-110.52	728	40.0	348	1665	20.4	-66	-59	-167	-161	-163
Cluff Pond*	AZ	32.81	-109.86	1006	37.0	463	1743	18.1	-69	-39	-150	-152	-153
Roper Lake*	AZ	32.76	-109.72	948	36.0	512	1734	11.3	-68	-57	-159	-157	-158
Dankworth Pond*	AZ	32.71	-109.71	978	36.0	503	1770	11.3	-68	-80	-166	-154	-155
Crescent Lake*	AZ	33.00	-109.00	1975	42.5	305	1650	15.1	-82	-88	-184	-176	-177
Animas Ditch*	AZ	32.28	-108.89	1268	43.0	305	1715	15.6	-70	4	-142	-141	-142
Caballo Lake*	NM	32.91	-108.31	1271	47.0	258	1572	15.7	-71	-66	-159	-160	-162
Elephant Butt Lake*	NM	33.17	-107.21	1335	54.0	215	1499	13.1	-71	-78	-183	-176	-178
Lake Escondida*	NM	34.11	-106.89	1423	60.0	127	1383	13.9	-74	-80	-174	-174	-175
Upper Glacier	NM	36.82	-105.05	2524	68.0	358	1246	9.7	-96	-94	-212	-215	-219
Lake #1	NM	36.08	-105.04	2420	65.0	396	1246	4.4	-92	-49	-177	-191	-196
Mary's Lake	NM	36.00	-105.00	2155	63.0	-	-	11.0	-88	-27	-191	-186	-188
Santa Rosa Lake*	NM	35.01	-104.69	1466	51.0	394	1537	14.4	-75	-83	-192	-190	-193
Conchas Lake*	NM	35.39	-104.19	1283	53.0	419	1547	11.9	-73	-21	-168	-158	-159
UTE Lake*	NM	35.33	-103.43	1155	53.0	194	1547	12.1	-69	-8	-165	-163	-165
Buffalo Spring Creek	TX	33.52	-101.71	919	51.0	583	1699	15.6	-56	-39	-131	-136	-136

Lake Meredith*	TX	35.65	-101.63	616	57.0	455	1654	12.9	-59	-9	-152	-154	-155
Lake Colorado City	TX	32.34	-100.92	631	53.0	338	1589	17.6	-48	-3	-106	-134	-134
Champion Creek	TX	32.29	-100.86	616	53.0	615	1589	16.7	-48	-18	-126	-143	-143
EV Spence Reservoir	TX	32.00	-100.67	607	54.0	483	1589	17.4	-47	-7	-105	-129	-128
Lake Nasworth	TX	31.37	-100.60	565	56.0	483	1663	17.4	-45	9	-108	-139	-140
Lake Junction	TX	30.49	-99.46	579	61.0	702	1461	18.2	-41	-34	-141	-142	-142
Lake Medina*	TX	29.57	-98.70	324	67.0	611	1375	18.5	-35	-18	-150	-162	-163
Lake Bastrop	TX	30.18	-97.29	137	73.0	850	1341	19.4	-31	16	-126	-127	-126
Cedar Creek Lake	TX	29.93	-96.73	98	76.0	995	1138	20.4	-30	13	-148	-141	-142
Somerville Lake	TX	30.33	-96.60	73	76.0	1108	1138	19.6	-29	-7	-116	-124	-124
Lake Houston	TX	29.70	-95.17	13	82.0	1150	1175	20.7	-27	-26	-135	-134	-134

*Dammed reservoir; Elv - elevation; RH – Mean annual relative humidity; P – mean annual precipitation; E - evaporation; T - temperature; δD_P - mean annual δD of precipitation; δD_{lake} – δD of lake water; δD_{C26}, δD_{C28}, δD_{C28} – δD values of C_{26}, C_{28}, C_{30} *n*-acids.

Table 2. δD values of long chain n-alkanoic acids and mean values ± standard deviation from individual species cultured in growth chamber

Species	Life form	RH=80%			RH=60%			RH=40%		
		C26	C28	C30	C26	C28	C30	C26	C28	C30
Fraxinus americana	tree	-156	-142	-136	-	-141	-129	-136	-139	-133
Fraxinus americana	tree	-160	-162	-160	-	-145	-152	-134	-156	-141
Fraxinus americana	tree	-163	-152	-155	-	-135	-136	-132	-139	-139
Fraxinus americana	tree	-143	-134	-132	-	-134	-121	-	-121	-125
Mean for F.A.		-156±9	-147±13	-146±14	-	-139±5	-135±13	-134±2	-139±14	-134±8
Carya glabra	tree	-157	-153	-142	-	-152	-144	-	-152	-140
Acer rubrum L.	tree	-171	-167	-160	-149	-157	-148	-138	-144	-133
Acer rubrum L.	tree	-169	-163	-151	-138	-143	-135	-141	-146	-135
Acer rubrum L.	tree	-162	-154	-147	-128	-136	-136	-139	-150	-144
Mean for A.R.		-168±5	-161±7	-153±7	-138±11	-145±11	-140±7	-139±1	-146±3	-137±6
Quercus rubra L.	tree	-183	-171	-166	-169	-177	-169	-167	-173	-166
Quercus rubra L.	tree	-170	-163	-159	-146	-159	-159	-145	-153	-153
Quercus rubra L.	tree	-155	-165	-170	-150	-172	-178	-125	-167	-173
Mean for Q.R.		-169±14	-167±4	-165±5	-155±12	-170±9	-168±9	-145±21	-164±11	-164±10
Thuja occidentalis	tree	-154	-134	-128	-141	-136	-125	-140	-139	-133
Thuja occidentalis	tree	-138	-133	-134	-143	-140	-131	-140	-141	-136
Mean for T.O.		-146±11	-134±1	-131±4	-142±1	-138±3	-128±4	-140±0	-140±1	-135±2
Picea glauca	tree	-158	-141	-139	-152	-138	-138	-156	-147	-153
Picea glauca	tree	-161	-146	-145	-156	-141	-139	-151	-144	-144
Mean for P.G.		-159±2	-143±4	-142±4	-154±3	-139±2	-139±1	-154±4	-145±3	-149±6
Zea mays L.	grass	-165	-156	-160	-162	-154	-151	-158	-157	-166
Zea mays L.	grass	-164	-154	-146	-159	-159	-164	-155	-164	-163
Mean for Z.M.		-164±0	-155±2	-153±10	-161±2	-156±3	-157±9	-157±2	-160±5	-165±3
Dactylis glomerata L.	grass	-208	-190	-178	-	-192	-189	-	-188	-183
Dactylis glomerata L.	grass	-	-191	-189	-	-194	-183	-	-174	-170
Mean for D.G.		-208±0	-190±1	-184±7	-	-193±1	-186±4	-	-181±10	-177±9
Alopecurus spp.	grass	-162	-158	-147	-170	-167	-160	-	-	-
Alopecurus spp.	grass	-169	-162	-149	-161	-164	-159	-	-	-
Alopecurus spp.	grass	-165	-160	-157	-157	-163	-159	-	-	-
Mean for A.		-166±4	-160±2	-151±5	-163±6	-165±2	-159±1	-	-	-
Phleum pratense L.	grass	-166	-160	-150	-166	-159	-143	-147	-144	-135
Phleum pratense L.	grass	-166	-152	-150	-159	-158	-158	-141	-138	-131
Phleum pratense L.	grass	-169	-160	-132	-158	-152	-130	-146	-144	-136
Mean forP.P.		-167±2	-157±4	-144±10	-161±4	-156±4	-144±14	-145±3	-142±4	-134±3

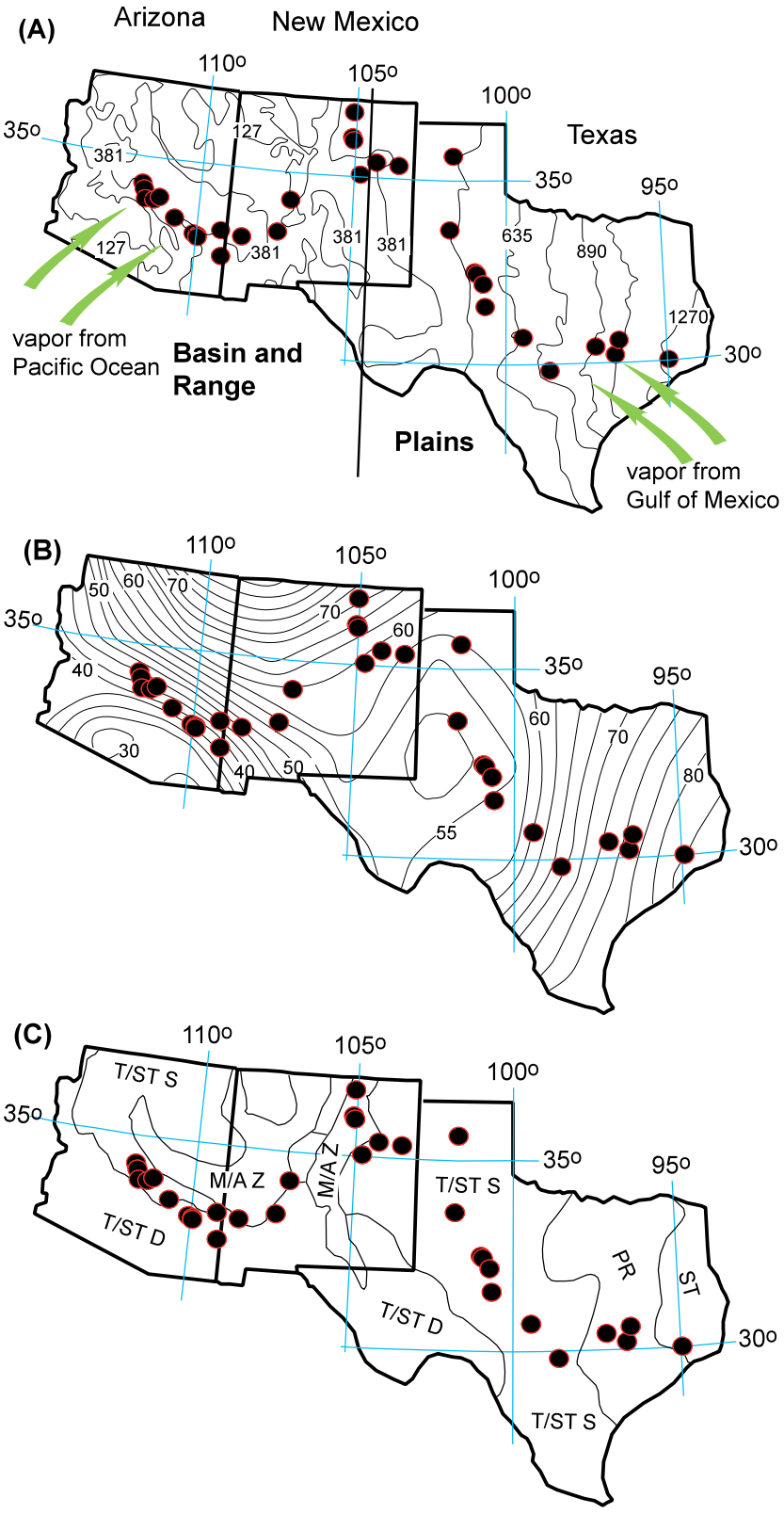
(A)
Arizona
New Mexico
Texas
110º
105º
100º
95º
35º
30º
127
381
635
890
1270
vapor from
Pacific Ocean
Basin and
Range
Plains
vapor from
Gulf of Mexico
(B)
50
60
70
40
30
55
80
(C)
T/ST S
M/A Z
T/ST D
PR
ST

Figure 1. The modern lake transect in the southwestern United States. (A) Precipitation gradient (mean annual precipitation (mm/yr) from 1961 to 1990; data from NOAA Cooperative Station Normals climate observations); (B) relative humidity (RH) gradient and mean annual relative humidity (%) (data from http://www.cdc.noaa.gov); (C) vegetation cover (data from http://www.nationalatlas.gov); ST – Subtropical forests; PR – Prairie; T/ST D – Tropical/subtropical Desert; T/ST S – Tropical/subtropical Steppe; M/A Z Mountain with Altitudinal Zonation. The arrows in (A) indicate the moisture source (Tropical Pacific Ocean from west, Gulf of Mexico from east) for precipitation in this region. The lakes are divided into two groups according to the geographic division and mean annual precipitation: Plains (including lakes from Texas); Basin and range (including lakes from New Mexico and Arizona).

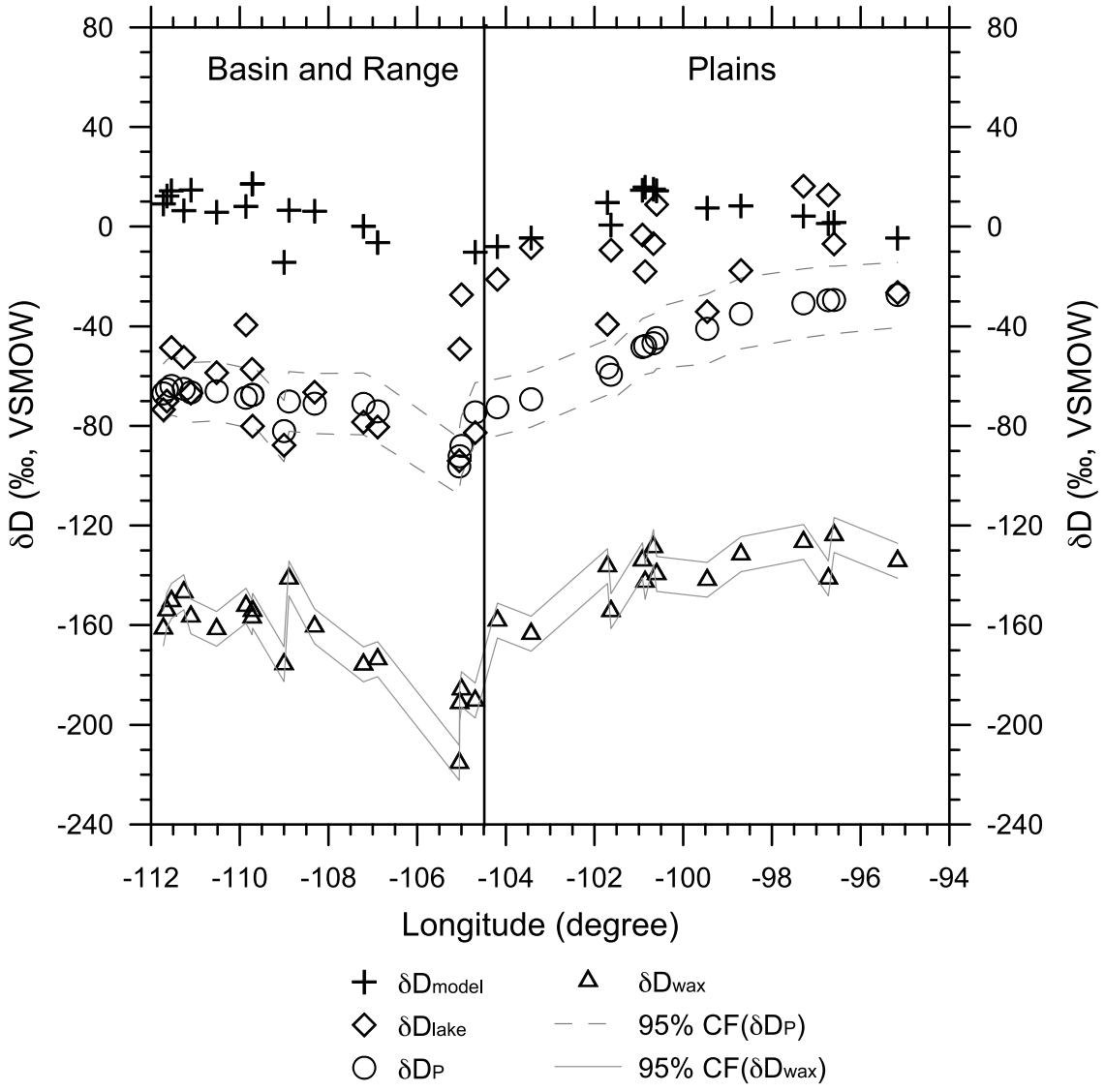

Figure 2. Hydrogen isotope data for the SW transect: δD_{wax}= measured D/H ratios of sedimentary leaf waxes; δD_P= D/H ratios of precipitation calculated from OIPC; δD_{lake}= measured D/H ratios of lake water; δD_{model}= modeled D/H ratios of lake water; 95% CF (δD_P)= 95% confidence interval for δD_P; 95% CF (δD_{wax})= 95% confidence interval for δD_{wax}.

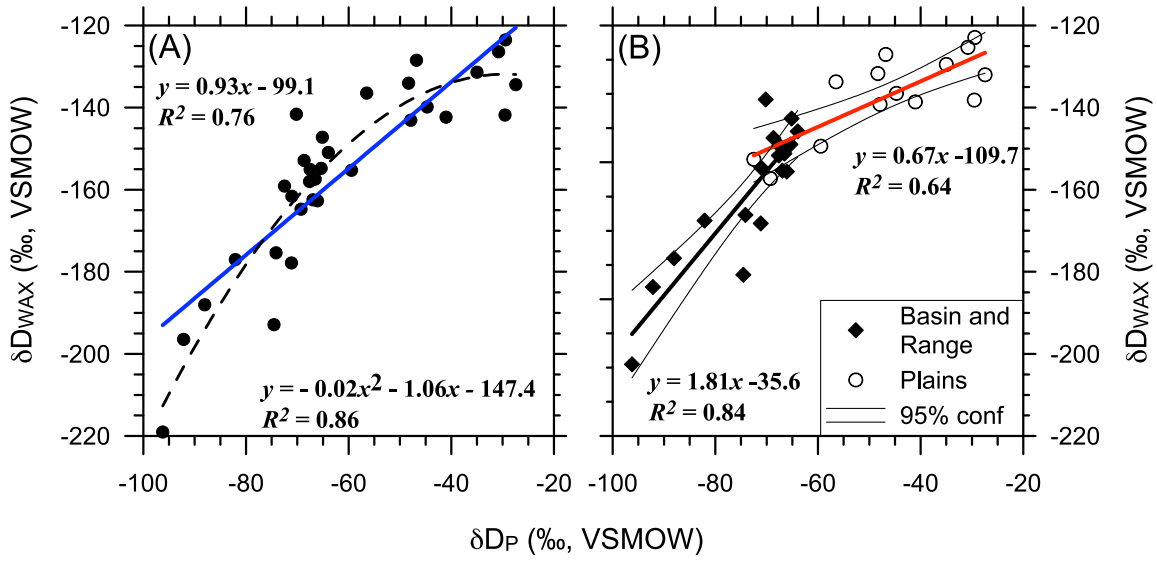

Figure 3. Correlation between δD_{wax} and δD_P for the lake surface sediment samples along the SW transect. (A) Correlation for the entire data set showing both linear and polynomial regressions. (B) Correlation for data from distinct geographical provinces (Basin and Range, and Plains). 95% confidence intervals are shown.

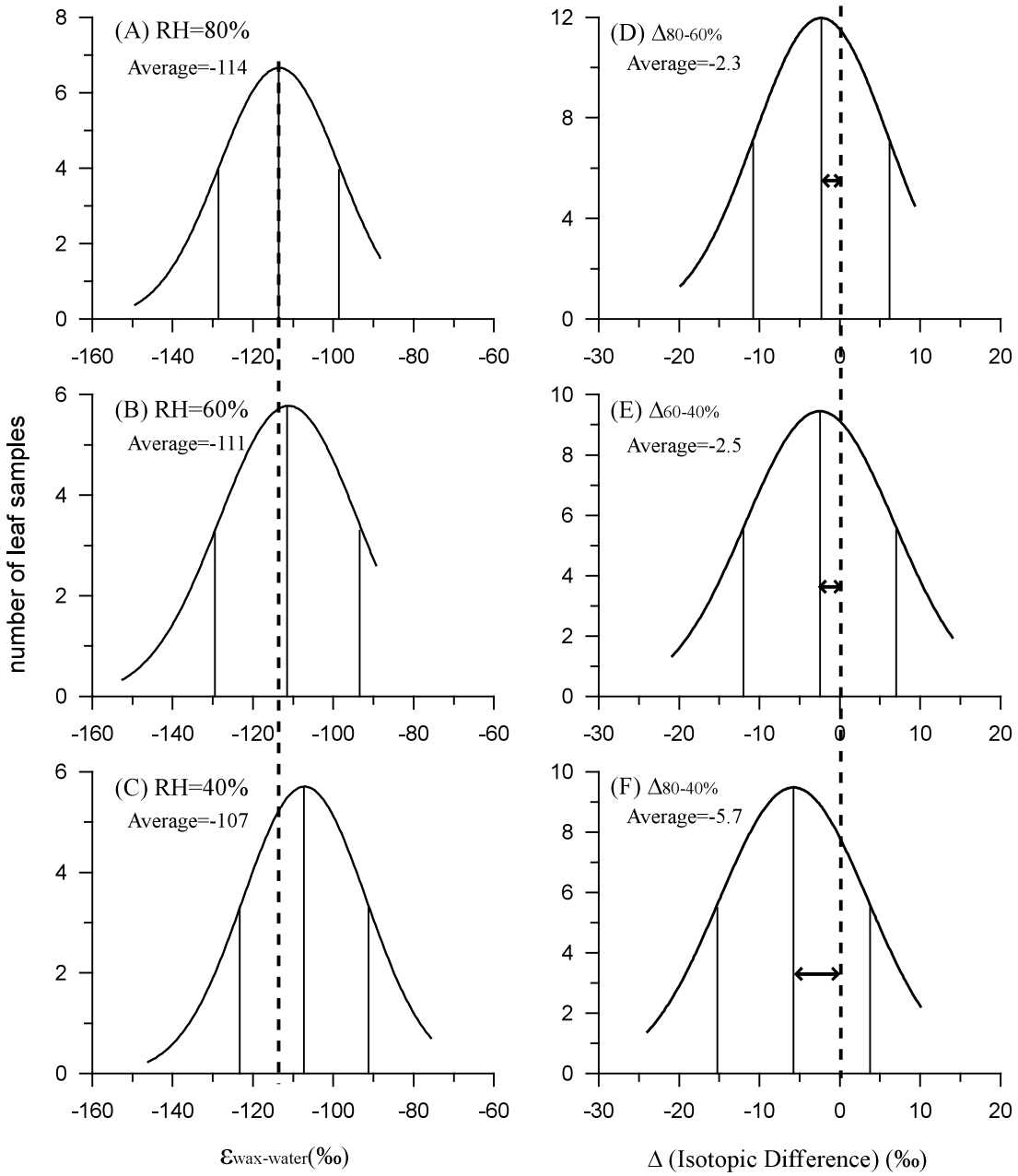

Figure 4. Differences in the apparent isotopic enrichment of leaf waxes for plants grown in growth chamber at three humidity levels. The left-hand plots depict changes in enrichment factor ($\varepsilon_{wax\text{-}water}$) as RH changes from 80% to 40% (A: RH = 80%; B: RH = 60%; C: RH = 40%). The vertical dashed line represents the average $\varepsilon_{wax\text{-}water}$ value at RH = 80%. The righthand plots show hydrogen isotopic differences (Δ values) between different RH levels. (D = $\Delta D_{80\text{-}60\%}$; E = $\Delta D_{60\text{-}40\%}$; F = $\Delta D_{80\text{-}40\%}$).

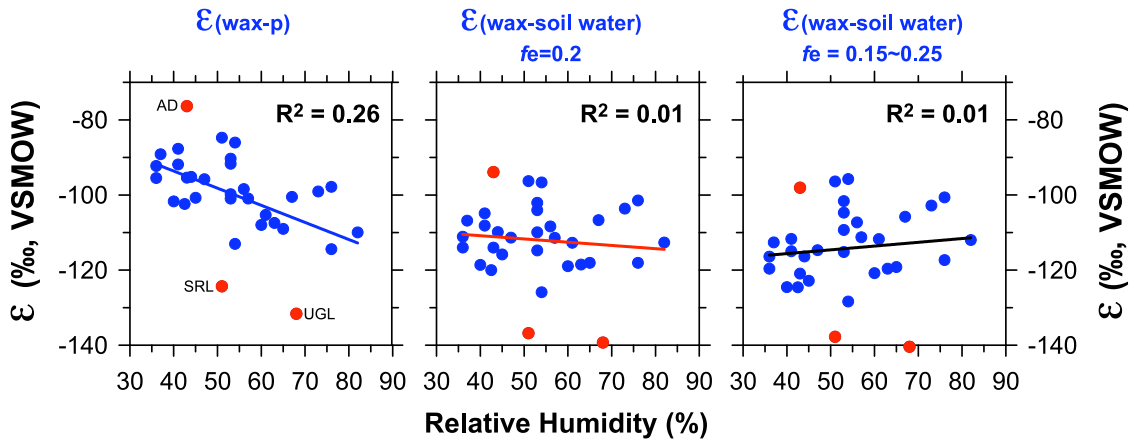

Figure 5. The correlation between RH and apparent isotopic enrichment of sedimentary leaf waxes relative to (A) precipitation ($\varepsilon_{wax\text{-}p}$), (B) modeled soil water ($\varepsilon_{wax\text{-}soil\ water}$) assuming *f*e = 15%, (C) modeled soil water ($\varepsilon_{wax\text{-}soil\ water}$) assuming a linear east to west gradient of *f*e from 15% to 25% for our study sites. $\varepsilon_{wax\text{-}soil\ water} = [(D/H)_{wax}/(D/H)_{soil\ water} - 1] \times 1000$ ‰. Three of the lakes, AD (Animas Ditch), UGL (Upper Glacial Lake) and SRL (Santa Rosa Lake) show different $\varepsilon_{wax\text{-}p}$ values (see text for discussion).

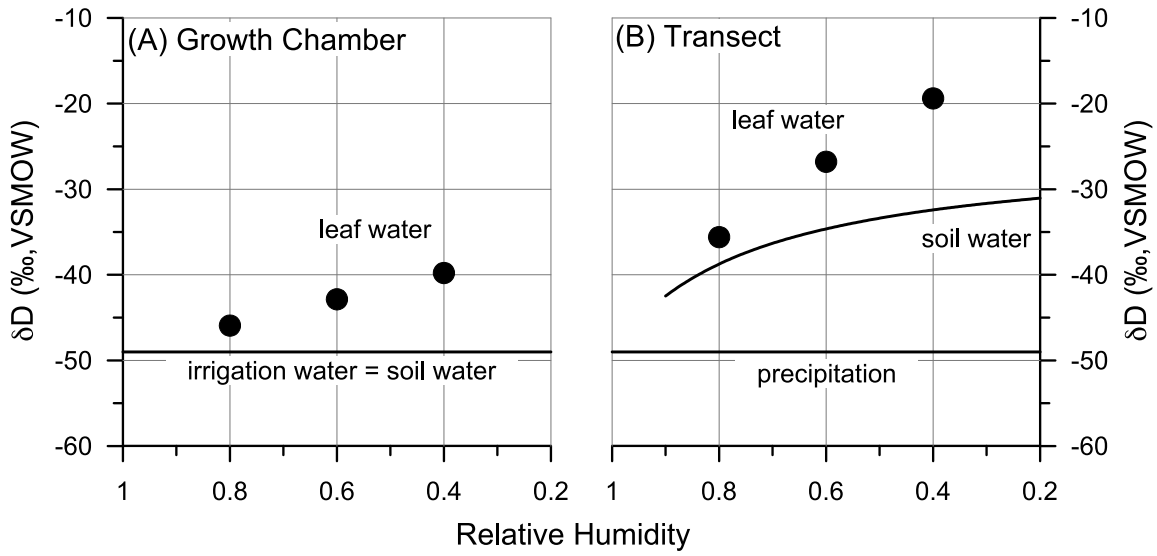

Figure 6. Modeled D/H ratios of soil water and leaf water for plants (A) in the growth chamber and (B) in the field. To facilitate the comparison between the plants from the growth chamber and the field, the D/H ratio of precipitation is set to the δD value of irrigation water in the growth chamber (-49 ‰).

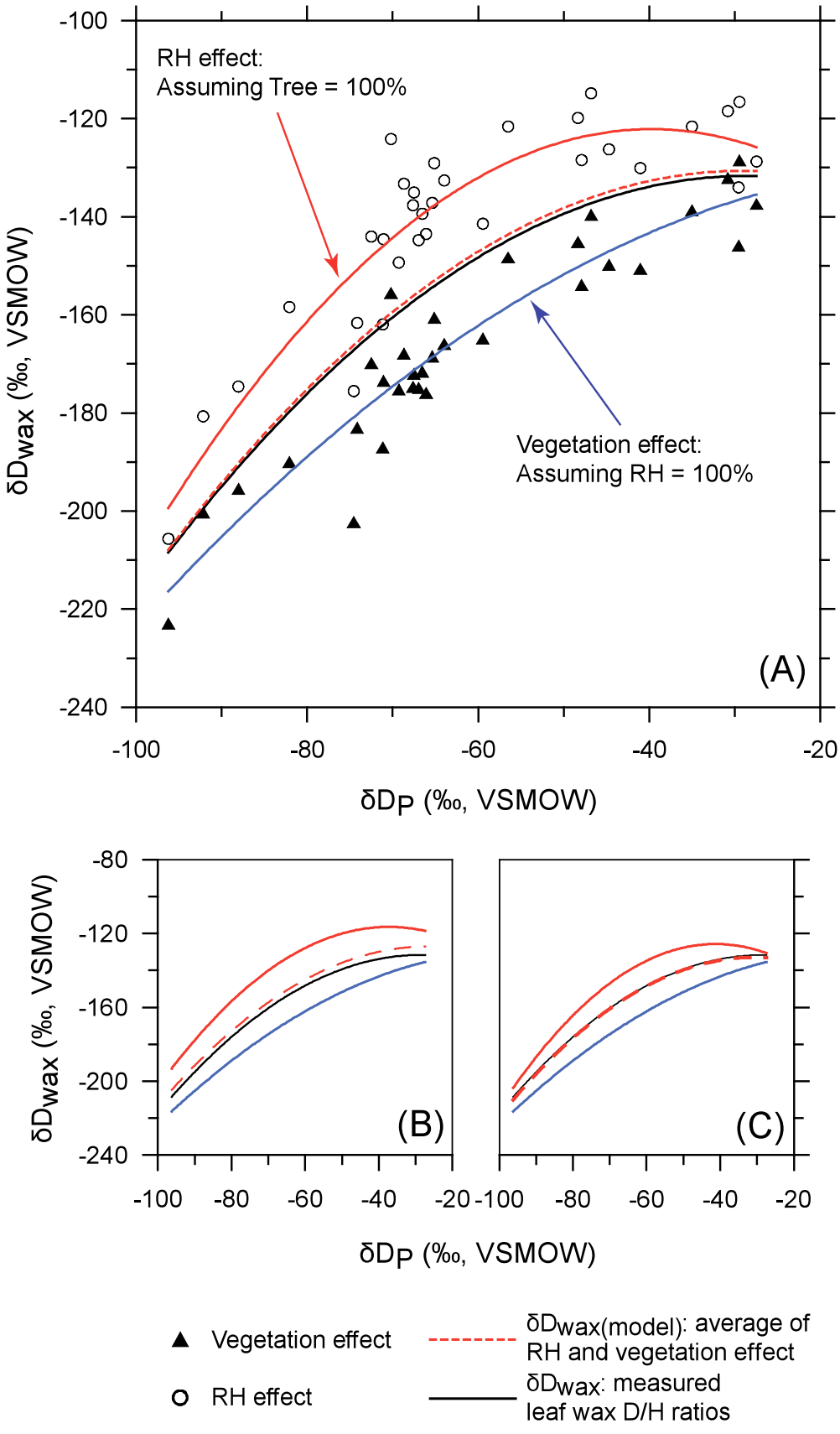
RH effect:
Assuming Tree = 100%
Vegetation effect:
Assuming RH = 100%
(A)
(B)
(C)
δDwax (‰, VSMOW)
δDP (‰, VSMOW)
-100
-120
-140
-160
-180
-200
-220
-240
-80
-60
-40
-20
Vegetation effect
RH effect
δDwax(model): average of RH and vegetation effect
δDwax: measured leaf wax D/H ratios

Figure 7. (A) Models showing the opposing effects of RH and vegetation on the sedimentary δD_{wax}. The data for RH effect (circles) are obtained by assuming the production percentage of tree leaf waxes is 100%, whereas the data for vegetation effect (triangles) are obtained by assuming RH is 100% for all lakes. The average of the RH effect and vegetation effect for all sites ($\delta D_{wax(model)}$, dashed line) is then compared with measured D/H ratios of leaf waxes from the lake sediments ($\delta D_{wax,}$ black line). To facilitate comparison, second order polynomial regressions are shown for all four datasets. (B) and (C) Sensitivity tests for the model combining RH and vegetation effects. As the percentage of tree cover increases from 0.7RH (B) to 1.2RH (C), the modeled δD_{wax} vs. δD_p relationship does not change significantly.

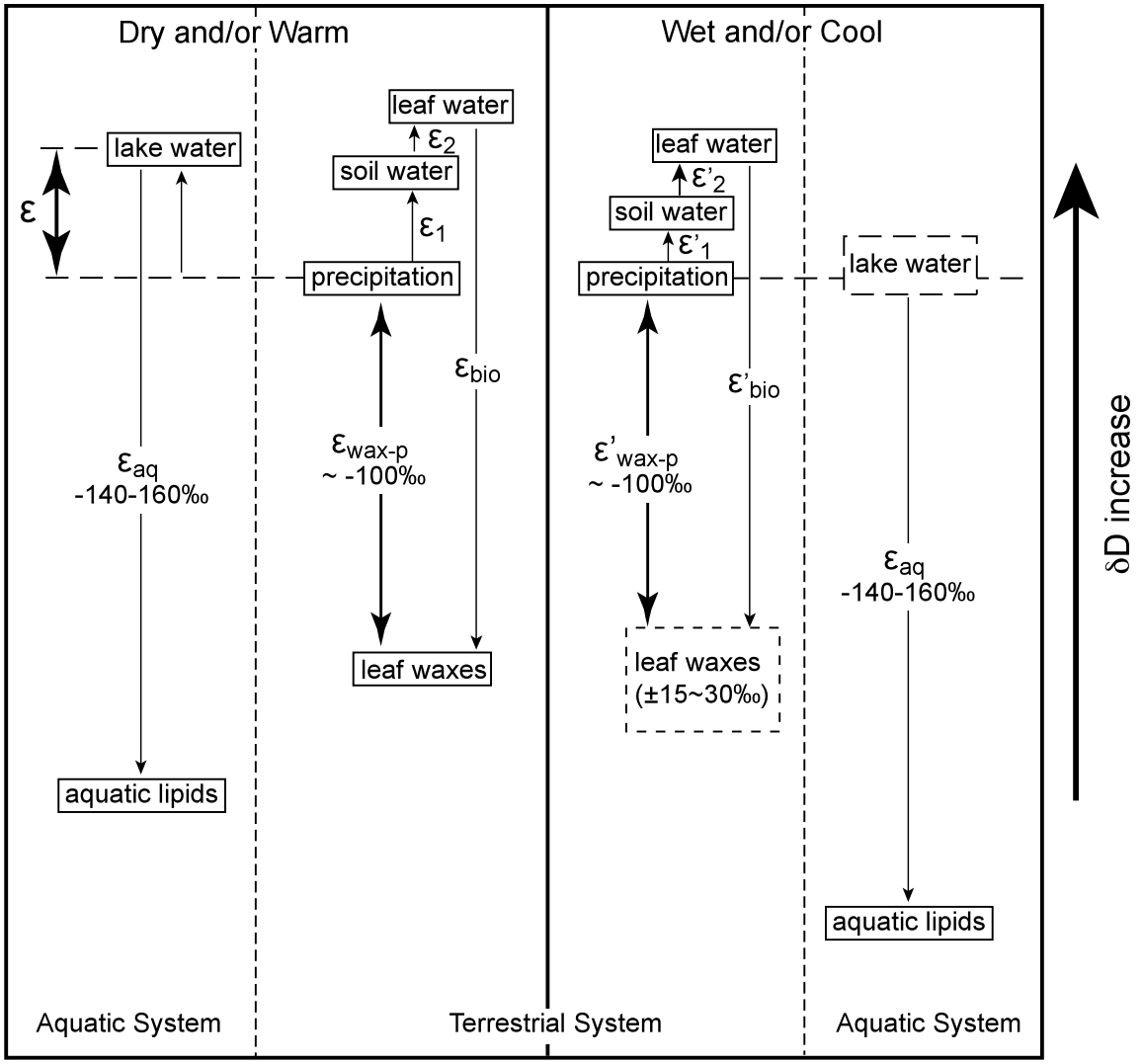

Figure 8. The schematic variation of D/H ratios for low RH and/or warm regions (left panel), and high RH and/or cool regions (right panel; This panel is adapted from Sachse et al. (2006)). ε_1, ε_2, ε'_1, ε'_2 represent the evaporation effect from precipitation to soil water, then to leaf water; ε_{bio} and ε'_{bio} are the hydrogen isotopic enrichment during biosynthesis. ε_{aq} is the biosynthesis effect for aquatic plants. $\varepsilon_{wax\text{-}p}$ and $\varepsilon'_{wax\text{-}p}$ are the apparent hydrogen isotopic enrichment from precipitation to leaf waxes. E is the isotopic enrichment between precipitation and lake water due to evaporation.

CHAPTER 4

Centennial-scale compound-specific hydrogen isotope record of Pleistocene - Holocene climate transition from southern New England

Co-authors: Yongsong Huang, W. Wyatt Oswald, David R. Foster, Bryan Shuman

Published in ***Geophysical Research Letters***, 2007, v. 34, L19706,

doi:10.1029/2007GL030303

ABSTRACT

Northeastern North America experienced major climate shifts during the Pleistocene – Holocene transition. However, there have been no high-resolution isotopic records of climate change from this region. Here, we present a centennial-scale record of climate change during the transition based on D/H ratios of behenic acid (C_{22} *n*-acid) or δD_{BA} from a sediment core in Blood Pond, Massachusetts. Surface calibrations from a transect of 19 lakes in eastern North America show that δD_{BA} values track mean annual atmospheric temperature variations. The abrupt climate events observed in Blood Pond records show remarkable similarity with Greenland ice core $\delta^{18}O$ records during the Pleistocene. During the early Holocene, the northeastern North America δD_{BA} record was more variable than Greenland, possibly due to the close proximity of the Laurentide ice sheet, and impact of freshwater outbursts as the ice sheet rapidly retreated.

INTRODUCTION

The Pleistocene - Holocene transition is characterized by abrupt climatic fluctuations around North Atlantic Ocean (e.g., Stuiver et al., 1995; Hughen et al., 1996). However, the spatial variations in the timing, amplitude, and phasing of the abrupt events are less understood on the adjacent continents. This is particularly true for the northeastern North America where the driving forces for climate were particularly complex, comprising a combination of changes in North Atlantic sea surface temperature, Laurentide ice sheet (LIS) extent, atmospheric composition, and insolation (e.g., Webb et al., 1993). Centennial-scale quantitative records from the northeastern North America are thus extremely important for better understanding marine-terrestrial-atmosphere-cryosphere connections and regional climatic responses.

Existing paleoclimate records from the northeastern North America are mainly based on paleoecological approaches, such as assemblages of pollen (e.g., Peteet et al., 1990; Webb et al., 1993; Shuman et al., 2002a) and Chironomidae (midge, e.g., Cwynar and Spear, 2001; Walker et al., 1997) from lake sediments. However, the possibility of transient vegetation responses to short-term, small-magnitude climate variations (e.g., Davis and Botkin, 1985), and the non-analogue conditions for Chironomidae (e.g., Kurek et al., 2002) could increase the difficulty of using pollen and Chironomidae data to assess abrupt (<centennial-scale) climate variability.

Compound-specific hydrogen isotope analyses of aquatic lipids in sediments (e.g., Sauer et al., 2001; Huang et al., 2002; 2004; Dawson et al., 2004) offer a new way to quantify past climate variations. The technique is especially useful for regions like northeastern North America where the lake sediments lack carbonate deposit. Organic compounds produced by algae and macrophytes track lake water isotopic variations (e.g., Huang et al., 2002; 2004; Hou et al., 2006; Sauer et al., 2001), which in regions of high precipitation-evaporation (P-E) ratio, mimic precipitation isotopic variations. For example, the low resolution record of D/H ratios of behenic acid (C_{22} *n*-acid) or δD_{BA} tracks general climate variation for the past 16,000 yr at Blood Pond (Hou et al., 2006). The objectives of this study are: 1) to establish a transfer function between δD_{BA} and surface air temperature; 2) to quantify the temperature variations of the abrupt climate events during the Pleistocene – Holocene transition; and 3) to integrate with other isotopic records and pollen data to probe the mechanisms of abrupt climate events in northeastern North America.

SAMPLES AND METHODS

Blood Pond (42.081^{o}N, 71.961^{o}W, 212.1 m above sea level) is a kettle pond located in Massachusetts (Figure 1). The lake is mainly recharged by ground water and precipitation, with a southerly overflow outlet. The sediment core was collected in 2001, and samples for isotope analyses were selected at 6 cm intervals. Chronology for the core is provided by AMS-^{14}C dating of bulk organic matter which were converted to calendar years before present (cal yr B.P.) using OxCal 3.9 (Hou et al., 2006). The preparation of the samples and the measurement of hydrogen isotopes have been described previously (Hou et al., 2006). Briefly, lipids were extracted from freeze-dried sediment using an Accelerated Solvent Extractor 200 (Dionex). Acid fractions were isolated, methylated, and purified. A HP 6890 GC interfaced to a Finnigan Delta^{+} XL stable isotope spectrometer through a high-temperature pyrolysis reactor was used for hydrogen isotopic analysis. The precession (1σ) of triplicate analyses was $<\pm 2‰$. The accuracy was routinely checked by measuring laboratory isotopic standards every six measurements. Temperature changes of precipitation were also reconstructed based on pollen assemblages in the same sediment core using the modern analog technique described in Webb et al. (2003).

RESULTS AND DISCUSSIONS

Relationship between δD_{BA} and surface air temperature

D/H ratios of C_{22} *n*-acid (δD_{BA}) from lake surface sediment track lake water D/H ratios along lake transects in eastern North America (Hou et al., 2006). However, the relationship between the δD_{BA} values and surface air temperature (T) has not been established. Here, we establish the relationship between δD_{BA} and T along the N-S transect (Figure 1; see Huang et al., 2004 for details of the transect) across a temperature gradient (2 to 23^{o}C) in eastern North America (Figure 2a),

$$\delta D_{BA} = 4.3T - 208.4,\ R^2 = 0.96,\ p < 0.001 \qquad (1)$$

Based on this relationship, a 1^{o}C change in T corresponds to ~ 4.3 ± 0.2‰ variation in δD_{BA}. To validate this relationship, we determined the relationship between T and precipitation δD value (δD_P) using the data from Global Network of Isotopes in Precipitation (GNIP) stations in eastern North America (Figure 1, Rozanski et al., 1993). The δD_P data show a linear correlation with T (Figure 2b),

$$\delta D_P = 5.2T - 113.0,\ R^2 = 0.97,\ p < 0.001 \qquad (2)$$

This suggests that 1°C change in T corresponds to a change of ~ 5.2 ± 0.2‰ in δD_P. The apparent isotopic fractionation (α) for C_{22} *n*-acid relative to lake water is constant along the transect (Hou et al., 2006):

$$\alpha = 0.8681 = \frac{1000 + \delta D_{BA}}{1000 + \delta D_P} \qquad (3) \qquad \text{or}$$

$$0.8681\ (1000 + \delta D_P) = 1000 + \delta D_{BA} \qquad (4)$$

Substituting (1) and (2) into (4), we obtain 4.5 (± 0.2) T + 770 ≈ 4.3 (± 0.2) T + 792. This suggests that the relationship between δD_{BA} and T is consistent with that between δD_P and T, when the D/H fractionation during the biosynthesis of BA is taken into consideration.

δD_{BA} fluctuations and climatic implications

δD_{BA} values from Blood Pond sediments show pronounced variations during the Pleistocene – Holocene transition (Figure 3, see auxiliary material). D/H ratios increased by ~ 20‰ between 16 and 14.8 ka. The Bølling and Allerød warm periods were indicated by higher δD values at 14.8 -14.4 ka and 14.2-13.7 ka, which were separated by one sample with low δD_{BA} value. The most significant δD variations were observed at the beginning and the end of Younger Dryas chronozone (YD). YD was indicated by lower δD_{BA} values with some fluctuations. The lowest δD_{BA} value occurred around 12.3 ka. The δD_{BA} records show similar fluctuations with $\delta^{18}O$ records from GISP2 ice core and

Crawford Lake during late Pleistocene (Figure 3). During early Holocene, δD values showed more frequent fluctuations with smaller amplitudes, occurred at 10.9, 10.6, 10.3 to 10.1, 9.7, 9.3 and 8.9 ka, respectively. Although δD_{BA} values in the transect show strong correlation with T (Figure 2A), δD_{BA} variations with small magnitude (<10‰) and defined by a single sample could be attributed to other factors in addition to temperature, such as P-E ratios, hydrological balance of lake water, seasonal shifts in precipitation. We will focus on major downcore δD_{BA} shifts to avoid over-interpreting the data as temperature changes.

Late Pleistocene (16 to 13.2 ka): Surface air temperature increased by ~ 5^{o}C between 16 and 14.8 ka. The warmest period of the Late Pleistocene occurred between 14.8 and 14.4 ka, coinciding with the Bølling period (B). The Allerød period (A) is about 2^{o}C cooler than Bølling. Warmth during the B-A periods inferred from the δD_{BA} data matches the warming pattern found in Greenland. Three short cold periods defined by single samples show similar temperature amplitude as those from GISP2 $\delta^{18}O$ (Oldest Dryas, Older Dryas, and Intra Allerød cold period (IACP), Figure 3), although variation in P/E ratios and seasonal changes in precipitation may affect the δD_{BA} changes. The onset of the Bølling period, and the step-change during B-A periods at Blood Pond appear to lead the GISP2 temperature changes by about 100 to 300 years. This may not reflect a real difference in phasing, as the chronological inaccuracies in Blood Pond records (100-350 year uncertainties, Figure 3) and/or the reservoir effect in Blood Pond could readily lead to observed chronological differences.

Younger Dryas chronozone (13.2-11.6 ka): The most significant temperature shifts in the record occurred at the beginning and end of the YD. The beginning of YD (13.2-13 ka) is marked by ~ 5.6°C decline in temperature. Temperatures fluctuated during the YD, with the lowest temperature occurring at ~ 12.3 ka. The YD ended abruptly at 11.6 ka, ~ 5.4°C increase in less than 200 years. The δD_{BA}-inferred temperature variations from Blood Pond can be compared with carbonate $\delta^{18}O$ variation from Crawford Lake in Ontario (Yu et al., 1998; Figure 3), White Lake in New Jersey (Yu, 2006), and with opal $\delta^{18}O$ change from Linsley Lake in Connecticut (Shemesh and Peteet, 1998). The $\delta^{18}O$-inferred temperature variation in Crawford Lake and White Lake was ~6 and 8°C (Yu et al., 1998; Yu, 2006). The opal $\delta^{18}O$-inferred temperature change in Connecticut was ~ 6°C (Shemesh and Peteet, 1998). Temperature changes during the YD have also been estimated using Chironomidae assemblages from lakes in the White Mountains of New Hampshire (Cwynar and Spear, 2001) and from pollen data in New England (e.g. Huang et al., 2002) and New York (Webb et al., 2003). The observed temperature decline in the Chironomidae records was ~ 5 to 6°C (Cwynar and Spear, 2001); pollen data show ~8°C increase in January temperatures and ~4°C increase in July temperatures after the YD (Huang et al., 2002; Webb et al., 2003). The Blood Pond pollen data were used to infer a 3°C decline in the mean temperature of precipitation at the beginning of the YD, and an 8°C increase at the end of YD (Figure 3).

Early Holocene (11.6-8 ka): A series of abrupt temperature excursions is evident in the early Holocene interval of the record. A temperature decrease of ~ 3°C follows a warming trend at the end of the YD (just before 11.5 ka). This cooling may represent the

Preboreal Oscillation (PBO). After 11.5 ka, temperature increased ~ 6^{o}C in ~400 years, which is also observed in the $\delta^{18}O$ record from Crawford Lake (Yu et al., 1998), but was not seen in pollen-based climate reconstructions from northeastern North America and in the Greenland ice core records (Figure 3). In addition to PBO, some other potential cold periods are also revealed by the lower δD_{BA} record, around on 10.9, 10.6, 10.3 to 10.1, 9.7, 9.3 and 8.9 ka.

Comparison of pollen and isotope-based temperature reconstructions

Mean temperature of annual precipitation inferred from pollen assemblages in the same sediment core using the modern analog method (Webb et al., 2003) show similar variations as inferred from the δD_{BA} especially for the YD (Figure 3, note the absolute values of pollen and δD inferred temperatures differ due to independent calibrations). However, there are discrepancies between pollen and δD_{BA} inferred temperatures. For example, between 15 and 13.5 ka, pollen data suggest lower temperature than inferred by δD_{BA} record. Despite similar sampling resolution, multiple fluctuations of δD_{BA} during the early Holocene are not observed in the pollen data (Figure 3). The discrepancies may result from misrepresentation of dry conditions as cool conditions by the pollen method, and/or the misrepresentation of dry conditions as warm conditions by the isotopic data (both δD_{BA} from Blood Pond and carbonate $\delta^{18}O$ from Crawford Lake). Although the northeastern North America is known for positive P-E ratio, which favors relatively small evaporative enrichment, a radical decrease in the P-E balance could enrich D/H ratios of lake water. The low lake level between 15 to 13.5 ka (Shuman et al., 2001) may have

enriched lake water D/H ratios, causing higher δD_{BA} values. Alternatively, the close proximity to the Laurentide ice sheet during the pre-YD period could alter the moisture source for precipitation, the precipitation seasonality. Local hydrologic factors also have altered the residence time of the lake, the balance of groundwater and surface runoff into the lake, and/or the source of groundwater. More studies are needed to reconcile these discrepancies.

Overall patterns of the abrupt climate change in northeastern North America

Comparison of the Blood Pond δD_{BA} data with the GISP2 $\delta^{18}O$ record reveals similarity in the number and timing of abrupt climate events during the late Pleistocene (Figure 3). Five Greenland cold regimes have been centered around 14.8 (OD1), 14 (OD2), 13.2 (IACP), 12.3 (YD, 12.9 – 11.6) and 11.4 ka (PBO). Consistent with this, five cold periods are found in Blood Pond. The $\delta^{18}O$ data from Crawford Lake, Ontario and White Lake, New Jersey also suggest similar climate shifts (Yu et al., 1998; Yu, 2006). The similarity in the sequence of the climate events implies that repeated reversals during the late Pleistocene in the North Atlantic region is related to a common cause i.e., the changes in thermohaline circulation due to freshwater outbursts (Clark et al., 2001).

During the early Holocene, the linkage of the climate regimes of Greenland and northeastern North America appears to have weakened. There is more variability in the northeastern North America than in the Greenland, and the amplitude of the temperature increase after the PBO is larger in the northeastern North America records (~ $6^{o}C$) than in

Greenland (~2^{o}C). The GISP2 $\delta^{18}O$ data show a more gradual temperature increase until 10 ka (Figure 3). Melting of the Laurentide ice sheet (LIS) from 12 to 10 ka accelerated due to the elevated summer insolation in North Hemisphere (COHMAP, 1988). The combination of the high insolation and rapidly retreating LIS may have resulted in a faster warming trend on the North American continent than in Greenland after the YD. Additionally, Blood Pond δD_{BA} values show six negative isotopic shifts, indicating cold events lasting decades to centuries which are not observed in the Greenland record (Figure 3). The timing of these events is close to the freshwater outbursts of relatively smaller magnitudes from Lake Agassiz, centered at ~10.6, 10.4, 10.3, 10.0, 9.5, and 9.2 ka (e.g., Clark et al., 2001; Teller et al., 2002). The cold freshwater may influence northeastern North America by cooling coastal waters and the local atmosphere, rather than strongly affecting the thermohaline circulation and altering the climate around the North Atlantic basin, as has been suggested for the YD, PBO and 8.2 ka events(e.g., Clark et al., 2001; Alley and Agustsdorrit, 2005). Therefore, the effect of these smaller freshwater outbursts on the Greenland ice sheet was minimal.

CONCLUSIONS

D/H ratios of behenic acid (C_{22} *n*-acid) or δD_{BA} are strongly correlated to the surface air temperature (T) along a 19-lake transect in eastern North America. The temperature dependence of δD_{BA} is 4.3‰/^{o}C. This is consistent with the relationship between isotopic precipitation and T in eastern North America (5.2‰/^{o}C), when the isotopic fractionation of behenic acid ($\alpha = 0.8681$) is taken into consideration. In Blood Pond, isotope-inferred temperatures closely track pollen-inferred temperatures. Therefore, the general features of the δD_{BA} are robust, although some disagreement between pollen and isotopic values demonstrates the potential for different responses of lake water δD values and terrestrial vegetation to climate change. Abrupt climate events observed in the GISP2 ice core during the Late Pleistocene are also detected in δD_{BA} record from Blood Pond. This implies that climate change in both Greenland and northeastern North America during this time was related to a common cause, namely the changes in thermohaline circulation in North Atlantic Ocean due to freshwater outbursts. During the early Holocene, climate in northeastern North America showed greater variability than in Greenland, possibly reflecting multiple climate forcing factors in northeastern North America versus a more uniform control by solar insolation above Greenland ice sheet. Multiple episodes of fresh water outbursts from Lake Agassiz may have induced a number of abrupt climate cooling events in northeastern North America during the early Holocene, each lasting several decades.

ACKNOWLEDGEMENTS

We thank two anonymous reviewers for their helpful comments on the early version of this paper. This work was supported by grants from the National Science Foundation (NSF 0318050, 0318123, 0402383) to Y. Huang.

REFERENCES

Alley R.B. and Agustsdottir A.M. (2005) The 8k event: cause and consequences of a major Holocene abrupt climate change. *Quaternary Science Reviews* 24, 1123-1149.

Clark P.U., Marshall S.J., Clarke G.K.C., Hostetler S.W., Licciardi J.M. and Teller, J.T. (2001) Freshwater forcing of abrupt climate change during the last glaciation, *Science* 293, 283-287.

COHMAP Members. (1988) Climatic changes of the last 18,000 years: Observations and model simulations. *Science* 241, 1043-1052.

Cwynar L.C. and Spear R.W. (2001) Late glacial climate change in the White Mountains of New Hampshire. *Quaternary Science Reviews* 20, 1265-1274.

Davis M.B. and Botkin D.B. (1985) Sensitivity of cool-temperate forests and their fossil pollen record to rapid temperature-change. *Quaternary Research* 23, 327-340.

Dawson D., Grice K., Wang S.X., Alexander R. and Radke J. (2004) Stable hydrogen isotopic composition of hydrocarbons in torbanites (Late Carboniferous to Late

Permian) deposited under various climatic conditions. *Organic Geochemistry* 35, 189-197.

Hou J., Huang Y., Wang Y., Shuman B., Oswald W.W., Faison E. and Foster D.R. (2006) Postglacial climate reconstruction based on compound-specific D/H ratios of fatty acids from Blood Pond, New England, *Geochemistry Geophysics Geosystems* 7, doi:10.1029/2005GC001076.

Huang Y., Shuman B., Wang Y. and Webb T.III. (2002) Hydrogen isotope ratios of palmitic acid in lacustrine sediments record late Quaternary climate variations, *Geology* 30, 1103-1106.

Huang Y., Shuman B., Wang Y. and Webb T.III. (2004) Hydrogen isotope ratios of individual lipids in lake sediments as novel tracers of climatic and environmental change: a surface sediment test. *Journal of Paleolimnology* 31, 363-375.

Hughen K.A., Overpeck J.T., Peterson L.C. and Trumbore S. (1996) Rapid climate changes in the tropical Atlantic region during the last deglaciation. *Nature* 380, 51-54.

Kurek J., Cwynar L.C. and Spear R.W. (2004) The 8200 cal yr BP cooling event in eastern North America and the utility of midge analysis for Holocene temperature reconstructions. *Quaternary Science Reviews* 23, 627-639.

Peteet D.M., Vogel J.S., Nelson D.E., Southon J.R., Nickmann R.J. and Heusser L.E (1990) Younger Dryas Climatic Reversal in Northeastern USA - AMS Ages for an Old Problem. *Quaternary Research*, 33 219-230.

Rozanski K., Araguás-Araguás L. and Gonfiantini R. (1993) Isotopic patterns in modern global precipitation. *In* "Climate change in continental isotopic records." (P. K.

Swart, K. C. Lohmann, J. McKenzie, and S. Savin, Eds.), pp. 1-36. AGU Monographs. American Geophysical Union, USA.

Sauer P.E., Eglinton T.I., Hayes J.M., Schimmelmann A. and Sessions A.L. (2001) Compound-specific D/H ratios of lipid biomarkers from sediments as a proxy for environmental and climatic conditions. *Geochimica et Cosmochimica Acta* 65, 213-222.

Shemesh A. and Peteet D. (1998) Oxygen isotopes in fresh water biogenic opal - Northeastern US Allerød-Younger Dryas temperature shift. *Geophysical Research Letters* 25, 1935-1938.

Shuman B., Bravo L., Kaye J., Lynch J.A., Newby P. and Webb T.III. (2001) Late Quaternary water-level variations and vegetation history at Crooked Pond, Southeastern Massachusetts. *Quaternary Research* 56, 401-410.

Shuman B., Bartlein P.J., Logar N., Newby P. and Webb T.III. (2002) Parallel climate and vegetation responses to the early Holocene collapse of the Laurentide Ice Sheet. *Quaternary Science Reviews* 21, 1793-1805.

Stuiver M., Grootes P.M. and Braziunas T.F. (1995) The GISP2 $\delta^{18}O$ climate record of the past 16,500 years and the role of sun, ocean, and volcanoes. *Quaternary Research* 44, 341-354.

Teller J.T., Leverington D.W. and Mann J.D. (2002) Freshwater outbursts to the oceans from glacial Lake Agassiz and their role in climate change during the last deglaciation. *Quaternary Science Reviews* 21, 879–887.

Walker I.R., Levesque A.J., Cwynar L.C. and Lotter A.F. (1997) An expanded surface-water palaeotemperature inference model for use with fossil midges from eastern Canada. *Journal of Paleolimnology* 18, 165-178.

Webb T.III., Bartlein P.J., Harrison S.P. and Spaulding W.G. (1993) Vegetation, lake levels, and climate in Eastern North America for the past 18,000 years, in *Global Climates since the Last Glacial Maximum*, edited by H.E. Wright Jr, J. E. Kutzbach, T. Webb, III, W. F. Ruddiman, F. A. Street-Perrot, and P. J. Bartlein, University of Minnesota Press, Minneapolis, 415-467.

Webb T.III., Shuman B., Leduc P., Newby P. and Miller N. (2003) Late Quaternary climate history of western New York State. *Bulletin of the Buffalo Society of Natural Sciences* 37, 11-17.

Yu Z. and Eicher U. (1998) Abrupt climate oscillations during the last deglaciation in central North America. *Science* 282, 2235-2238.

Yu Z. (2006) Rapid response of forested vegetation to multiple climatic oscillations during the last deglaciation in the northeastern United States. *Quaternary Research* 67, 297-303.

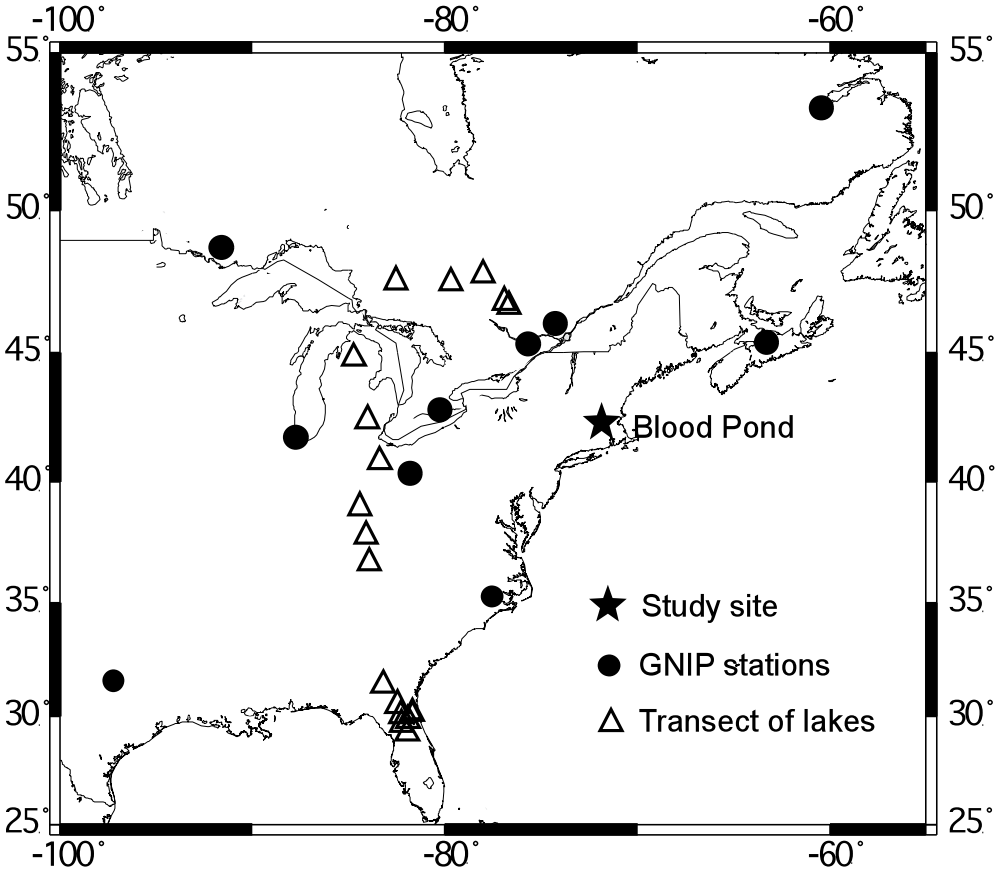

Figure 1. Map showing the location of Blood Pond (star), the GNIP stations (solid circles) and lakes along north-south transect (solid triangles).

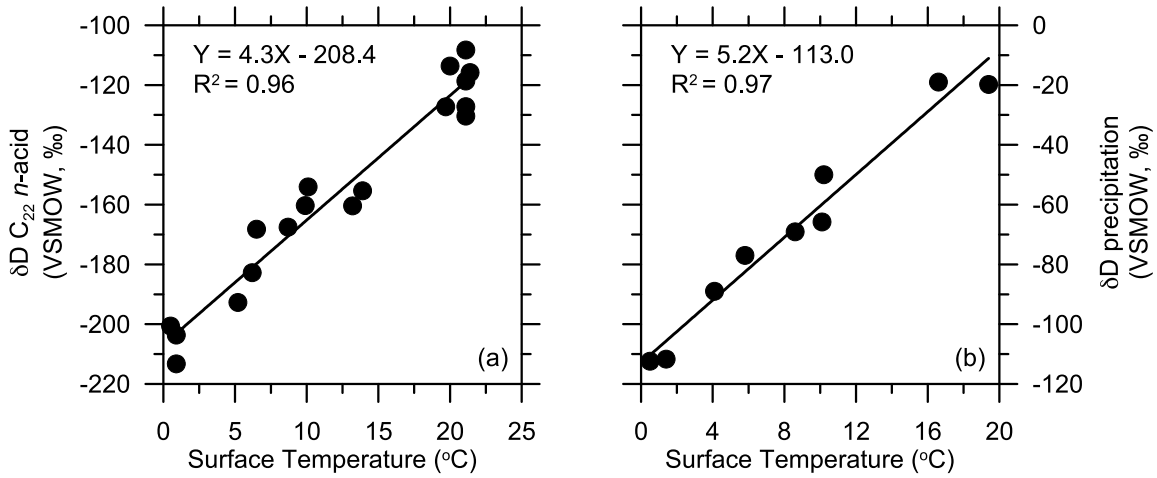

Figure 2. Correlation between (a) D/H ratios of behenic acid (C_{22} *n*-acid) or δD_{BA} and surface air temperature (T) along the north-south transect in eastern North America, (b) mean annual δD of precipitation (δD_P) and surface air temperature (T) in eastern North America (1961-1987, data from Rozanski et al., 1993).

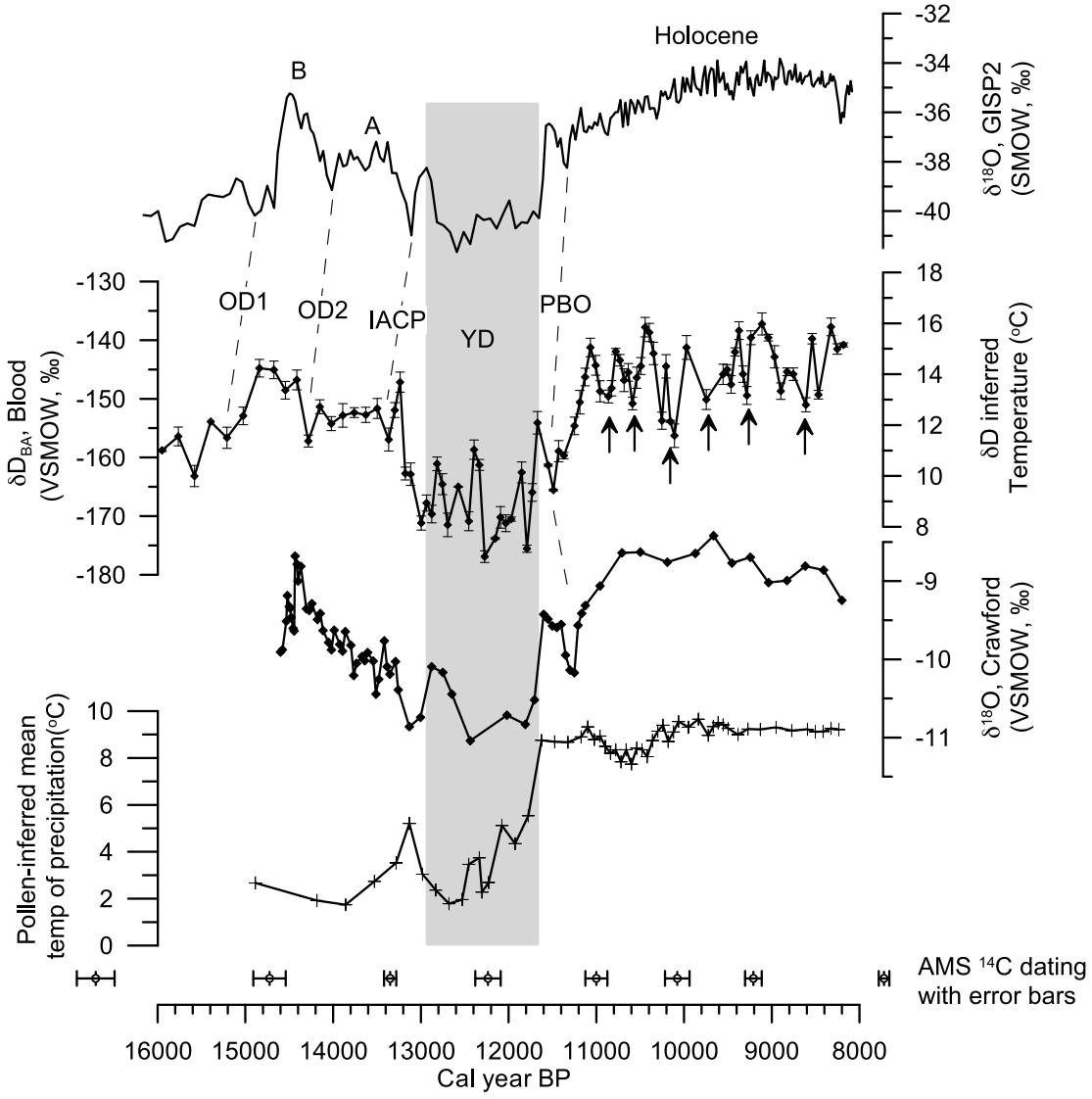

Figure 3. δD_{BA} record and pollen-inferred temperature from Blood Pond during the transition from late Pleistocene to Holocene in comparison with $\delta^{18}O$ data from Greenland Ice Sheet Project 2 (GISP2), and carbonate $\delta^{18}O$ from Crawford Lake. The dashed lines indicate the corresponding cold periods, OD1: Oldest Dryas; OD2: Older Dryas, IACP: Intra-Allerød cold period; YD: Younger Dryas; PBO: Pre-Boreal oscillation; B: Bølling; A: Allerød. The arrows besides of δD_{BA} curve indicate the freshwater outburst from proglacial lakes. Calibrated ages from accelerator mass spectrometry radiocarbon (AMS ^{14}C) dating with errors are shown.

CHAPTER 5

An abrupt and prominent climatic reversal at 9.2 ka in the northeastern North America

Co-authors: Yongsong Huang, Bryan N. Shuman, W. Wyatt Oswald, David R. Foster

To be submitted to

Proceedings of National Academy of Sciences of the United States of America

ABSTRACT

Continental climate during the early Holocene (from 10 to 7 ka) is characterized by multiple abrupt climatic reversals such as the well-known 8.2 ka event that has been observed worldwide and attributed to the terminal collapse of the Laurentide Ice Sheet (LIS) in the North American continent. However, many episodes of meltwater releases occurred prior to the final collapse of LIS, their impact on the continental climate is much less understood. We present in this paper decadal-scale hydrogen isotopic records of aquatic and terrestrial plant biomarkers from Blood Pond, Massachusetts during the early Holocene. Our isotopic records infer a cooling of 3~4 °C between 9.3 and 9.1 ka against the millennial scale climate background, mainly induced by changes in precipitation seasonality. In comparison, the 8.2 ka event displays smaller amplitude of temperature cooling of 1~2 °C at our southern New England site. We interpret our observed climatic reversal at ~ 9.2 ka as representing increased proportion of winter precipitation in conjunction with a drier and cooler summer, triggered by slowdown in thermohaline circulation as a result of freshwater release from the proglacial lakes. We attribute the difference in climate response at 8.2 ka and 9.2 ka events to the configuration of LIS, with 9.2 ka LIS having a much stronger blocking effect on the moisture from the Gulf of Mexico during the summer. Our data suggest that the seasonality of the precipitation at the southern New England was highly sensitive to meltwater releases, especially prior to the final collapse of the LIS.

Abrupt climate changes are of great societal concern because they have great impacts and far-reaching consequences on natural ecosystems and human societies. Better understanding of the mechanisms driving the abrupt climate changes is among the most important tasks in climate prediction research. One much discussed triggering mechanism for abrupt climate shifts is a rapid slowdown in the thermohaline circulation (THC) as a result of freshwater release from the proglacial lakes (Lake Agassiz and Ojibway) on the North American continent during the late Pleistocene to early Holocene (e.g., Clark et al., 2002). A series of freshwater release events occurred between 14 to 8 ka (e.g., Teller and Leverington, 2004), triggering widespread abrupt climate shifts, such as the well-known Younger Dryas (e.g., Alley, 2000) and 8.2 ka event (e.g., Alley and Agustsdottir, 2005).

Recently, Fleitmann et al. (2008) suggest that there might be another widespread climate reversal at 9.2 ka associated to freshwater release occurred at 9.17±0.15 ka. Paradoxically, however, the climatic responses so far observed at 9.2 ka appear to be disproportionally large, given that the estimated freshwater volume centered at 9.17±0.15 ka was only ~ 5% of the freshwater release that triggered the 8.2 ka event at 8.45±0.03 ka (Teller and Leverington, 2004). For example, the reduction in Indian and East Asian monsoons around 9.2 ka is several times larger than that during the 8.2 ka event (Dykoski et al., 2005). However, the isotopic variation at 9.2 ka in Greenland ice cores is slightly smaller than that at 8.2 ka event (Vinther et al., 2006). Currently the spatial distributions and amplitude of climate shift at 9.2 ka around the globe are poorly established, especially in comparison with the widely reported 8.2 ka event (e.g., Alley and

Agustsdottir, 2005). It is still highly uncertain if the suggested "9.2 ka event" is truly worldwide and the amplitude of climate shift is indeed exceptional.

Northeastern North America is among the most critical regions to understanding abrupt climate changes induced by the freshwater releases. Theoretically, this region should be highly sensitive to the freshwater release due to its proximity to the freshwater paths from the proglacial lakes, as exemplified by the dramatic climate reversal during the late Pleistocene (e.g. Younger Dryas, Shuman et al., 2005; Hou et al., 2007). However, existing paleoecological records in this region (e.g., Webb et al., 1993; Shuman et al., 2002; Cwynar and Spear, 2001) could be complicated by the insufficient sensitivity to the transient, abrupt forcing (e.g., Davis and Botkin, 1985) and do not provide clear indications for the short climate reversals at ~ 9.2 ka. Compound-specific hydrogen isotope analyses of aquatic lipids in sediments offer a new, highly sensitive approach to quantify past abrupt climate variability. The technique is especially useful for regions like northeastern North America where the lake sediments lack carbonate deposit. Organic compounds produced by algae and aquatic plants track lake water isotopic variations (e.g., Huang et al., 2002; 2004; Hou et al., 2006; Sauer et al., 2001) and mean annual surface air temperature (Hou et al., 2007) in regions of high precipitation-evaporation (P-E) ratio. In addition, D/H ratios of terrestrial plant leaf waxes record D/H ratios of water for plant biosynthesis, which reflect a combination of groundwater and/or growing season precipitation in northeastern North America (White et al., 1981). The combination of the D/H ratios of both aquatic and terrestrial biomarkers would provide more comprehensive

information on past climate and environment changes because of the general instantaneous response of precipitation isotopic ratios to climate change.

Here, we present decadal-scale D/H records of C_{22} and C_{28} *n*-alkanoic acids to quantify the centennial-scale climate variability during the early Holocene, especially the relative amplitudes of climate reversals around the 9.2 ka and 8.2 ka; and to better understand the mechanisms for centennial-scale temperature variability in northeastern North America.

DECADAL-SCALE, PRECIPITATION-WEIGHTED TEMPERATURE RECORDS FROM BLOOD POND

D/H ratios of C_{22} *n*-alkanoic acid (δD_{BA}) have been demonstrated as a reliable proxy for lake water isotopic composition (Hou et al., 2006) and mean annual surface air temperature (Hou et al., 2007). The relationship between δD_{BA} and surface air temperature (T) (δD_{BA} = 4.3T -208.4‰, R^2= 0.96, p <0.001) is consistent with the relationship between precipitation δD variability and temperature from the GNIP stations in eastern North America (Hou et al., 2007) as the lake water derives ultimately from precipitation. Besides of the impact of temperature, the δD_{BA} values are also influenced by the precipitation seasonality (relative proportion of seasonal precipitation) because the C_{22} *n*-acid is produced mainly by aquatic macrophytes using lake water (Ficken et al., 2000; Hou et al., 2006). The lake water in the New England region is recharged mainly by ground water and cool season precipitation (Shuman and Donnelly, 2006).

The δD_{BA} and inferred temperature records from Blood Pond sediment core do not show pronounced variations during the early Holocene from 10 to 7 ka, in contrast to the significant variability of δD_{BA} and temperature records between 15 to 10 ka from the same sediment core (Hou et al., 2007; Fig.1, also see supplemental material). Two features of the Blood Pond δD_{BA} records during the early Holocene (10 – 7 ka) are particularly noticeable (Fig.1). First, there are two prominent and abrupt isotopic shifts during the early Holocene, one occurring between 9.3 and 9.1 ka with ~ 35 ‰ δD shift, and the other 8.5-8.35 kyr BP with ~ 15 ‰ δD shift. Secondly, the δD values increased

gradually between 9.7 and 8.3 kyr BP by 10‰, then decreased slightly until 7.2 ka by 10‰. If the observed δD_{BA} variation of ~ 35 ‰ around the 9.2 ka represents only mean annual air temperature variability, the amplitude of change would be >6 °C. This is unlikely, given that our estimated temperature change during the YD event is approximately the same amplitude (Hou et al., 2007). We attribute our observed isotopic change as a combination of seasonal shift in precipitation and temperature around 9.2 ka, with the former factor predominating. We have no means to separate these two effects at this time, and therefore designate changes in δD_{BA} to precipitation-weighted temperature, which integrates both factors. The duration of the 9.2 ka event in Blood Pond records defined by CLIM-X-DETECT (Mudelsee, 2006) spans 9.3 to 9.1 ka, which is consistent with the visual observation. The amplitude defined by CLIM-X-DETECT is ~ 3°C, which is slightly smaller than the visual observation. Therefore, the 9.2 ka event revealed by Blood Pond δD_{BA} records spans about 200 years (9.3-9.1 ka) and the precipitation weighted temperature variability is about 3°C cooler than the millennial-scale background temperature during early Holocene. Suggestions of a ~9.2 ka climate reversal are recently found in Wildwood Pond, New York, where an evident sandy layer suggests a brief period of cold and dry climate around 9.2 kyr BP (Oswald et al., in review).

The Blood Pond temperature record also reveals a clear climate reversal from 8.45 to 8.3 kyr BP, spanning ~ 150 yrs (Figs. 1 & 2). The maximal precipitation weighted temperature change is ~ 3 ^{o}C, or 1.5 ^{o}C relative to millennial background temperature based on the CLIM-X-DETECT program. Many published lake sediment records in northeastern North America have identified climate reversals at ~ 8.4 to 8.2 ka. For

example, δD records of both aquatic (C_{16} *n*-acid) and terrestrial (C_{28} *n*-acid) biomarkers from Berry and Crooked Ponds, Massachusetts suggest a multi-century period of cold conditions from 8.4 to 8.0 ka (Shuman et al., 2006). Pollen records from North Pond (Shuman et al., 2004) and Makepeace Cedar Swamp (Newby et al., 2000) also reveal abrupt climate changes around this time. Midge assemblages and LOI records from two lakes in White Mountain also reflect cooling between 8.4 and 8.2 kyr BP (Kurek et al., 2004). LOI and sediment grain size records from Brown's Lake in Ohio also showed abrupt variations from 8.9 to 8.0 ka (Lutz et al., 2008). Due to the uncertainties in radiocarbon chronology, it is likely that all these observed climate reversals in northeastern North America occurred around the same time and correspond directly to the so called 8.2 event in Greenland (Alley et al., 1997) and other regions of the world (e.g., Alley and Agustsdottir, 2005). However, it is also likely that the climate reversal at New England indeed proceeded the 8.2 event on top of Greenland ice sheet by ~ 200 years, because a number of independently dated lake records show a similar timing of climate reversal at ~ 8.4 ka (Shuman et al., 2002; Shuman et al., 2006). Most importantly, the freshwater release that has been suggested to trigger the "8.2 event" occurred at 8.4 ka rather than 8.2 ka (Teller and Leverington, 2004). Therefore, it is possible that the climate reversal in New England show different sensitivity and timing of response to the 8.4 ka freshwater release from Greenland ice core records. We will fully discuss possible scenarios in the next section of this paper.

δD records of leaf waxes (δD_{wax}) at Blood Pond show significantly different variability from δD_{BA} records during the early Holocene (Fig.2). δD_{wax} records revealed

gradually decreasing trend from 10 to 7 ka by ~ 10‰, with abrupt increase of 10‰ around 9.3 – 9.1 ka, and 10‰ at 8.5 – 8.35 ka. Higher plants use a combination of summer precipitation and ground water as their source water in the northeastern United States (White et al., 1985; Hou et al., 2008), with summer precipitation has much higher D/H ratios than groundwater. The gradual decrease trend of δD_{wax} records from 10 to 7 ka probably suggest a slowly decreased contribution of summer precipitation and/or increased contribution of groundwater to the plant source water. This is supported by the increase in regional lake level during the same period (Fig.2; Shuman et al., 2001; Newby et al., 2000). The abrupt increase in δD_{wax} around 9.3 – 9.1 and 8.5 – 8.5 ka may imply abrupt increases in contribution from summer precipitation as the higher plant source water.

MECHANISMS FOR THE ABRUPT CLIMATE SHIFTS DURING THE EARLY HOLOCENE

The slowdown in thermohaline circulation in North Atlantic Ocean caused by the freshwater releases from the proglacial lakes (Lake Agassiz and Ojibway) have been suggested to be responsible for the 8.2 event (e.g., Barber et al., 1999; Alley and Agustsdottir, 2005) and the recently suggested 9.2 ka event (Fleitmann et al., 2008). The slowdown in THC resulted in a decrease of the northward heat transport by the North Atlantic Ocean, probably leading to increased sea-ice cover in northern North Atlantic Ocean (Wiersma and Renssen, 2006). The increased sea-ice cover would result in steeper thermal gradient between high and low latitudes, which decreases the precipitation at high latitudes (including Europe, North Atlantic Ocean, Asia and North America) associated with modifications to atmospheric circulation (Renssen et al., 2002;Wiersma and Renssen, 2006). The climate effect of the slowdown in THC as a result of meltwater outburst have also been simulated in various models (e.g., Renssen et al., 2002; Alley and Agustsdottir, 2005; Wiersma and Renssen, 2006), suggesting generally cool and dry climate in Northern Hemisphere around 8.2 ka.

Fleitmann et al. (2008) suggest that there might be a worldwide “9.2 ka event”, as shown by the widespread and nearly synchronous climatic perturbation during the early Holocene. The evidence for the possible existence of such an event is based on the alignment of a set of high-quality climate records across climate zones, including speleothem records from Dongge Cave in China (Dykoski et al., 2005) and Qunf Cave in

Oman (Cai et al., 2008), Greenland ice cores (NGRIP, GRIP and DYE-3) (Vinther et al., 2006), and oxygen isotope records from Lake Ammersee, Germany (von Grafenstein et al., 1999). Fleitmann et al. (2008) suggest that freshwater release to the North Atlantic Ocean centered at 9.17±0.15 ka caused the slowdown in THC, which then induced widespread climate changes. Our hydrogen isotopic records of the C_{22} and C_{28} *n*-acids from Blood Pond represent the first quantitative indicators for abrupt climatic reversal at ~ 9.2 ka in the northeastern North America, where the climate is likely to be highly responsive to meltwater releases, such as demonstrated by the large cooling during the Younger Dryas event (Webb et al., 1993; Hou et al., 2007). The abrupt isotopic shift at 9.2 ka from Blood Pond is concurrent with Greenland ice core records (Vinther et al., 2006), lake sediment records (e.g., von Grafenstein et al., 1999), speleothem records(e.g., Dongge Cave, China (Dykoski et al., 2005), Qunf Cave, Oman (Fleitmann et al., 2007), and Dongshiya Cave, China (Cai et al., 2008) (Fig.1).

There is a significant conflict if one assumes that amount of meltwater released into north Atlantic is proportional to the degree of climate reversal. The volume of the meltwater outburst triggered the 8.2 ka event was the largest freshwater release during the early Holocene (5.2 Sv if released within one year, 1 Sv = 10^6 m^3/s) (Teller and Leverington, 2004). The volume of the freshwater release centered at 9.17 ka was only ~5% of the meltwater outburst triggered 8.2 ka event. However, the climate responses to the two freshwater release events are very different for the currently available, high resolution records during the early Holocene. The precipitation weighted temperature variability at 9.2 ka is at least 2 times larger than that at 8.4 ka in the Blood Pond record

(Figs.1 & 2). There are several records around the world that show greater 9.2 ka climate response than the response at 8.2 ka, including the speleothem $\delta^{18}O$ records from Dongge Cave, China which show 1‰ and 0.5‰ for 9.2 and 8.2 ka events respectively (Dykoski et al., 2005) and the ostracod $\delta^{18}O$ records from Lake Ammersee which show 1.0‰ and 0.7‰ variation for the two abrupt events (von Grafenstein et al., 1999). However, the ice core oxygen isotope records from Greenland show very similar response for the climate change at 9.2 and 8.2 ka (Fig.1; Vinther et al., 2006).

AMPLITUDES OF THE ABRUPT CLIMATE SHIFTS DURING THE EARLY HOLOCENE

We attribute the amplitude difference between the two abrupt climate reversals in northeastern North American continent during the early Holocene primarily to two possible factors 1) the difference in geographic distribution of Laurentide Ice sheet (LIS) and associated atmospheric circulation at 9.2 ka and 8.2 ka (Fig.3); and 2) to lesser extent, different meltwater paths at 9.2 and 8.4 ka. The LIS extent varied dramatically in North American continent during the 9.2 ka event and the 8.2 ka event, in contrast to the relatively invariable Greenland Ice Sheet (Fig.3; Peltier, 1994). The relatively large and southerly LIS at 9.2 kyr BP may have created a strong anticyclone system (Fig.3A) that can effectively reduce the moisture input from Gulf of Mexico into northeastern North America. This could also interfere with the heat transport by Gulf Stream to the north, leading THC to a less stable status. The freshwater release into North Atlantic Ocean around 9.2 ka would further slowdown the THC, which then amplified the effect of anticyclone on the climate in this region. However, as the LIS collapsed around 8.4 ka (Fig.3B), the anticyclone system over the North American continent would disappear or be very weak, which cannot effectively block the moisture from Gulf of Mexico. The THC would be more stable as the interference from the anticyclone was minimal. The slowdown in THC as a result of freshwater release into North Atlantic Ocean around 8.4 ka would influence the climate in northeastern North American continent to a less extent because of lack of positive feedback to the anticyclone system around 9.2 ka. Therefore, the climate response in New England to freshwater release is likely amplified at 9.2 ka

than at 8.4 ka, about doubled as exemplified by Blood Pond temperature records. The positive feedback between the anticyclone over North America and slowdown in THC would be propagated to Europe and Asia via atmospheric circulation. In comparison, the climate responses of Greenland at 9.2 ka and during the 8.2 ka event were not significantly different because the Greenland ice sheet did not change in size significantly from 9.2 to 8.2 ka.

The amplitude difference between the 8.2 and 9.2 ka events could also result from the routes of the freshwater release events from the proglacial lakes. The freshwater release occurred at 9.17 ka routed east through Nipigon Basin, the Great Lakes to the North Atlantic Ocean, a routing that injects freshwater close to key areas of North Atlantic Deep Water formation (Teller and Leverington, 2004). However, the final freshwater release, triggering the 8.2 ka event, routed north to Hudson Bay. It is likely that the former route may have a greater influence on the stability of the thermohaline circulation.

However, there is currently no direct evidence to support the above assumptions. Climate models have so far mostly focused on the 8.2 ka events when the Laurentide Ice Sheet (LIS) was very small or nearly absent. There are currently no models to simulate the climate effect of the meltwater outburst which triggered to the 9.2 ka event, when the LIS was still relatively large in North American continent. High spatial resolution GCM models could probably provide more insightful ideas. Moreover, high resolution (both spatial and temporal) climate records from North Atlantic Ocean and surrounding

continents will also be helpful to resolve the different regional response to the meltwater pulse from the proglacial lakes.

ABRUPT CHANGES IN PRECIPITATION SEASONALITY AT 9.2 AND 8.4 KA IN NEW ENGLAND

The hydrogen isotope records from Blood Pond suggest dramatic changes in precipitation seasonality (relative proportion of summer and winter precipitation) in northeastern North America during the early Holocene, which was caused by the changes in THC and associated atmospheric circulation. The precipitation seasonality strongly influences the D/H ratios of C_{22} *n*-alkanoic acid, which reflects the D/H ratios of lake water (Hou et al., 2006) since Blood Pond is recharged by ground water that represents annual mean precipitation. On the other side, the precipitation seasonality also affects the δD values of leaf waxes from lake sediment, as the higher plants use soil water for biosynthesis. The soil water in New England represents a combination of ground water and summer precipitation (White et al., 1985). During 10 - 9 ka, the LIS and associated anticyclone (high pressure system) prevented the moisture originated from Gulf of Mexico transporting to northeastern North America (Fig.3A). This leads to less mean annual precipitation, but mostly decreased summer precipitation, which in turn increased the proportion of winter precipitation. The LIS collapsed around 8.4 ka, therefore the associated anticyclone became very small or disappeared, and then the water vapor from Gulf of Mexico could freely penetrate into the northeastern North American continent (Fig.3B). This would lead increase in annual precipitation, but mostly increased summer precipitation, which in turn decreased the proportion of winter precipitation. The precipitation pattern would affect the isotopic composition of groundwater and lake water.

In northeastern North American continent, the groundwater isotopic ratios are generally equivalent to annual mean precipitation (Darling and Bath, 1988).

The general trends in δD records of C_{22} and C_{28} *n*-acids can be explained by the changes in precipitation seasonality. The lower C_{22} *n*-acid δD values and higher C_{28} *n*-acid δD values between 10 and 8.5 ka can be attributed to less annual precipitation (decreased proportion of summer precipitation and increased proportion of winter precipitation). Because of less mean annual precipitation, the groundwater and lake level were relatively low, the terrestrial plants mainly used summer precipitation for biosynthesis. Summer precipitation was also enriched due to the amount effect (since smaller amount of low latitude moisture will reach our study site, representing more evolved moisture along Rayleigh fractionation path). This results in higher D/H ratios in plant source water and hence the leaf waxes. The lake water in New England, recharged mainly by groundwater and cool season precipitation, would be isotopically lighter, which is recorded by C_{22} *n*-acid. After 8.4 ka when LIS collapsed, the increased annual precipitation (mainly increase in summer precipitation) led elevated groundwater and lake level. The terrestrial plants could use both groundwater and summer precipitation for biosynthesis, which results in lower D/H ratios in leaf waxes. The generally high δD values of C_{22} *n*-acid also suggest that the lake water was isotopically higher because of more contribution from summer precipitation. The changes in precipitation seasonality are supported by the lake level records from Crooked Pond (Shuman et al., 2001) and Makepeace Cedar Swamp (Newby et al., 2000) (Fig.2).

The abrupt changes in δD records at Blood Pond during the 8.2 ka and 9.2 ka events indicate the dramatic changes in precipitation seasonality in northeastern North America. The lower C_{22} *n*-acid δD values (representing depleted lake water) and higher C_{28} *n*-acid δD values (more contribution of summer precipitation) suggest extreme seasonality at the two abrupt climate reversals during the early Holocene. The less annual precipitation was dominated by winter precipitation. Simulation of precipitation seasonality could also produce similar changes in lake water isotopic composition and precipitation-weighted temperature. The average δD value of modern warm season precipitation is ~82‰, and the cool season precipitation is ~ 40‰, which were calculated from the online isotopes in precipitation calculator (OIPC, Bowen and Revenaugh, 2003). A binary isotope model shows that 20% decrease in summer precipitation would produce a 13‰ decrease in mean annual precipitation if the annual precipitation amount does change, which corresponds to variability of 2.5°C in precipitation weighted temperature.

CONCLUSION

We report the first quantitative record of an abrupt and prominent climatic reversal at 9.2 kyr BP based on hydrogen isotopic records from Blood Pond, northeastern North America. The 9.2 ka event spans ~200 yr, from 9.3 to 9.1 kyr BP, with an average ~3 °C precipitation weighted cooling against the millennium background. The "8.2 ka event" was also shown in the Blood Pond records, with a smaller response, ~1.5 °C cooling over 150 yrs and earlier timing (8.45-8.3 kyr BP) than Greenland. Both abrupt climate shifts could be triggered by the slowdown of thermohaline circulation as a result of meltwater outbursts into North Atlantic Ocean from proglacial lakes (Lake Agassiz and Ojibway) in North American continent. The difference in extent of Laurentide Ice Sheet and associated atmospheric circulation during the two abrupt climate shifts at 9.2 ka and 8.4 ka was critical in determining the climate response as a result of meltwater releases. The climate was much more sensitive to the meltwater at 9.2 ka when LIS was and large and in a more southerly position. Even though the meltwater volume at 9.2 ka was only ~5 % of that at 8.4 ka, the changes in precipitation weighted temperature was more than twice as large. The main characteristic of the 9.2 ka climate reversal in New England is the dramatic shift in precipitation seasonality. High spatial resolution GCM models, and high resolution (both spatial and temporal) climate records from North Atlantic Ocean and surrounding continents will be helpful to resolve the different regional response to the meltwater pulse from the proglacial lakes when boundary conditions were different during the early Holocene.

ACKNOWLEDGEMENTS

This work was supported by grants from the National Science Foundation (NSF 0318050, 0318123, 0402383) to Y. Huang.

REFERENCE

Alley R.B. (2000) The Younger Dryas cold interval as viewed from central Greenland. *Quaternary Science Reviews* 19, 213-226.

Alley R.B. and Agustsdottir A.M. (2005) The 8k event, cause and consequences of a major Holocene abrupt climate change. *Quaternary Science Reviews* 24,1123-1149.

Alley R.B., Marotzke J., Nordhaus W.D., Overpeck J.T., Peteet D.M., Pielke R.A.J., Pierrehumbert R.T., Rhines P.B., Stocker T.F., Talley L.D. and Wallace J.M. (2003) Abrupt climate change. *Science* 299, 2005-2010, doi:10.1126/science.1081056.

Alley R.B., Mayewski P.A., Sowers T., Stuiver M., Taylor K.C. and Clark P.U. (1997) Holocene climatic instablity: A prominent, widespread event 8200 yr ago. *Geology* 25, 483-486.

Banner J.L., Guilfoyle A., James E.W., Stern L.A. and Musgrove M. (2007) Seasonal variations in modern speleothem calcite growth in Central Texas, U.S.A. *Journal of Sedimentary Research* 77, 615-622.

Barber D.C., Dyke A., Hillaire-Marcel C., Jennings A.E., Andrews J.T., Kergin M.W., Bilodeau G., McNeely R., Southon J., Morehead M.D. and Gagnon J.M. (1999) Forcing of the cold event of 8200 years ago by catasrophic drainage of Laurentide lakes. *Nature* 400, 344-348, doi:10.1038/22504.

Bowen G.J. and Revenaugh J. (2003) Interpolating the isotopic composition of modern meteoric precipitation. *Water Resources Research* 39, 1299, doi:10.129/2003WR002086.

Broecker W.S. (2007) Abrupt climate change revistied. *Global and Planetary Change* 54, 211-215, doi:10.1016/j.gloplacha.2006.06.019.

Cai B., Edwards R.L., Cheng H., Tan M., Wang X. and Liu T. (2008) A dry episode during the Younger Dryas and centennial-scale weak monsoon events during the early Holocene, A high-resolution stalagmite record from southeast of the Loess Plateau, China. *Geophysical Research Letters* 35, doi:10.1029/2007GL030986.

Clark P.U., Pisias N.G., Stocker T.F. and Weaver A.J. (2002) The role of the thermohaline circulation in abrupt climate change. *Nature* 415, 863-869.

Darling W.G. and Bath A.H. (1988) A stable isotope study o recharge processes in the English chalk. *Journal of Hydrology* 101, 31-46.

Davis M.B. and Botkin D.B. (1985) Sensitivity of cool-temperate forests and their fossil pollen record to rapid temperature-change. *Quaternary Research* 23, 327-340.

Denton G.H., Alley R.B., Comer G.C. and Broecker W.S. (2005) The role of seasonality in abrupt climate change. *Quaternary Science Reviews* 24, 1159-1182.

Denton G.H. and Karlén W. (1973) Holocene climatic variations, their pattern and possible cause. *Quaternary Research* 3, 155-205.

Dykoski C.A., Edwards R.L., Cheng H., Yuan D., Cai Y., Zhang M., Li Y., Qing J., An Z. and Revenaugh J. (2005) A high-resolution, absolute-dated Holocene and deglacial Asian monsoon record from Dongge Cave, China. *Earth and Planetary Science* Letters 233, 71-86, doi:10.1016/j.epsl.2005.01.036.

Ficken K.J., Li B., Swain D.L. and Eglinton G. (2000) An *n*-alkane proxy for the sedimentary input of submerged/floating freshwater aquatic macrophytes. *Organic Geochemistry* 31, 745-749.

Fleitmann D., Burns S.J., Mangini A., Mudelsee M., Kramers J., Villa I., Neff U., Al-Subbary A.A., Buettner A., Hippler D. and Matter A. (2007) Holocene ITCZ and Indian monsoon dynamics recorded in stalagmites from Oman and Yemen (Socotra). *Quaternary Science Reviews* 26, 170-188, doi:10.1016/j.quascirv.2006.04.012.

Fleitmann D., Mudelsee M., Burns S.J., Bradley R.S., Kramers J. and Matter A. (2008) Evidence for a widespread climatic anomaly at around 9.2 ka before present. *Paleoceanography* 23, doi:10.1029/2007PA001519.

Hou J., D'Andrea W.J. and Huang Y. (2008) Can sedimentary leaf waxes record D/H ratios of continental precipitation? Field, model, and experimental assessments. *Geochimica et Cosmochimica Acta* 72, doi:10.1016/j.gca.2008.04.030.

Hou J., Huang Y., Wang Y., Shuman B., Oswald W.W., Faison E. and Foster D.R. (2006) Postglacial climate reconstruction based on compound-specific D/H ratios of fatty acids from Blood Pond, New England. *Geochemistry Geophysics Geosystems* 7, doi:10.1029/2005GC001076.

Hou J., Huang Y., Oswald W.W., Foster D.R. and Shuman B. (2007) Centennial-scale compound-specific hydrogen isotope record of Pleistocene-Holocene climate transition from southern New England. *Geophysical Research Letters* 34, doi:10.1029/2007GL030303.

Kurek J., Cwynar L.C. and Spear R.W. (2004) The 8200 cal yr BP cooling event in eastern North America and the utility of midge analysis for Holocene temperature reconstructions. *Quaternary Science Reviews* 23, 627-639.

Lanzante J.R. (1996) Resistant, robust and non-parametric techniques for the analysis of climate data, theory and examples, including applications to historical radiosonde station data. *International Journal of Climatology* 16, 1197-1226.

Lie Ø. and Paasche Ø. (2006) How extreme was northern hemisphere seasonality during the Younger Dryas. *Quaternary Science Reviews* 25, 404-407.

Lutz B., Wiles G., Lowell T. and Michaels J. (2007) The 8.2 ka abrupt climate change event in Brown's Lake, northeast Ohio. *Quaternary Research* 67, 292-296, doi:10.1016/j.yqres.2006.08.007.

Mickler P.J., Stern L.A. and Banner J.L. (2006) Large kinetic isotope effects in modern speleothems. *Geological Society of America Bulletin* 118, 65-81.

Mudelsee M. (2006) CLIM-X-DETECT, A Fortran 90 program for robust detection of extremes against a time-dependent background in climate records. *Computers & Geosciences* 32, 141-144, doi:10.1016/j.cageo.200505.010.

Newby P.E., Killoran P., Waldorf M.R., Shuman B., Webb R.S., Webb T.III. (2000) 14,000 years of sediment, vegetation, and water-level changes at the Makepeace Cedar Swamp, Southeastern Massachusetts. *Quaternary Research* 53, 352-368.

Overpeck J.T. and Cole J.E. (2006) Abrupt change in Earth's climate system. *Annual review of Environment and Resources* 31, 1-31.

Peltier W.R. (1994) Ice age paleotopography. *Science* 265, 195-201.

Renssen H., Goosse H. and Fichefet T. (2002) Modeling the effect of freshwater pulses on the early Holocene climate, the influence of high frequency climate variability. *Paleoceanography* 17, doi:10.1029/2001PA000649.

Shuman B., Bartlein P.J. and Webb T.III. (2005) The magnitudes of millennial- and orbital-scale climatic change in eastern North America during the Late Quanternary. *Quaternary Science Reviews* 24, 2194-2206.

Shuman B., Bravo J., Kaye J., Lynch J.A., Newby P. and Webb T.III. (2001) Late Quaternary water-level variations and vegetation history at Crooked Pond, Southeastern Massachusetts. *Quaternary Research* 56, 401-410.

Shuman B. and Donnelly J.P. (2006) The influence of seasonal precipitation and temperature regimes on lake levels in the northeastern United States during the Holocene. *Quaternary Research* 65, 44-56.

Shuman B., Newby P., Huang Y. and Webb T.III. (2004) Evidence for the close climatic control of New England vegetation history. *Ecology* 85, 1297-1310.

Shuman B., Huang Y., Newby P. and Wang Y. (2006) Compound-specific isotopic analyses track changes in the seasonality of precipitation in the Northeastern United States at ca. 8200 cal yr BP. *Quaternary Science Reviews* 25, 2992-3002.

Teller J.T. and Leverington D.W. (2004) Glacial Lake Agassiz, A 5000 yr history of change and its relationship to the delta O-18 record of Greenland. *Geological Society of America Bulletin* 116, 729-742.

Vinther B.M., Clausen H.B., Johnsen S.J., Rasmussen S.O., Andersen K.K., Buchardt S.L., Dahl-Jensen D., Seierstad I.K., Siggaard-Andersen M.L., Steffensen J.P., Svensson A., Olsen J. and Heinemeier J. (2006) A synchronized dating of three Greenland ice cores throughout the Holocene. *Journal of Geophysical Research* 111, doi:10.1029/2005JD006921.

von Grafenstein U., Erlenkeuser H., Brauer A., Jouzel J. and Johnsen S.J. (1999) A mid-European decadal isotope-climate record from 15,500 to 5000 years BP. *Science* 284, 1654-1657.

Webb T.III., Bartlein P.J., Harrison S.P. and Spaulding W.G. (1993) Vegetation, lake levels, and climate in Eastern North America for the past 18,000 years, in Global Climates since the Last Glacial Maximum, edited by H.E. Wright Jr, J. E. Kutzbach, T. Webb, III, W. F. Ruddiman, F. A. Street-Perrot, and P. J. Bartlein, University of Minnesota Press, Minneapolis, 415-467.

Wiersma A.P. and Renssen H. (2006) Model-data comparison for the 8.2 ka BP even, confirmation of a forcing mechanism by catastrophic drainage of Laurentide Lakes. *Quaternary Science Reviews* 25, 63-88, doi:10.1016/j.quascirev.2005.07.009.

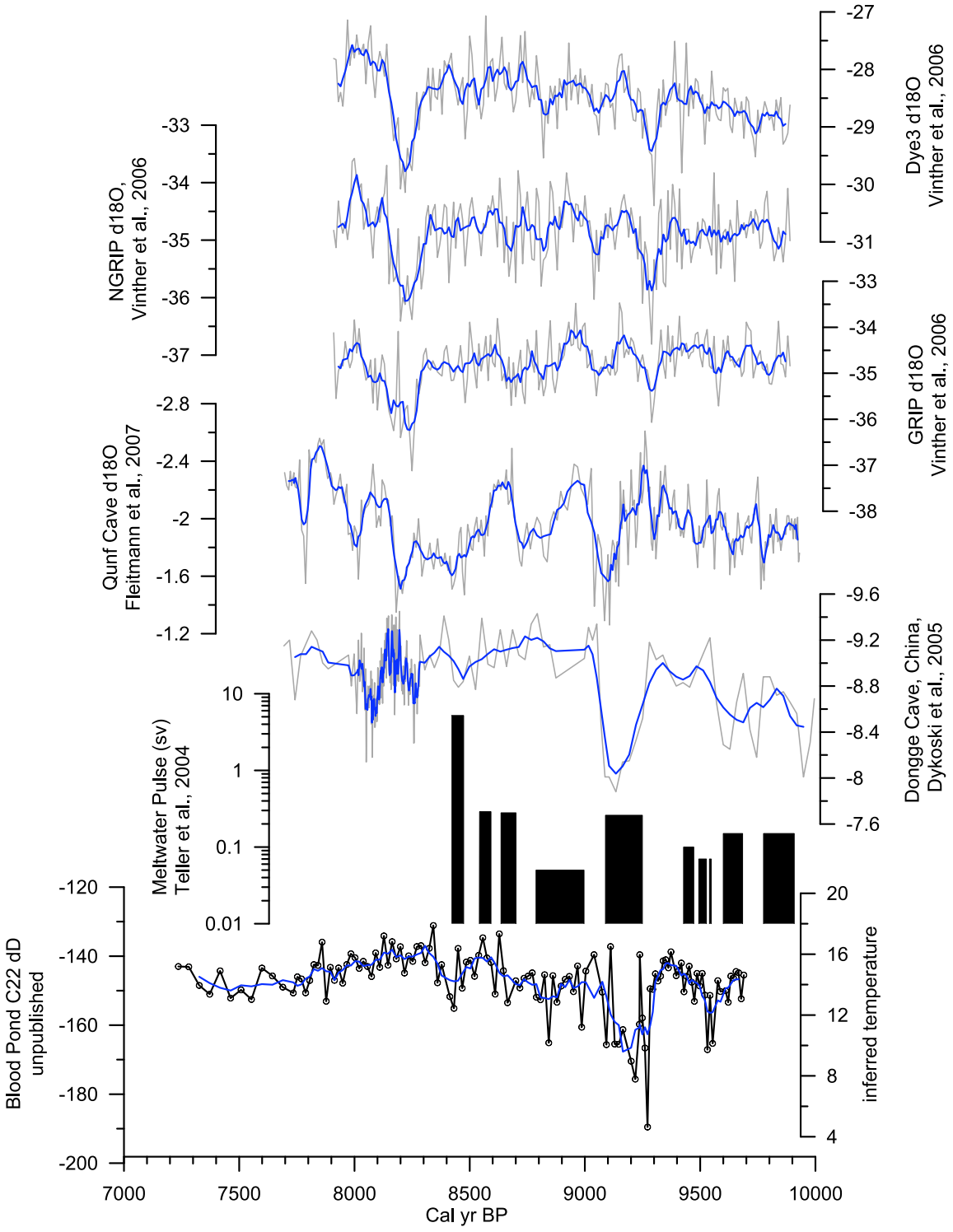

Figure 1. The 9.2 and 8.2 ka events were revealed in Blood Pond δD records, speleothem $\delta^{18}O$ records and Greenland ice core $\delta^{18}O$ records. Also shown the meltwater outbursts from proglacial lakes during the early Holocene.

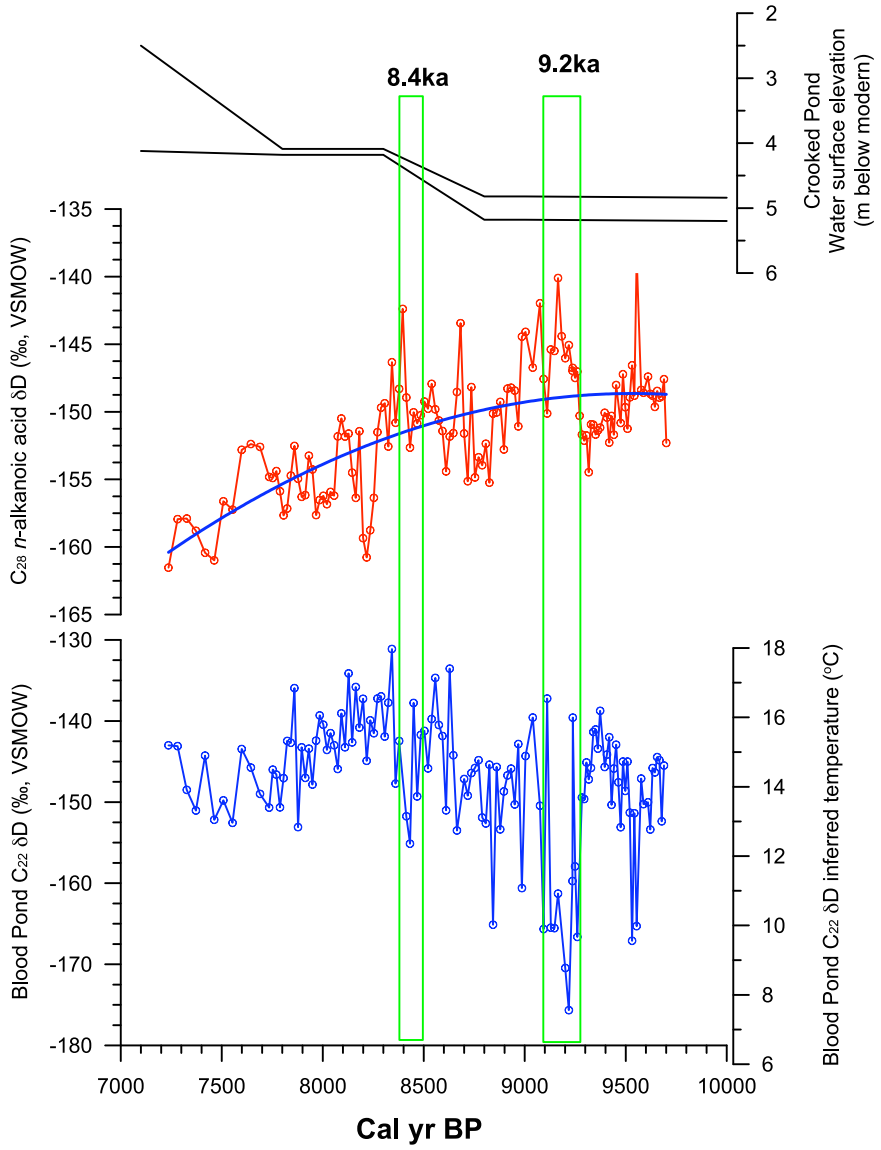

Figure 2. Comparison between δD records of C_{22} and C_{28} n-alkanoic acids. D/H ratios of C_{22} *n*-alkanoic acid represent the precipitation-weighted temperature; D/H ratios of C_{28} *n*-alkanoic acid reflect the available water for plant biosynthesis. Lake level records from Crooked Pond (Shuman et al., 2001) are also shown to indicate the elevated lake level from 10 to 7 ka.

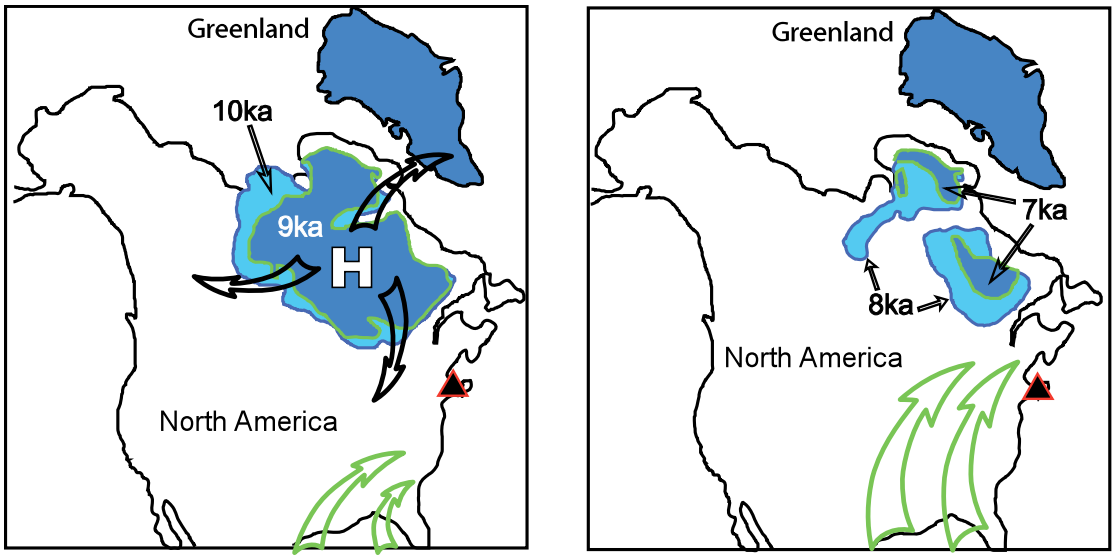

Figure 3. The extent of Laurentide Ice Sheet (LIS) in North American continent between 10 and 9 kyr BP (left), between 8 and 7 kyr BP (right), and associated anticyclone (marked as H) over LIS between 10 and 9 kyr BP. The Greenland ice sheet did not show significant variation during the early Holocene. The triangles show the location of Blood Pond in northeastern North America. The green arrows indicate the trajectories of water vapor originated from Gulf of Mexico (see text for discussion).

SUPPLEMENTARY MATERIALS

1. METHODS

We examined a sediment core from the Blood Pond, Massachusetts, the United States. The age model of the core was established by C-14 dating of bulk sediments and plant macrofossils and published previously (Hou et al., 2006). Ages are reported as thousands of calibrated years before present (kyr BP). Average sedimentation rate for the study section in this study is 1.2 mm/yr. Each sample spans 1 cm, and the distance between two neighboring samples is 2 cm, which leads to the average sampling resolution of ~25 yr. Compound-specific hydrogen isotope analysis of *n*-alkanoic acids was performed using gas chromatography – isotope ratio monitoring mass spectrometry. Each sample was run in triplicate and the standard deviation of all samples is <± 2‰. Method details and the isotope are available in supplemental material. Detailed procedures and instrumental conditions for the isotopic analyses are reported previously (Huang et al., 2002, 2004).

In order to detect the duration and amplitude of the abrupt climate reversal, we performed a robust, statistical method to detect the anomaly in order to avoid highly inflated values in presence of extremes (Lanzante, 1996). A Fortran 90 program CLIM-X-DETECT (Mudelsee, 2006), specifically designed for the purpose of anomaly detection, is used to calculate the running median ($2k$+1 window point) as estimator of the time-dependent trend and the running median of absolute distances to the median (MAD) as estimator of the time-dependent variability. The 95% confidence band, which

is employed to define the extremes detection threshold, is given by median ± 2.96MAD. The duration of an anomaly is given by the time points that the detection threshold is crossed. The size of an anomaly is the maximum of the peak value minus median, divided by the MAD. We selected k = 45, which leads to average window width on the order of 1000 years. It permits us to explore millennial-scale background and variability.

2. CHRONOLOGY

The chronology of the Blood Pond sediment core during the early Holocene was based on five radiocarbon dates (Figure S1).

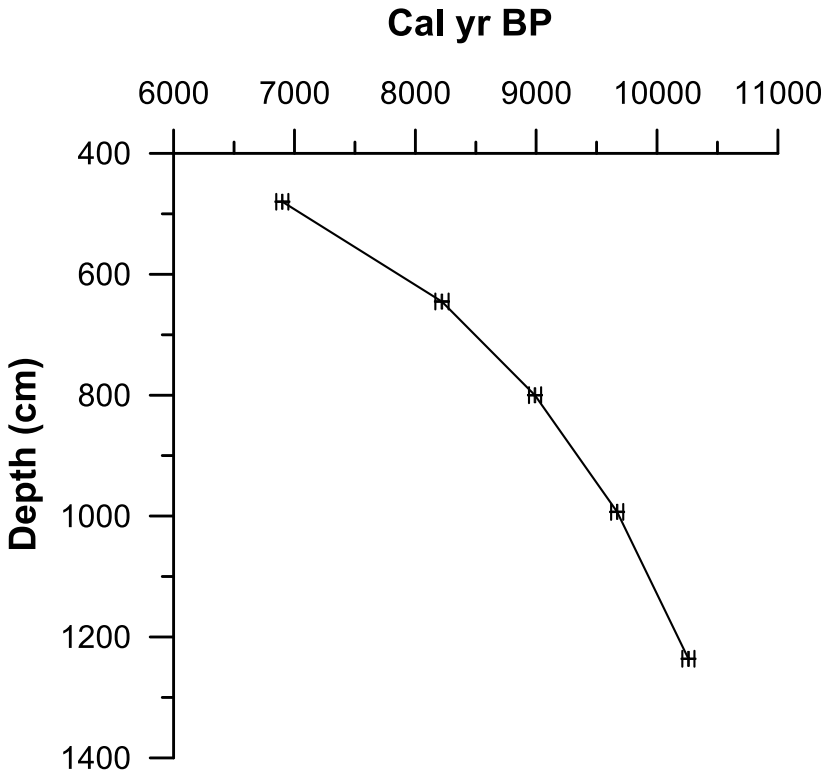

Figure S1. Five radiocarbon dates provide the chronology for the Blood Pond sediment core during the early Holocene.

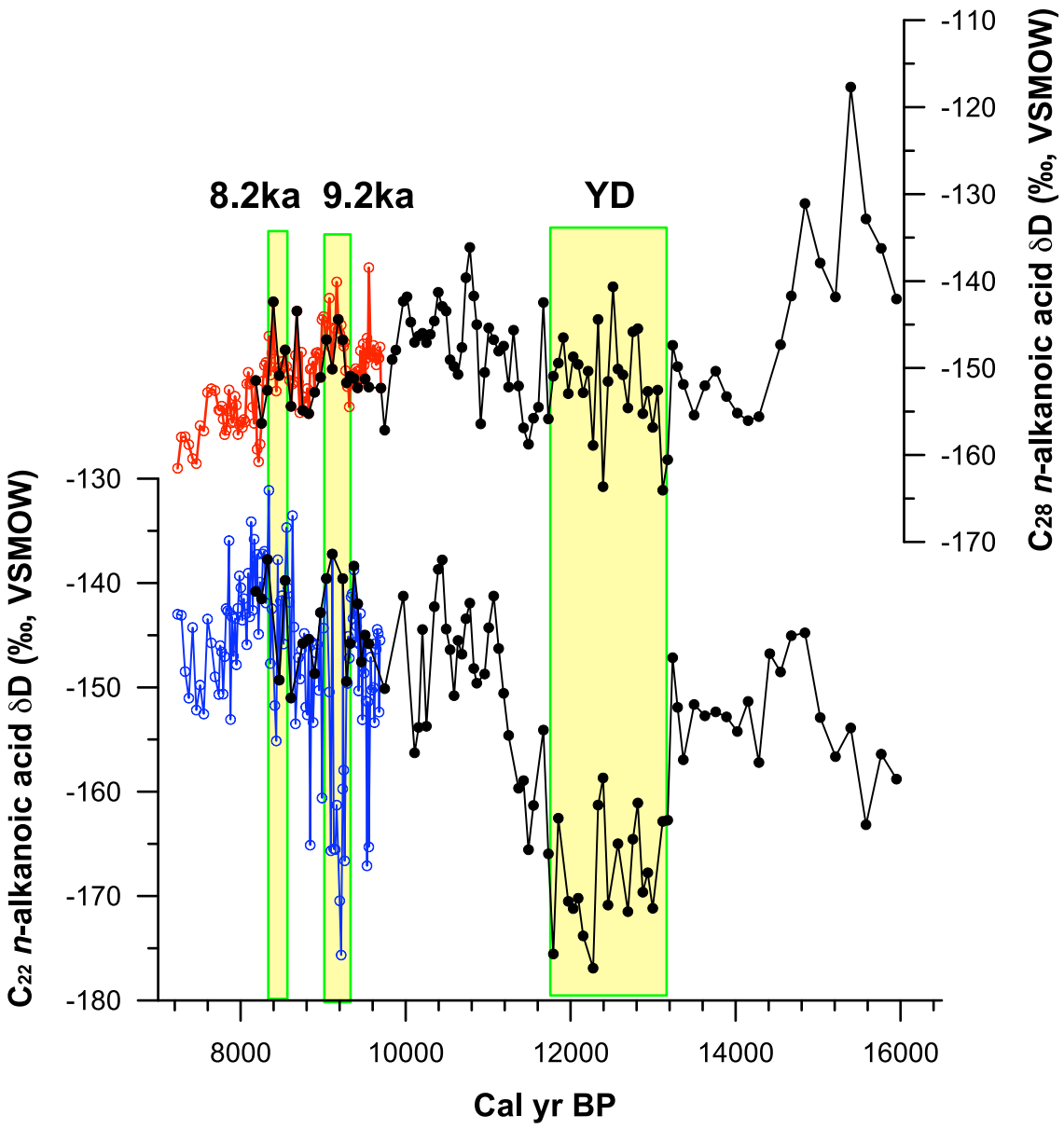

Figure S2. Comparison between Blood Pond hydrogen isotope records during the early Holocene and records from the late Pleistocene. The late Pleistocene records show prominent variability, while the early Holocene records show less variability. However, two abrupt climate shifts (9.2 and 8.4 ka) were shown during the early Holocene.

CHAPTER 6

Solar activity induced pronounced temperature oscillations during the late Pleistocene to the early Holocene in the northeastern North America

Co-author: Yongsong Huang

To be submitted to

Science

Sensitivity of the Earth's climate to the solar activity has profound implications for modeling future climate changes, but is a subject of intense scientific debate. GCM modeling considering solar forcing can successfully simulate climatic variations in the past millennia such as the Little Ice Age (LIA), but volcanic forcing during the same time period can also yield similar climatic effect and confound interpretations. Here we present decadal to centennial resolution compound-specific hydrogen isotopic records from two lakes in the northeastern North America to investigate the relationship between solar activity and temperature changes during the late Pleistocene to early Holocene. Our temperature reconstructions from the two lakes 100 km apart in New England are highly consistent with each other and agree well with established general climatic scenarios. More importantly, our records contain centennial-scale cyclicities related to the solar cycles (88 and 232 yr), indicating strong links between the pronounced 1 to 2^{o}C temperature oscillations and solar activity during the late Pleistocene. Our results strongly support the presence of an internal amplification mechanism for the solar forcing that is capable of causing disproportionally large climatic responses with relative small changes in the incoming solar radiation.

The causes and controlling mechanisms for the Earth climatic change on different time scales have been subjected to intensive study in order to better predict future climatic changes. On relatively long time scale (several thousands to tens and hundreds of thousands years) in the past few million years, changes in the Earth orbital configuration played a dominant role in the prominent climatic oscillations such as the glacial – interglacial variations (e.g., Imbrie et al., 1992). However, the mechanisms for the climate changes of relatively short time (e.g., decadal to centennial), which are more relevant to the human society, remain much less understood. Solar forcing has been proposed to be one plausible mechanism for the decadal- to centennial- scale climate changes, such as those observed during the well known little ice age (LIA, mid-1600s to early 1700s) and medieval warm period (MWP, 1100s-1500s) (Bard et al., 2000). However, the impact of solar variability on climate changes has been highly controversial, because of the minute amplitude of solar irradiance variation over decadal to centennial time scales (e.g., decrease by only ~ 0.1 % of the total irradiance during LIA; Bard et al., 2000). Although solar-forced climate model have successfully simulated the climate changes on northern hemisphere continents during LIA by involving changes of ozone chemistry and the North Atlantic Oscillation or NAO (Shindell et al., 2001), the credibility of the solar forcing of the LIA is questioned by the evidence for the coincident enhanced volcanic activity (e.g., Mann et al., 2005; Briffa et al., 1998). Increased volcanic eruptions would produce similar cooling effects during the LIA as changes in solar forcing, making the two factors virtually impossible to distinguish.

Here we present new evidence for prominent solar forcing of the temperature variations in New England based on a high-resolution hydrogen isotopic record from Rocky Pond, MA (Fig.1). Rocky Pond sediment has high sedimentation rate (2 m/kyr) during the late Pleistocene to early Holocene transition, allowing decadal scale down core analysis (see Fig.S1 in Supplementary Material). The modeling results of Shindell et al. (2001) indicate that the Northeastern North America is an exceptionally sensitive region to the solar variability on Earth, because of internal amplification mechanisms related to the North Atlantic Oscillation. For example, the relatively small variations in solar irradiance during the LIA (~0.1 %) induced up to 1.0 °C temperature change, especially during the winter (Shindell et al., 2001). However, so far there have been no paleo-temperature records from northeastern North America beyond the last 1000 years that have sufficient time resolution to detect the solar forcing on the climate change, and to support the model results. Because our new isotopic record is from the late Pleistocene to early Holocene, we avoid the overlap with volcanic forcing factor during the LIA that has so far confounded the interpretation (Briffa et al., 1998). In this paper, we will first demonstrate that our hydrogen isotopic data from Rocky Pond record the regional temperature changes during the late Pleistocene to early Holocene, and are consistent with previous published results. We will then show that the spectral components in our records are related to the solar variability. Our results strongly support that solar cycles can indeed drive disproportionably large climatic oscillations through Earth's internal feedback mechanisms.

We measured hydrogen isotope (D/H) ratios of C_{22} *n*-alkanoic acid (behenic acid) from solvent extractable fraction and sediment bound C_{16} *n*-alkanoic acid (palmitic acid) from the Rocky Pond sediment core (Huang et al., 2004). D/H ratios of C_{22} *n*-alkanoic acid (δD_{BA}) have been demonstrated to be a reliable temperature proxy (δD_{BA} = 4.3T - 208.4‰, Hou et al., 2007). D/H ratios of bound C_{16} *n*-alkanoic acid (δD_{PA}) from lake surface sediment track lake water D/H ratios with constant isotopic fractionation along lake transects in eastern North America (Huang et al., 2004). δD_{PA} also show strong correlation with annual mean temperature variability (δD_{PA} = 3.3 T – 202, R^2 = 0.95, p <0.001. See supplementary materials for method and data).

Temperature variations during the Pleistocene – early Holocene transition inferred from C_{22} and C_{16} *n*-alkanoic acids at Rocky Pond show remarkable similarity to those of Blood Pond and record well-known climate fluctuations (Fig.2). For example, the Bølling and Allerød warm periods were indicated by the increase in δD values and temperature. The short cool periods, Older Dryas (OD, ~14.1 ka) and Intra-Allerød cold period (IACP, ~13.5 ka) during the late Pleistocene, which were indicated by single samples in Blood Pond records, were clearly revealed in Rocky Pond records (Fig.2). The amplitude of OD and IACP were similar, ~3 ^{o}C cooler than Allerød warm period. The most significant temperature variability occurred at the beginning and end of the Younger Dryas (YD). All records show about ~6-7 °C cooler than the early Holocene. The Preboreal Oscillation (PBO), an abrupt and short cool period around 11.4 ka, was also revealed by multiple samples in Rocky Pond records, which is similar to OD and IACP. Temperature increased ~ 6 ^{o}C abruptly at the end of YD. Following PBO, temperature increased ~ 6 ^{o}C

gradually until 10 ka. The consistent results from two different lakes further support that δD_{BA} and δD_{PA} are reliable temperature proxies and record regional temperature variability. There are some differences between the temperature records from Rocky Pond and Blood Pond. Notably, the Rocky Pond temperatures are generally ~2^{o}C higher than Blood Pond. The temperature difference is likely due to the proximity of Rocky Pond to the Atlantic coast (100 km). The modern temperature around Rocky Pond is 1.5 °C higher than Blood Pond. Blood Pond record also shows slightly smaller temperature fluctuations during OD, Allerød warm period and IACP than Rocky Pond record. This probably results from the lower temporal resolution of the Blood Pond records. In addition, based on independent radiocarbon dates, the end of YD at Rocky Pond is ~ 11.9 ka, about 100 years earlier than the Blood Pond record, which the YD ends ~11.8 ka. We will discuss this chronology issue in the next section.

Chronology for the two lake sediment cores was established independently by 5 radiocarbon dates from two lakes, respectively, between 15 to 10 ka (Fig.2). Ages between individual dates are linearly interpolated. Unfortunately, one of the dates (11995.5±245.5 yr) for the Rocky Pond prior to the termination of YD has large errors due to the coincidence with the radiocarbon plateau (Goslar et al., 1999). We have previously compared with our Blood Pond chronology and isotopic records with pollen data (Hou et al., 2007). Our results indicate Blood Pond chronology is accurate, especially for the termination of the YD. In order to avoid inconsistencies for the spectral analysis, we tuned the end of YD as indicated by δD_{BA} at Rocky Pond to the same timing as Blood Pond (Fig.2). The revised chronology for Rocky Pond is consistent with

regional paleoecological and paleoclimate records (e.g., Hou et al., 2007; Shuman et al., 2002; Yu et al., 1997; Ellis et al., 2004). The δD records from Rocky Pond were re-plotted using the tuned chronology in Fig.1s in the supplementary materials.

We performed singular spectrum analysis (multi-taper method) on the temperature records from both Rocky and Blood Pond. Both δD_{BA} and δD_{PA} records from Rocky Pond show prominent spectral peaks centered at 504-, 232-, 131- and 88 yr (Fig.3A, B). Temperature inferred from C_{22} *n*-alkanoic acid show additional peaks compared with C_{16} *n*-alkanoic acid record, centering at 805-, 427-, 299-, and 105-yr. Temperature records from Blood Pond also show spectral peak at 427- and 232 yr (Fig.3). The absence of 88 yr cycle at Blood pond is due to the relatively low time resolution (~80 yr). The spectra are confirmed by the Gaussian band-passing of all temperature records from Rocky and Blood Ponds (see Fig.S3 in supplementary materials).

The spectra peaks (88 and 232 yr) shown in Rocky and Blood Pond temperature records are well documented by the atmospheric ^{14}C production record, which is a proxy for solar variability (Damon and Sonett, 1990; Solanki et al., 2004, Fig.3). Moreover, the temperature variation from the northeastern North America appears to be coherent with time series of the cosmogenic nuclides, ^{14}C (Fig.4). Notably, the 232 yr cycle in both lakes shows stronger amplitude during the middle of Younger Dryas, whereas the 232 yr cycle in ^{14}C production record shows small amplitude and opposite trend during the same interval. This suggests a higher sensitivity of the regional climate during colder times.

The temperature in northeastern North America increased during periods of strong solar activity, as indicated by the lower ^{14}C production (Fig.4). The lower temperature was correlated with the periods of less solar activity. Our results suggest that the centennial-scale climate variability during the late Pleistocene to early Holocene from northeastern North America is closely related to solar activity.

The mechanisms how the relatively small amplitude irradiation change of the sunspot cycle may cause disproportionally large climatic response in the northern hemisphere continents have been discussed by Shindell et al. (1999, 2001) and Bard et al. (2000), Bard and Frank (2006). During the Little Ice Age, for example, the global average temperature changes that can be modeled by solar forcing alone are relatively small (~ 0.3 to 0.4^{o}C lower during the Maunder Minimum). However, a key component for the amplified temperature change in the northern hemisphere continents is the North Atlantic Oscillation (NAO) (Shindell et al., 1999; Shindell et al., 2001). The reduced solar irradiance leads to lower tropical and subtropical sea surface temperature (SST), reduced latitudinal temperature gradient at 100 to 200 mbar, and diminished stratospheric westerly winds. These changes then result in decreased angular momentum transport to high latitudes and reduced tropospheric westerlies and associated temperature and pressure changes corresponding to a low NAO/AO (Shindell et al., 1999a; Shindell et al., 2001a). The dynamic feedbacks of ozone chemistry in troposphere are also involved in the mechanism to enhance or dampen the climate response to solar forcing (Shindell et al., 1999b; Shindell et al., 2001b). This is because the solar irradiation variation is not spectrally averaged: the relative amplitude of the UV variability is an order of magnitude

larger than the total irradiance changes. When solar input increases, the strong UV variations lead to enhanced ozone formation in the stratosphere (Gille et al., 1984) and excess UV adsorption by ozone, which causes additional heating the stratosphere. Therefore, changes in ozone chemistry are a positive feedback to the solar forcing.

In the high-index NAO (positive phase), the eastern United States coast experiences mild and wet winter because the increased atmospheric pressure difference between subtropical high and polar low deviates the storm track on a more northerly track. On the other hand, in the low-index NAO (negative phase), the eastern United States coast experience much cold climate because the reduced press gradient bring the storm track more west-east pathway (Hurrell et al., 2003). Although the NAO is a mode of variability internal to the atmosphere, model results and paleoclimate records suggest the mean state of NAO also show centennial-scale variability. For example, lower SST records from Sargasso Sea and warm temperature in the area off Newfoundland during 16^{th} to 19^{th} centuries coincides with the reduced NAO during the same period (Keigwin and Pickart 1999). The GCM simulations also suggest low NAO index during the Maunder Minimum (Shindell et al., 2001b). Therefore, the decadal to centennial-scale temperature variability in northeastern North America can be attributed to solar irradiance changes combined with the changes in ozone chemistry, but strongly amplified by the changes in the mean state of NAO.

Our records provide the first evidence for a robust connection between solar irradiance and centennial-scale temperature variability during the late Pleistocene to early Holocene. In contrast to the records for the past millennia that contain the confounding effects of solar and volcanic forcing, our records extends ~5000 years and eliminates the fortuitous coincidence between the two confounding factors. Therefore, our results strongly supports that the relatively small solar forcing can lead to significant decadal to centennial scale climate change, especially on northern hemisphere continents. The amplification appears to be much stronger during the colder times (such as during the middle of YD in this study).

REFERENCE

Bard E. and Frank M. (2006) Climate change and solar variability: what's new under the Sun?. *Earth and Planetary Science Letters* 248, 1-14, doi:10.1016/j.epsl.2006.06.016.

Bard E., Raisbeck G., Yiou F. and Jouzel J. (2000) Solar irradiance during the last 1200 years based on cosmogenic nuclides. *Tellus* 52B, 985-992.

Briffa K.R., Jones P.D., Schweingruber F.H. and Osborn T.J. (1998) Influence of volcanic eruptions on Northern Hemisphere summer temperature over the past 600 years. *Nature* 393, 450-455.

Damon P.E. and Sonett C.P. (1991) Solar and terrestrial components of the atmospheric 14C variation spectrum, in Sonett, C.P., Giampapa, M.S., and Matthews, M.S., eds., The Sun in time: Tucson, The University of Arizona Press, 360-388.

Ellis K.G., Mullins H.T. and Patterson W.P. (2004) Deglacial to middle Holocene (16,000 to 6000 calendar years BP) climate change in the northeastern United States inferred from multi-proxy stable isotope data, Seneca Lake, New York. *Journal of Paleolimnology* 31, 343-361.

Gille J.C., Smythe, C.M. and Heath D.F. (1984) Observed ozone response to variations in solar ultraviolet radiation. *Science* 225, 315-317.

Goslar T., Wohlfarth B., Bjorck S., Possnert G. and Bjorck J. (1999) Variations of atmospheric ^{14}C concentrations over the Allerod - Younger Dryas transition. *Climate Dynamics* 15, 29-42, doi:10.1007/s003820050266.

Hou J., Huang Y., Oswald W.W., Foster D.R. and Shuman B. (2007) Centennial-scale compound-specific hydrogen isotope record of Pleistocene-Holocene climate transition from southern New England. *Geophysical Research Letters* 34, doi:10.1029/2007GL030303.

Huang Y., Shuman B., Wang Y. and Webb T.III. (2004) Hydrogen isotope ratios of individual lipids in lake sediments as novel tracers of climatic and environmental change: a surface sediment test. *Journal of Paleolimnology* 31, 363-375.

Hurrell J.W., Kushnir Y., Ottersen G. and Visbeck M. (2003) An overview of the North Atlantic Oscillation, in Hurrell, J.W., Kushnir, Y., Ottersen, G., and Visbeck, M., eds., The North Atlantic Oscillation - Climatic significance and environmental impact: (Geophysical Monograph; 134): Washington DC, American Geophysical Union, 1-35.

Imbrie J., Boyle E.A., Clemens S.C., Duffy A., Howard W.R., Kukla G., Kutzbach J., Martinson D.G., McIntyre A., Mix A.C., Molfino B., Morley J.J., Peterson L.C., Pisias N.G., Press W.L., Raymo M.E., Shackleton N.J. and Toggweiler J.R. (1992) On the structure and origin of major glaciation cycles. I. Linear response to Milankovitch forcing. *Paleoceanography* 7, 701-738.

Keigwin L.D. and Pickart R.S. (1999) Slope water current over the Laurentian Fan on the interannual to millennial time scales. *Science* 286, 520-523, doi:10.1126/science.286.5439.520.

Mann M.E., Cane M.A., Zebiak S.E. and Clement, A. (2005) Volcanic and Solar Forcing of the Tropical Pacific over the Past 1000 Years. *Journal of Climate* 18, 417 - 456.

Shindell D.T., Schmidt G.A., Miller R.L. and Rind D. (2001a) Northern Hemisphere winter climate response to greenhouse gas, ozone, solar and volanic forcing. *Journal of Geophysical Research* 106, 7193-7210.

Shindell D.T., Schmidt G.A., Mann M.E., Rind D. and Waple A. (2001b) Solar forcing of regional climate change during th Maunder Minimum. *Science* 294, 2149-2152, doi:10.1126/science.294.5528.2149.

Shindell D.T., Miller R.L., Schmidt G.A. and Pandolfo L. (1999a) Simulation of recent northern winter climate trends by greenhouse-gas forcing. *Nature* 399, 452-455.

Shindell D.T., Rind D., Balachandran N., Lean J. and Lonergan P. (1999b) Solar cycle variability, ozone, and climate: *Science* 284, 305-308, doi:10.1126/science.284.5412.305.

Shuman B., Bartlein P.J., Logar N., Newby P. and Webb T.III. (2002) Parallel climate and vegetation responses to the early Holocene collapse of the Laurentide Ice Sheet. *Quaternary Science Reviews* 21, 1793-1805.

Solanki S.K., Usoskin I.G., Kromer B., Schussler M. and Beer J. (2004) Unusual activity of the Sun during recent decaes compared to the previous 11,000 years. *Nature* 431, 1084-1087, doi:10.1038/nature02995.

Stuiver M., Reimer P.J., Bard E., Beck J.W., Burr G.S., Hughen K.A., Kromer B., McCormac F.G., Plicht J.v.d. and Spurk M. (1998) INTCAL98 radiocarbon age calibration, 24,000-0 cal BP. *Radiocarbon* 40, 1041-1083.

Yu Z., McAndrews J.H. and Eicher U. (1997) Middle Holocene dry climate caused by change in atmospheric circulation patterns: Evidence from lake levels and stable isotopes. *Geology* 25, 251-254.

Zanchettin D., Aubino A., Traverso T. and Tomasino M. (2008) Impact of variations in solar activity on hydrological decadal patterns in northern Italy. *Journal of Geophysical Research* 113, D12102, doi:10.1029/2007JD009157.

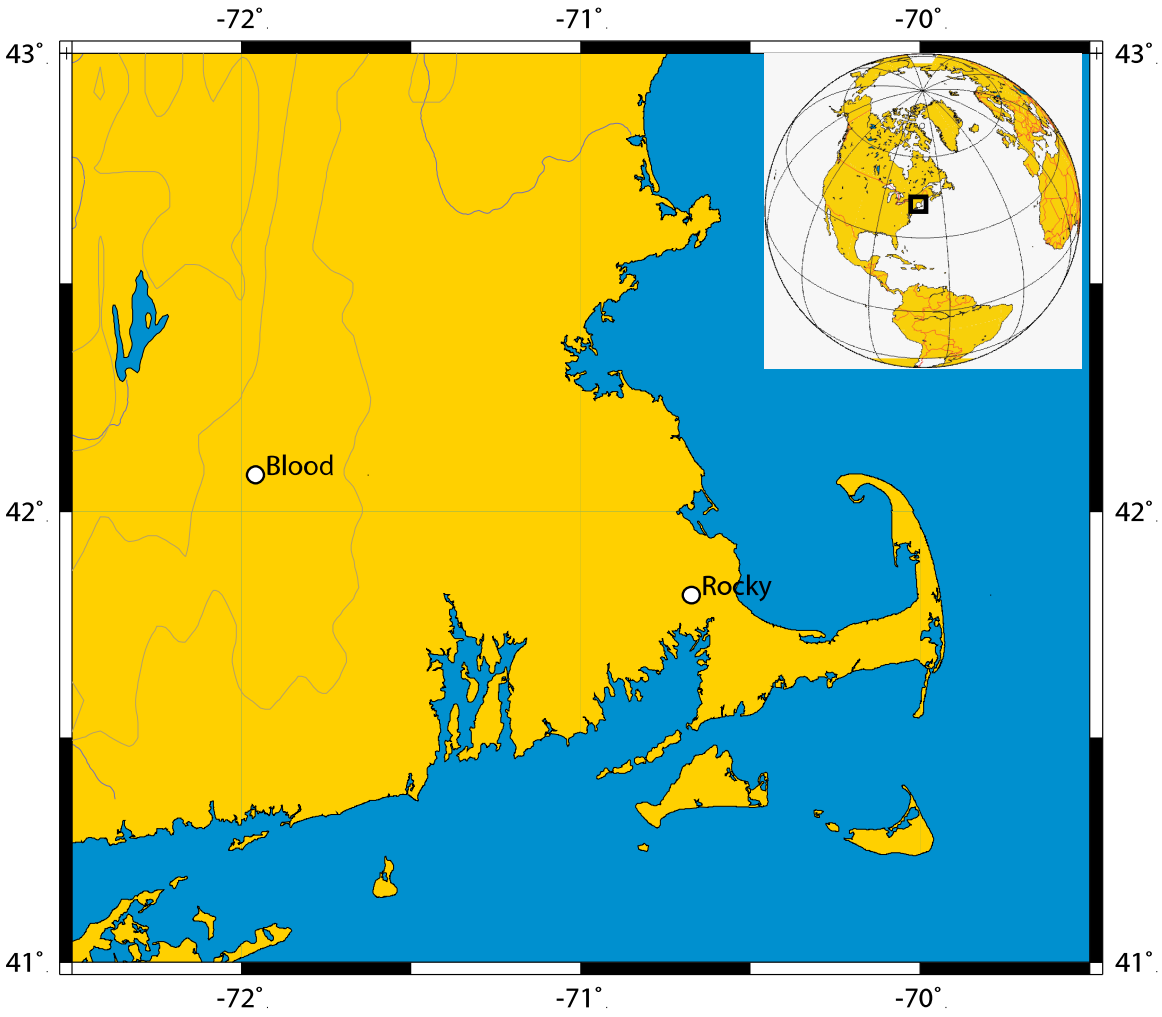

Figure 1. Location of the two lakes in northeastern North America. The two lakes are about 100 km apart, with Rocky Pond is close to the coast.

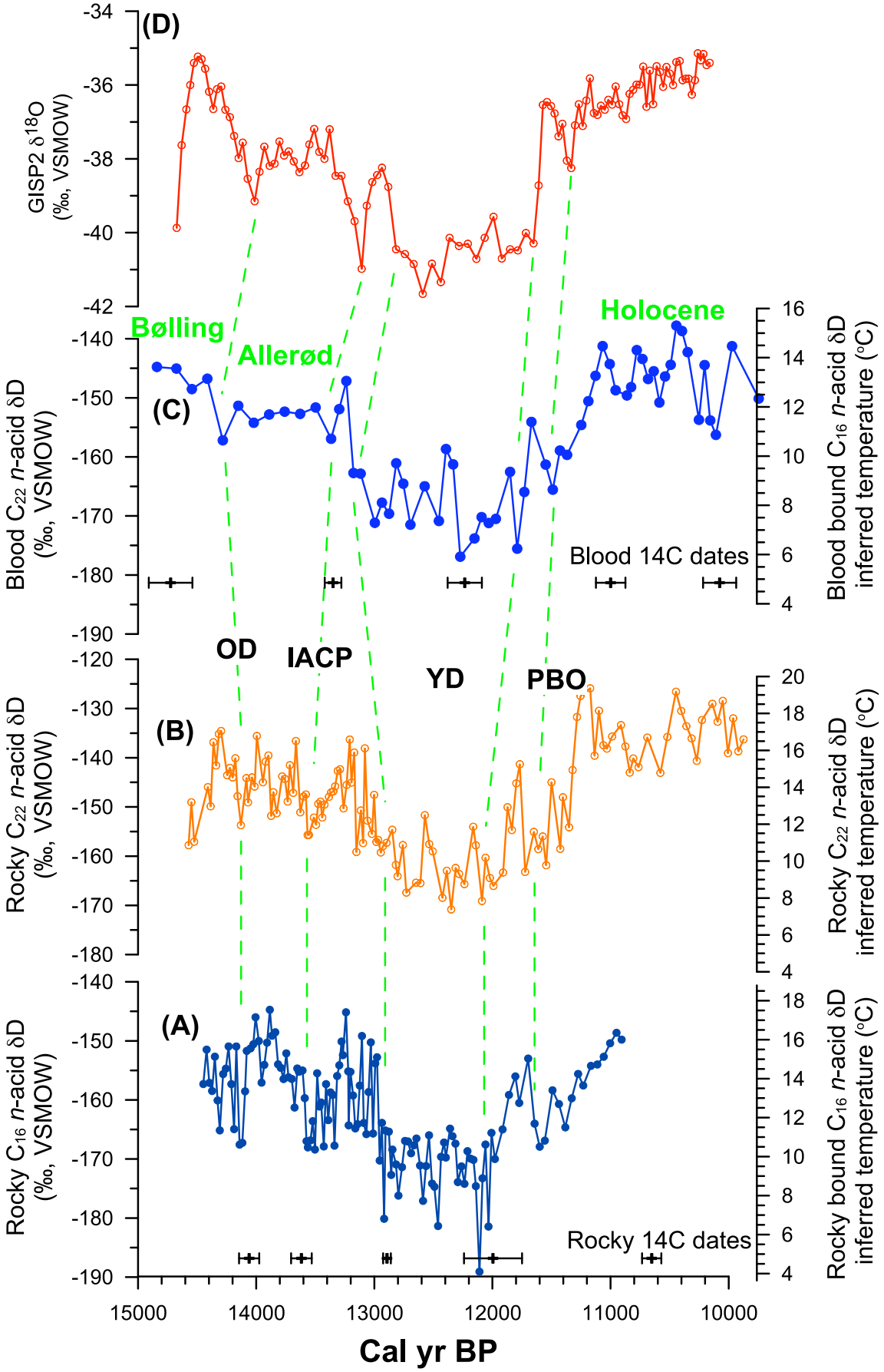
(D)
GISP2 δ18O (‰, VSMOW)
-34
-36
-38
-40
-42
Bølling
Allerød
Holocene
(C)
Blood C22 n-acid δD (‰, VSMOW)
-140
-150
-160
-170
-180
-190
Blood 14C dates
Blood bound C16 n-acid δD inferred temperature (°C)
16
14
12
10
8
6
4
OD
IACP
YD
PBO
(B)
Rocky C22 n-acid δD (‰, VSMOW)
-120
-130
-140
-150
-160
-170
-180
Rocky C22 n-acid δD inferred temperature (°C)
20
18
16
14
12
10
8
6
4
(A)
Rocky C16 n-acid δD (‰, VSMOW)
-140
-150
-160
-170
-180
-190
Rocky 14C dates
Rocky bound C16 n-acid δD inferred temperature (°C)
18
16
14
12
10
8
6
4
15000
14000
13000
12000
11000
10000
Cal yr BP

Figure 2. Hydrogen isotope records and inferred temperature from lakes in northeastern North America, (A) Rocky Pond C_{16} *n*-alkanoic acid; (B) Rocky Pond C_{22} *n*-alkanoic acid; (C) Blood Pond C_{22} *n*-alkanoic acid. The Y-axes at the left side are of hydrogen isotopic scale, the Y-axes at the right side are of temperature scale which were calculated based on the correlation between δD_{BA}, δD_{PA} and mean annual surface air temperature (T) ($\delta D_{BA} = 4.3T - 208.4‰$, $\delta D_{PA} = 3.3\ T - 202$). The GISP2 $\delta^{18}O$ records are also shown for comparison (D).

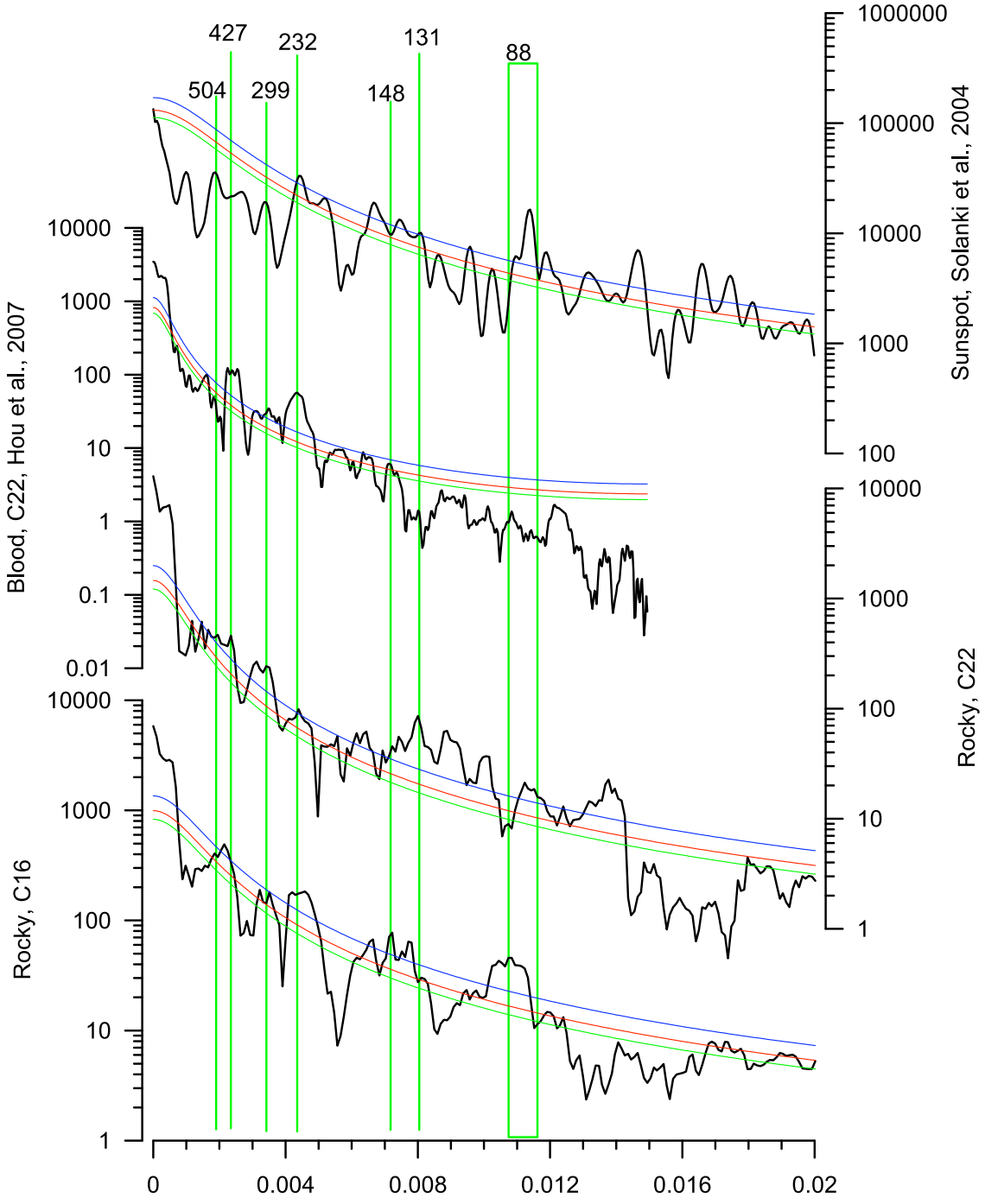

Figure 3. Spectral components of the temperature records from lakes in northeastern North America, (bottom to top), Rocky Pond C_{16}, Rocky Pond C_{22}, and Blood Pond C_{22}. The sunspot number records from Solanki et al. (2004) is also shown for comparison. All spectral analyses were performed by Singular Spectrum Analysis - MultiTaper Method (SSA-MTM) Toolkit.

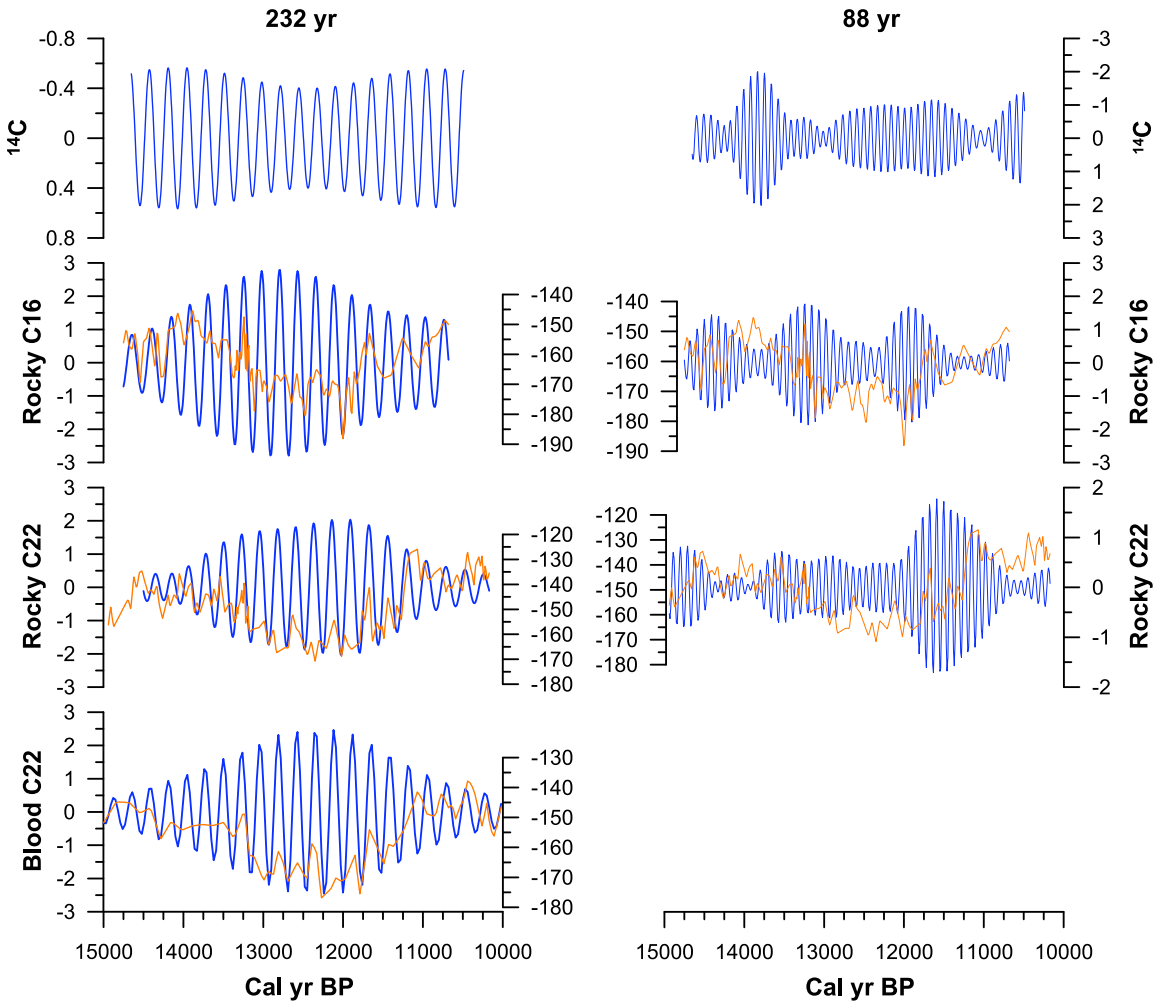

Figure 4. Band pass of two prominent solar cycles (232 and 88 years) of the Blood Pond C_{22}, Rocky Pond C_{16}, C_{22} and radiocarbon data (Stuiver et al., 1998). The hydrogen isotope data (orange curves) are also plotted to show the corresponding cyclicities. Notably, the 232 yr cycle in both lakes shows stronger amplitude during the middle of Younger Dryas, whereas the 232 yr cycle in ^{14}C production record shows small amplitude and opposite trend during the same interval.

SUPPLEMENTARY MATERIALS

1. METHODS

We examined lower part of the sediment core (15-10 ka) from Rocky Pond in northeastern North America (Fig.1). The age model of the core was established by five radiocarbon dates. The sedimentation rate was very high during the study period (~ 2mm/yr) (Fig.1). All sediment and leaf samples were freeze-dried. Sediment samples were extracted using an Accelerated Solvent Extractor (ASE200, Dionex) with dichloromethane: methanol (9:1 v/v) at 150^{o}C and 1200 psi for three 15-min cycles to get solvent-extractable lipids. Approximately 0.5-1 g of each dry sample was extracted. The bound lipids from sediment were released by saponifying the ASE extracted sediments under reflux using 2 N KOH/(Methanol + 5%water) (e.g., Meyers and Ishiwatari 1993). The solution was then acidified and extracted with hexane. The total lipid extract obtained from sediment was separated into neutral and acid fractions using Supelco® Supelclean™ LC-NH_2 silica gel using dichloromethane : isopropyl alcohol (2:1 v/v) and ether with 4% acetic acid (v/v), respectively. Acid fractions were methylated with 5% anhydrous HCl in methanol at 60 ^{o}C for 12 hours. Hydroxyl acids were removed by eluting the samples through silica gel columns using hexane, in order to further purify the fatty acid methyl esters to avoid chromatographic coelution.

Quantification and identification of compounds was performed by Gas Chromatography - Flame Ionization Detection (GC-FID) and Gas Chromatography-Mass Spectrometry (GC-MS) (HP 6890, Agilent). An HP 6890 GC interfaced to a Finnigan

DeltaPlus XL stable isotope spectrometer through a high-temperature pyrolysis reactor was used for hydrogen isotopic analysis (Huang et al., 2004). The compounds separated by the GC were pyrolyzed to H_2 and CO at 1445^{o}C. A tank of ultra high purity hydrogen gas with known δD values was used as the isotope standard during the measurements. The H_3^+ factor was determined daily prior to sample analysis (average value was 2.5 during the course of this study). The accuracy for the instrument was routinely checked by an injection of laboratory isotopic standards (C_{16}, C_{18}, C_{22}, C_{24} *n*-acid methyl esters) between every six measurements. The precisions (1σ) for the four laboratory standards were < ±2‰ throughout the entire process. The precision (1σ) for triplicate analyses of all samples was < ±2‰. δD values obtained from individual acids (as methyl esters) were corrected by mathematically removing the isotopic contributions from added groups before reporting. The δD value of the added methyl group was determined by acidifying and then methylating (along with the samples) the disodium salt of succinic acid with a predetermined δD value (using TC/EA-IRMS) (Huang et al., 2002).

2. CALIBRATION OF SEDIMENT BOUND C_{16} *n*-ALKANOIC ACID δD AS TEMPERATURE PROXY

We determined the relationship between δD_{PA} and T along the N-S transect across a temperature gradient (2 - 23^{o}C) in eastern North America (Fig.S1).

$$\delta D_{PA} = 3.3\ T - 202,\ R^2 = 0.95,\ p < 0.001 \qquad (1)$$

Based on this relationship, a 1^{o}C change in T corresponds to ~ 3.3 ± 0.2‰ variation in δD_{BA}.

The temperature dependence of δD_{PA} (3.3 ‰/^{o}C) is smaller than that of δD_{BA} (4.3‰/^{o}C) along the same transect in North America (Hou et al., 2007). This may be attributed to the sources of bound lipids and their isotopic fractionation during the production and diagenesis. Cranwell (1981) showed that the bound lipids in lake sediments were mainly produced from algal and microbial sources. Furthermore, Albaigés et al. (1984) demonstrated that the isotopic fractionation of bound lipids from microbial sources is much larger than the algal sources, which result in smaller isotopic fractionation factor. Nevertheless, the significant correlation between δD_{PA} and surface air temperature along the modern lake transect suggest that δD_{PA} could be a reliable proxy for surface air temperature. We estimated and compared the temperature variability from both C_{22} and C_{16} n-alkanoic acids from Rocky Pond during the late Pleistocene, which was also compared with regional temperature records.

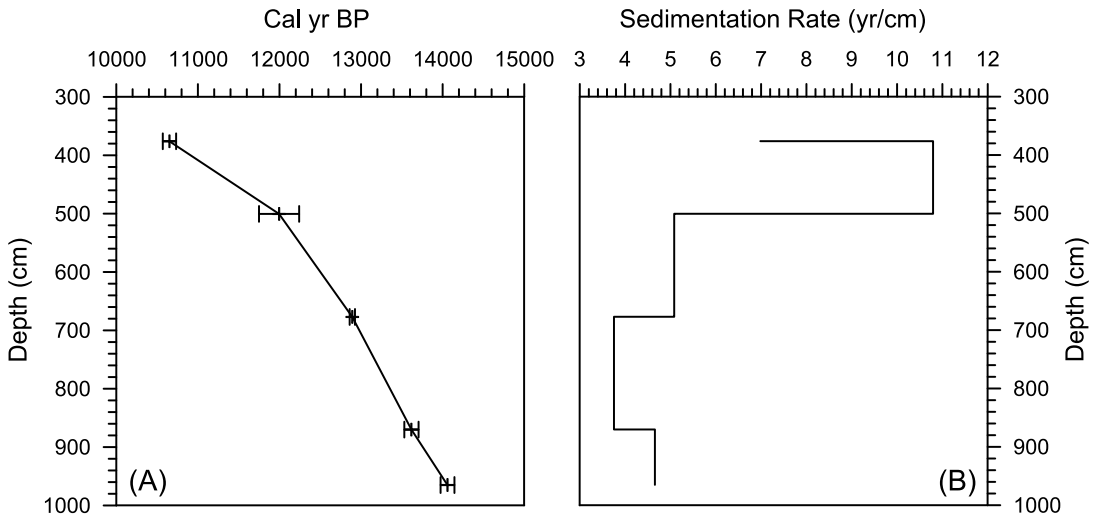

Figure S1. The Rocky Pond chronology based on five radiocarbon dates (left), and the sedimentation rate (right).

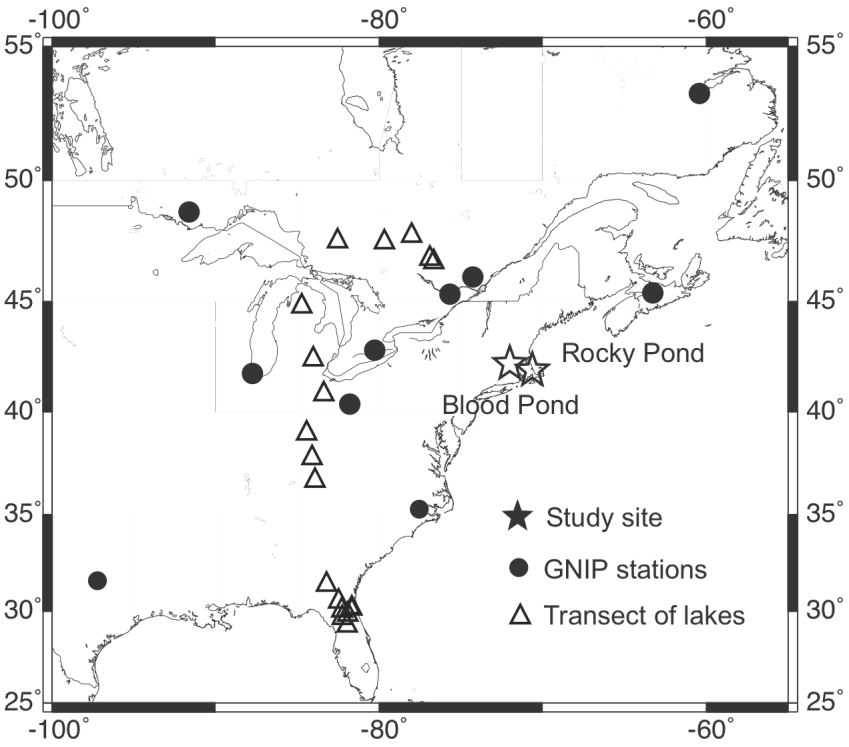

Figure S2. Map showing the location of the north-south transect of lakes (triangles) for calibration of C_{16} *n*-alkanoic acid δD values in eastern North America, the GNIP stations (solid circles) for comparison with temperature dependence of precipitation δD variation, and the study sites in the paper, Blood Pond and Rocky Pond (stars).

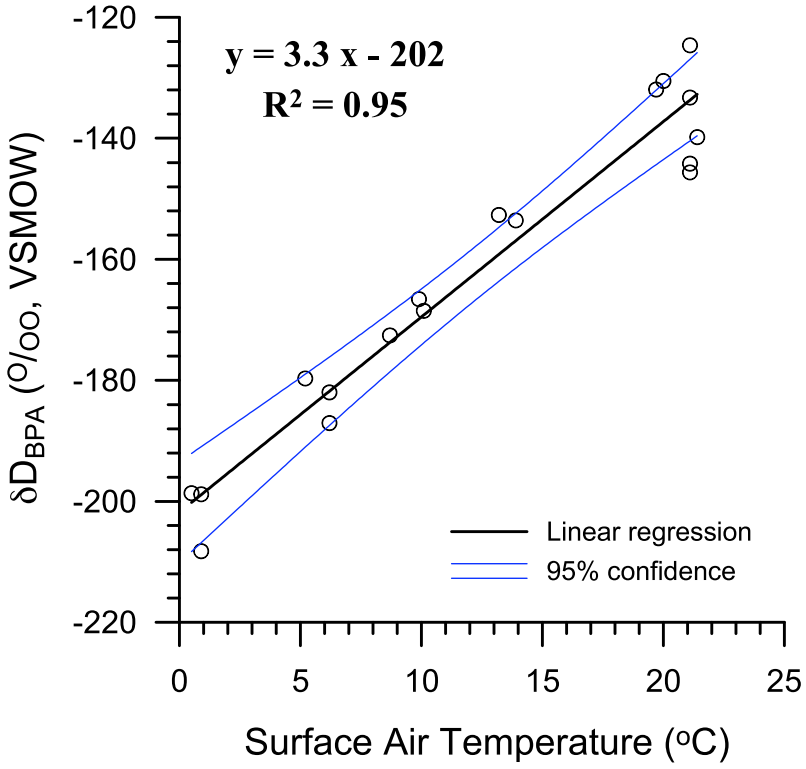

Figure S3. Calibration of δD values of sediment bound C_{16} *n*-alkanoic acid as a proxy for surface temperature. The transect of the lakes are shown in Figure S2. The relationship between δD_{PA} and temperature is y = 3.3x-202, which indicates the temperature dependence of the δD_{PA} is 3.3‰/°C.

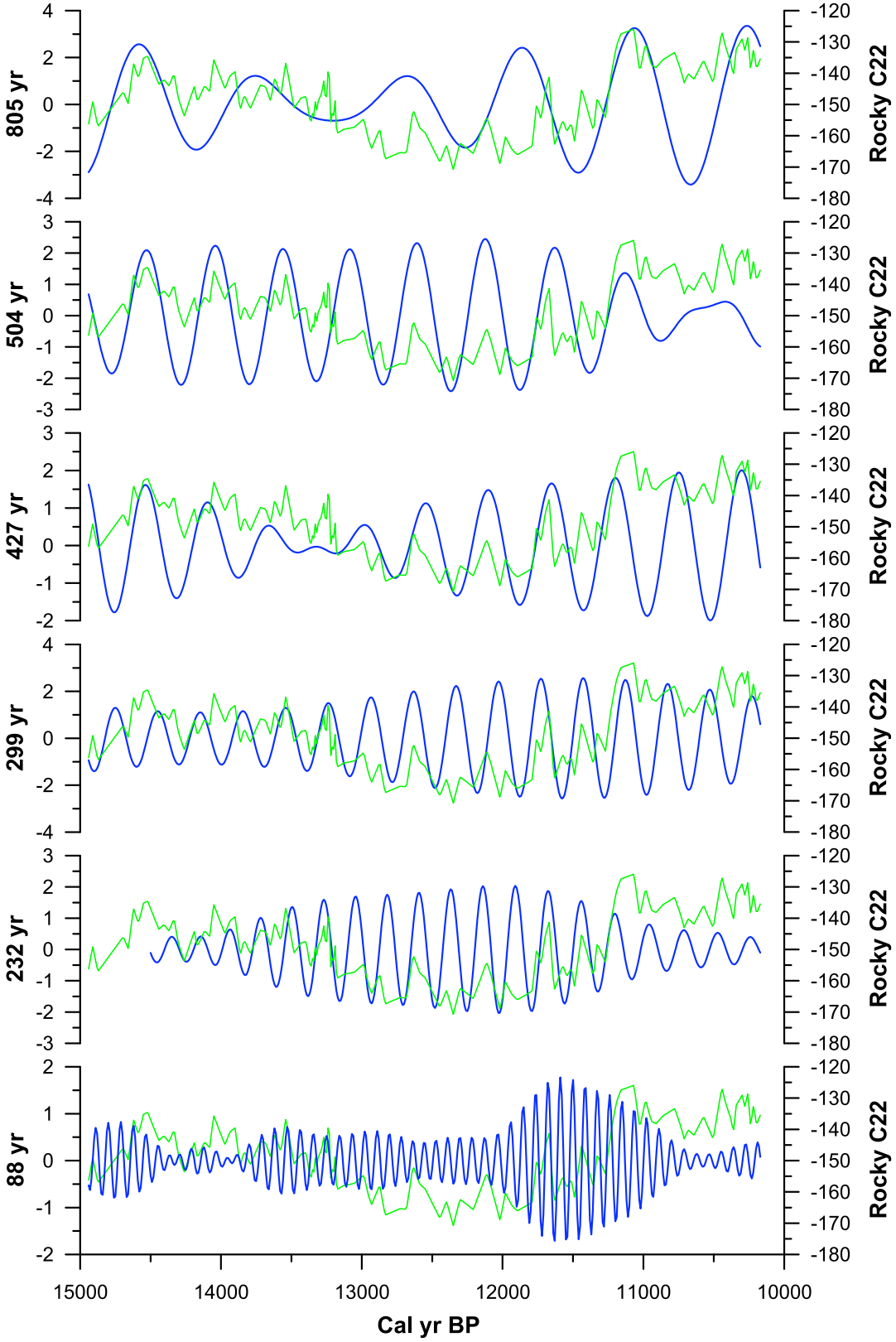
805 yr
504 yr
427 yr
299 yr
232 yr
88 yr
Rocky C22
Cal yr BP
15000
14000
13000
12000
11000
10000

Figure S4-A

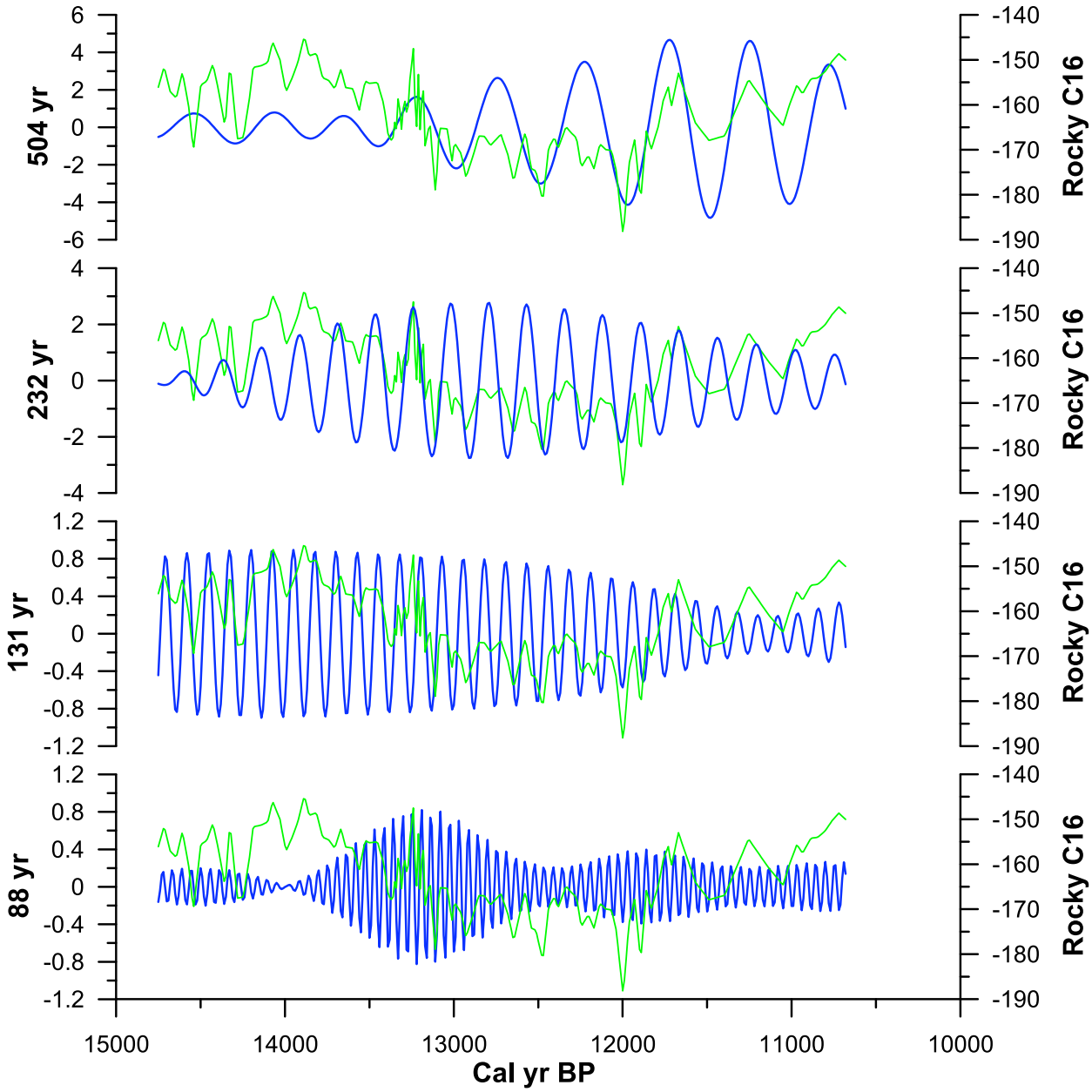
504 yr
232 yr
131 yr
88 yr
Rocky C16
Cal yr BP
15000
14000
13000
12000
11000
10000

Figure S4-B

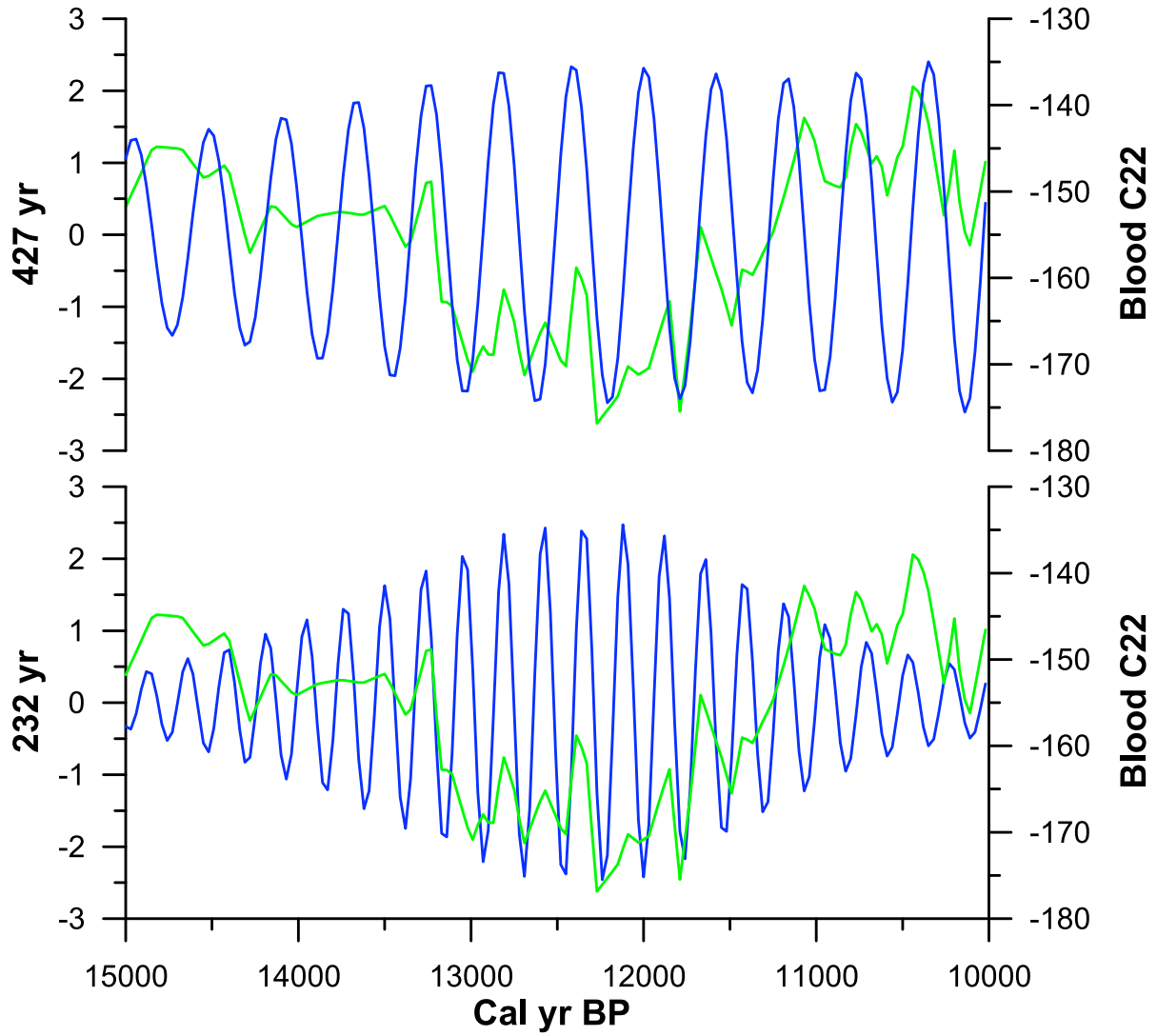

Figure S4-C

Figure S4. Band pass (Gaussian filter) of temperature records inferred from Rocky Pond C_{22} (A), C_{16} (B), and Blood Pond C_{22} (C). The overlap of band passed signal and original signal confirm the prominent spectral components in the temperature records from the two lakes.

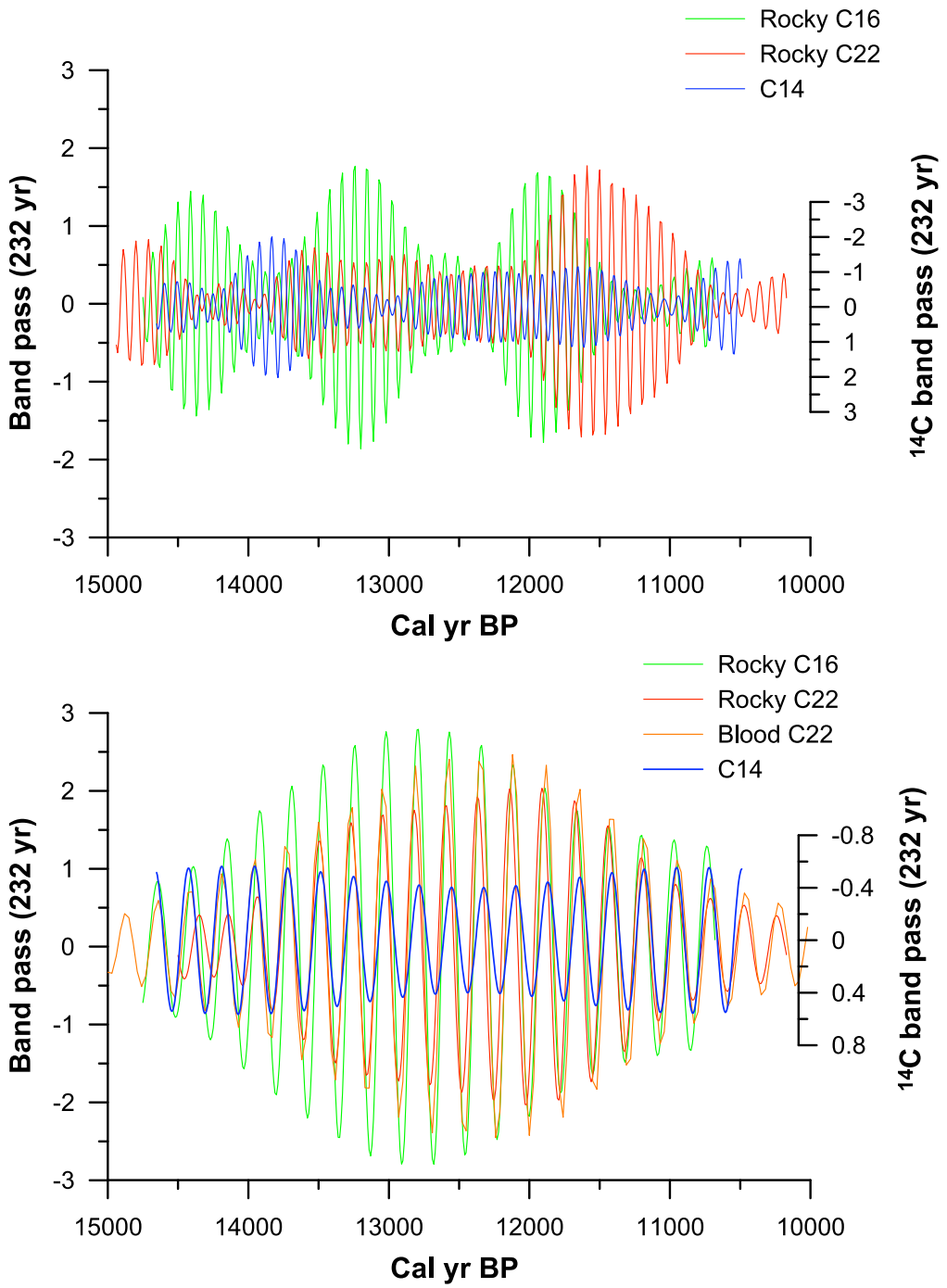

Figure S5. Band pass (Gaussian filter) of Rocky C_{22}, C_{16} δD records, Blood Pond C_{22} δD records and ^{14}C records (Stuvier et al., 1998). The in phase variation of all records suggests that the temperature records related with solar activity.

Appendix 1. Chapter 4: Hydrogen isotope and inferred temperature records during the late Pleistocene to early Holocene from Blood Pond, northeastern North America.

Sample I.D.	Depth (cm)	Age (yr BP)	C22 n-acid δD (‰, VSMOW)	Standard Deviation of 3 measurements (‰, VSMOW)	Temperature inferred from C22 δD (°C)
BP1418	1418	16320	-164	1.8	10.4
BP1410	1410	16135	-157	0.2	12.1
BP1402	1402	15950	-149	1.6	13.9
BP1394	1394	15765	-161	1.8	11.1
BP1386	1386	15580	-143	1.5	15.3
BP1378	1378	15395	-154	1.8	12.5
BP1370	1370	15210	-151	1.5	13.4
BP1362	1362	15025	-143	1.5	15.1
BP1354	1354	14840	-144	1.5	15.1
BP1346	1346	14675	-147	1.5	14.3
BP1338	1338	14544	-145	1.7	14.7
BP1330	1330	14413	-155	1.0	12.4
BP1322	1322	14283	-150	1.2	13.7
BP1314	1314	14152	-152	1.2	13.1
BP1306	1306	14021	-151	2.0	13.4
BP1298	1298	13890	-150	0.8	13.5
BP1290	1290	13759	-151	1.3	13.4
BP1282	1282	13628	-150	1.7	13.6
BP1274	1274	13497	-155	1.9	12.5
BP1266	1266	13366	-150	1.3	13.6
BP1258	1258	13297	-146	1.7	14.6
BP1250	1250	13237	-160	1.1	11.2
BP1242	1242	13176	-160	1.9	11.2
BP1234	1234	13116	-168	1.2	9.4

BP1226	1226	13056	-168	1.2	9.4
BP1218	1218	12996	-165	1.4	10.1
BP1210	1210	12935	-167	1.5	9.7
BP1202	1202	12875	-159	1.2	11.6
BP1194	1194	12815	-162	1.8	10.8
BP1186	1186	12755	-168	2.0	9.3
BP1178	1178	12694	-168	1.2	9.4
BP1170	1170	12634	-162	0.1	10.7
BP1162	1162	12574	-155	1.5	12.5
BP1154	1154	12514	-168	1.6	9.4
BP1146	1146	12453	-156	1.7	12.1
BP1138	1138	12393	-159	0.9	11.5
BP1130	1130	12333	-173	1.0	8.1
BP1122	1122	12273	-157	1.1	12.0
BP1114	1114	12212	-171	0.2	8.8
BP1106	1106	12152	-167	1.8	9.6
BP1098	1098	12092	-168	1.4	9.4
BP1090	1090	12031	-167	0.4	9.5
BP1082	1082	11971	-149	0.9	13.7
BP1074	1074	11911	-160	1.8	11.3
BP1066	1066	11851	-172	0.6	8.4
BP1058	1058	11790	-163	1.5	10.5
BP1050	1050	11730	-152	1.9	13.1
BP1042	1042	11670	-146	1.6	14.6
BP1034	1034	11610	-159	0.2	11.5
BP1026	1026	11549	-163	0.1	10.6
BP1018	1018	11489	-157	1.8	12.0
BP1010	1010	11429	-157	0.6	11.9
BP1002	1002	11369	-141	1.7	15.6
BP994	994	11308	-153	1.5	13.0

BP986	986	11248	-152	2.0	13.2
BP978	978	11188	-158	1.5	11.7
BP970	970	11128	-154	1.6	12.6
BP962	962	11067	-149	1.7	13.7
BP954	954	11007	-152	1.8	13.0
BP946	946	10958	-156	0.4	12.1
BP938	938	10910	-152	1.1	13.0
BP930	930	10862	-157	1.3	11.9
BP924	924	10826	-156	0.5	12.2
BP916	916	10778	-150	1.0	13.6
BP908	908	10730	-151	1.9	13.2
BP900	900	10683	-155	1.5	12.5
BP892	892	10635	-153	1.1	12.8
BP884	884	10587	-158	1.8	11.6
BP876	876	10539	-154	1.4	12.6
BP868	868	10491	-152	1.7	13.0
BP860	860	10443	-146	1.5	14.5
BP852	852	10396	-147	1.9	14.3
BP844	844	10348	-150	0.4	13.5
BP836	836	10300	-152	1.5	13.0
BP828	828	10252	-161	2.0	11.0
BP820	820	10204	-152	0.2	13.0
BP812	812	10156	-161	2.0	11.0
BP804	804	10108	-164	1.8	10.4
BP796	796	10062	-151	0.9	13.4
BP788	788	10017	-141	2.0	15.6
BP780	780	9972	-149	1.7	13.7
BP764	764	9881	-145	1.7	14.9
BP756	756	9836	-147	2.0	14.4
BP740	740	9746	-158	1.7	11.8

BP706	706	9554	-154	1.5	12.7
BP698	698	9509	-153	1.4	12.9
BP690	690	9464	-155	1.5	12.3
BP682	682	9418	-150	1.2	13.5
BP674	674	9373	-147	0.4	14.3
BP666	666	9328	-154	1.9	12.7
BP658	658	9283	-157	0.6	11.9
BP650	650	9238	-148	1.9	14.1
BP642	642	9183	-140	1.4	15.9
BP634	634	9111	-146	0.7	14.6
BP626	626	9040	-148	1.1	14.1
BP618	618	8968	-151	1.2	13.4
BP610	610	8897	-156	1.2	12.1
BP602	602	8825	-153	0.9	12.8
BP594	594	8754	-154	0.7	12.7
BP586	586	8682	-149	1.1	13.7
BP578	578	8611	-159	1.5	11.6
BP570	570	8539	-148	0.9	14.0
BP562	562	8468	-157	0.3	12.0
BP554	554	8396	-150	1.1	13.6
BP546	546	8325	-146	1.1	14.5
BP538	538	8253	-150	1.6	13.7
BP530	530	8181	-149	1.2	13.8
BP522	522	8110	-151	1.3	13.3
BP514	514	8038	-150	1.2	13.7

Appendix 2. Chapter 5: Hydrogen isotope and inferred temperature records during the early Holocene from Blood Pond, northeastern North America.

Sample I.D.	Depth (cm)	Age (yr BP)	C_{22} *n*-acid δD (‰, VSMOW)	C_{22} *n*-acid δD Standard Deviation of three measurements (‰, VSMOW)	Temperature inferred from C_{22} δD (°C)	C_{28} *n*-acid δD (‰, VSMOW)	C28 n-acid dD Standard Deviation of three measurements (‰, VSMOW)
BP458	458	7236	-143	1.9	15.2	-162	0.6
BP460	460	7281	-143	1.8	15.2	-158	0.9
BP462	462	7327	-148	2.0	13.9	-158	0.8
BP464	464	7372	-151	1.5	13.3	-159	1.0
BP466	466	7417	-144	1.5	14.9	-160	0.6
BP468	468	7463	-152	1.9	13.1	-161	0.8
BP470	470	7508	-150	0.2	13.6	-157	0.3
BP472	472	7553	-153	0.9	13.0	-157	1.2
BP474	474	7599	-143	1.9	15.1	-153	1.5
BP476	476	7644	-146	1.5	14.6	-152	0.6
BP478	478	7689	-149	1.2	13.8	-153	0.7
BP480	480	7735	-151	1.7	13.4	-155	1.2
BP482	482	7752	-146	0.9	14.5	-155	1.2
BP484	484	7770	-147	0.9	14.4	-154	0.6
BP486	486	7788	-151	1.3	13.4	-156	2.0
BP488	488	7806	-147	1.9	14.3	-158	1.1
BP490	490	7824	-142	1.5	15.3	-157	1.1
BP492	492	7842	-143	2.0	15.3	-155	0.9
BP494	494	7860	-136	1.8	16.9	-153	1.5
BP496	496	7878	-153	1.4	12.9	-155	2.0
BP498	498	7895	-143	2.0	15.2	-156	0.7
BP500	500	7913	-147	2.0	14.3	-156	1.2
BP502	502	7931	-143	2.0	15.1	-153	1.4

BP504	504	7949	-148	1.5	14.1	-154	1.0
BP506	506	7967	-142	1.3	15.3	-158	1.5
BP508	508	7985	-139	1.7	16.1	-157	1.7
BP510	510	8003	-140	1.8	15.8	-156	1.6
BP512	512	8021	-144	1.9	15.1	-157	1.4
BP514	514	8038	-141	2.0	15.6	-156	0.5
BP516	516	8056	-143	1.5	15.2	-156	1.0
BP518	518	8074	-146	1.1	14.5	-152	0.6
BP520	520	8092	-139	1.5	16.1	-150	0.4
BP522	522	8110	-143	1.2	15.2	-152	2.0
BP524	524	8128	-134	0.6	17.3	-152	2.0
BP526	526	8146	-143	1.8	15.3	-155	1.8
BP528	528	8164	-136	0.7	16.9	-156	1.2
BP530	530	8181	-141	1.8	15.7	-151	1.5
BP532	532	8199	-137	0.9	16.5	-159	1.6
BP534	534	8217	-145	1.6	14.8	-161	1.0
BP536	536	8235	-140	1.8	15.9	-159	1.6
BP538	538	8253	-142	2.0	15.6	-156	1.1
BP540	540	8271	-137	1.8	16.6	-152	1.3
BP542	542	8289	-137	1.9	16.6	-150	0.9
BP544	544	8307	-142	0.5	15.5	-149	1.5
BP546	546	8325	-138	2.0	16.4	-153	1.4
BP548	548	8342	-131	1.5	18.0	-146	1.1
BP550	550	8360	-148	1.3	14.1	-151	0.4
BP552	552	8378	-142	0.8	15.3	-148	2.0
BP556	556	8414	-152	1.5	13.2	-149	1.9
BP558	558	8432	-155	2.0	12.4	-153	0.4
BP560	560	8450	-138	0.2	16.4	-150	1.5
BP562	562	8468	-149	1.4	13.7	-151	0.8
BP564	564	8485	-142	0.9	15.5	-150	0.8

BP566	566	8503	-141	1.7	15.6	-149	0.1
BP568	568	8521	-146	1.6	14.5	-150	0.7
BP570	570	8539	-140	0.9	16.0	-148	0.8
BP572	572	8557	-135	1.5	17.1	-150	0.2
BP574	574	8575	-140	1.2	15.8	-151	1.1
BP576	576	8593	-142	2.0	15.5	-151	2.0
BP578	578	8611	-151	2.0	13.3	-154	1.5
BP580	580	8628	-134	1.9	17.4	-152	0.6
BP582	582	8646	-144	1.2	14.9	-152	1.2
BP584	584	8664	-153	1.5	12.8	-149	0.9
BP586	586	8682		0.9		-143	0.6
BP588	588	8700	-147	1.5	14.2	-152	0.9
BP590	590	8718	-149	0.6	13.8	-155	1.1
BP592	592	8736	-146	0.1	14.4	-148	1.1
BP594	594	8754	-146	0.2	14.6	-155	1.6
BP596	596	8771	-145	0.8	14.8	-153	0.3
BP598	598	8789	-152	1.6	13.1	-154	1.1
BP600	600	8807	-153	1.9	13.0	-152	1.1
BP602	602	8825	-145	0.5	14.7	-155	0.3
BP604	604	8843	-165	2.0	10.1	-150	1.1
BP606	606	8861	-146	2.0	14.6	-150	1.7
BP608	608	8879	-153	0.9	12.8	-149	1.2
BP610	610	8897	-149	1.0	13.9	-153	0.5
BP612	612	8915	-147	1.5	14.3	-148	1.0
BP614	614	8932	-146	0.3	14.5	-148	1.3
BP616	616	8950	-150	0.7	13.5	-148	0.9
BP618	618	8968	-143	1.5	15.2	-151	1.4
BP620	620	8986	-161	1.3	11.1	-144	1.5
BP622	622	9004	-144	0.5	14.9	-144	1.3
BP626	626	9040	-140	1.5	16.0	-147	0.8

BP630	630	9075	-150	1.9	13.5	-142	1.5
BP632	632	9093	-166	0.1	9.9	-148	1.9
BP634	634	9111	-137	2.0	16.6	-150	1.8
BP636	636	9129	-165	1.5	10.0	-145	1.6
BP638	638	9147	-166	1.3	10.0	-145	0.7
BP640	640	9165	-161	1.5	11.0	-140	0.3
BP642	642	9183		0.1		-144	0.6
BP644	644	9201	-170	1.0	8.8	-146	0.5
BP646	646	9218	-176	1.0	7.6	-145	2.0
BP648	648	9236	-160	1.1	11.3	-147	1.0
BP650	650	9238	-140	5.0	16.0	-147	0.8
BP652	652	9249	-158	0.6	11.7	-147	0.6
BP654	654	9260	-167	1.4	9.7	-147	1.4
BP658	658	9283	-149	0.4	13.7	-152	0.8
BP660	660	9294	-150	0.2	13.7	-152	1.6
BP662	662	9306	-145	0.9	14.7	-152	1.5
BP664	664	9317	-147	1.5	14.2	-154	0.9
BP666	666	9328	-146	2.0	14.6	-151	1.1
BP668	668	9339	-141	1.5	15.6	-151	0.4
BP670	670	9351	-141	1.6	15.7	-152	2.0
BP672	672	9362	-143	1.7	15.1	-151	1.6
BP674	674	9373	-139	1.8	16.2	-151	1.5
BP678	678	9396	-146	0.4	14.6	-150	1.2
BP680	680	9407	-144	1.1	14.9	-150	1.5
BP682	682	9418	-142	1.3	15.4	-152	1.2
BP684	684	9430	-150	0.5	13.5	-150	1.0
BP686	686	9441	-146	1.0	14.5	-152	1.6
BP688	688	9452	-143	1.9	15.2	-148	1.1
BP690	690	9464	-148	1.5	14.1	-151	1.3
BP692	692	9475	-153	1.1	12.9	-147	0.9

BP694	694	9486	-145	1.8	14.7	-150	1.5
BP696	696	9497	-149	1.4	13.9	-151	1.4
BP698	698	9509	-145	1.7	14.7	-149	1.1
BP700	700	9520	-151	1.5	13.3	-147	0.4
BP702	702	9531	-167	1.9	9.6	-149	2.0
BP704	704	9543	-151	0.4	13.3	-138	1.9
BP706	706	9554	-165	1.5	10.0	-148	0.4
BP710	710	9576	-147	2.0	14.3	-149	1.5
BP712	712	9588	-150	0.2	13.5	-147	0.8
BP716	716	9610	-150	2.0	13.6	-149	0.8
BP718	718	9622	-153	1.8	12.8	-149	0.1
BP720	720	9633	-146	0.9	14.6	-150	0.7
BP722	722	9644	-146	2.0	14.4	-148	0.8
BP724	724	9656	-144	1.7	14.9	-149	0.2
BP726	726	9667	-145	1.2	14.8	-149	1.1
BP728	728	9678	-152	1.7	13.0	-148	2.0
BP730	730	9689	-145	1.7	14.6	-152	1.5

Appendix 3. Chapter 6: Hydrogen isotope and inferred temperature records from Blood Pond, northeastern North America.

Table 1. Hydrogen isotope of C_{22} *n*-acid and inferred temperature records from Blood Pond, northeastern North America.

Sample I.D.	Depth (cm)	Age (yr BP)	C_{22} *n*-acid δD (‰, VSMOW)	C_{22} *n*-acid δD Standard Deviation of three measurements (‰, VSMOW)	Temperature inferred from C_{22} δD (°C)
RP1075	1075	14572	-158	2.0	11.8
RP1070	1070	14549	-149	1.5	13.8
RP1065	1065	14525	-157	2.0	11.9
RP1040	1040	14409	-146	1.3	14.5
RP1035	1035	14386	-150	1.2	13.6
RP1030	1030	14362	-137	0.5	16.6
RP1025	1025	14339	-142	1.1	15.5
RP1020	1020	14316	-135	1.7	17.0
RP1016	1016	14297	-135	0.1	17.2
RP1005	1005	14246	-144	1.2	15.1
RP1000	1000	14223	-142	1.4	15.4
RP995	995	14199	-144	2.0	15.0
RP990	990	14176	-140	1.5	15.9
RP986	986	14157	-148	1.2	14.1
RP980	980	14129	-154	1.1	12.7
RP970	970	14083	-144	1.6	14.9
RP967	967	14069	-149	2.0	13.8
RP960	960	14036	-144	1.7	15.0
RP955	955	14013	-146	1.6	14.5
RP951	951	13994	-136	1.2	16.9

RP940	940	13943	-145	2.0	14.7
RP935	935	13920	-141	2.0	15.7
RP930	930	13896	-140	2.0	16.0
RP925	925	13873	-152	1.4	13.2
RP921	921	13855	-147	1.6	14.3
RP915	915	13827	-151	1.2	13.3
RP905	905	13780	-144	2.0	15.0
RP900	900	13757	-144	1.2	14.9
RP895	895	13733	-149	1.2	13.8
RP891	891	13715	-142	1.5	15.6
RP885	885	13687	-147	0.4	14.2
RP880	880	13664	-137	2.0	16.7
RP872	872	13626	-151	2.0	13.3
RP865	865	13598	-148	0.3	14.1
RP860	860	13579	-147	2.0	14.2
RP856	856	13564	-156	2.0	12.3
RP853	853	13553	-156	0.4	12.3
RP842	842	13512	-152	2.0	13.1
RP837	837	13493	-154	2.0	12.7
RP832	832	13474	-149	1.6	13.7
RP827	827	13456	-149	1.4	13.8
RP823	823	13441	-152	1.3	13.1
RP818	818	13422	-150	1.8	13.7
RP808	808	13384	-148	1.1	14.1
RP803	803	13365	-147	1.0	14.3
RP798	798	13347	-147	2.0	14.3
RP794	794	13332	-146	1.0	14.6
RP788	788	13309	-143	2.0	15.3
RP783	783	13290	-142	1.4	15.4
RP775	775	13260	-150	1.0	13.5

RP768	768	13234	-146	1.5	14.6
RP761	761	13208	-136	2.0	16.8
RP757	757	13193	-145	1.1	14.7
RP751	751	13170	-139	1.5	16.2
RP746	746	13152	-159	2.0	11.5
RP736	736	13114	-151	2.0	13.4
RP731	731	13095	-157	2.0	11.9
RP727	727	13080	-138	0.3	16.3
RP721	721	13058	-153	2.0	12.9
RP711	711	13020	-155	0.9	12.3
RP706	706	13001	-148	1.0	14.2
RP701	701	12983	-157	2.0	11.9
RP697	697	12968	-157	1.4	12.0
RP691	691	12945	-159	2.0	11.4
RP686	686	12926	-158	1.4	11.7
RP678	678	12896	-157	1.5	11.9
RP671	671	12848	-155	1.7	12.5
RP667	667	12818	-162	1.6	10.8
RP665	665	12803	-164	0.2	10.3
RP659	659	12758	-158	1.6	11.8
RP655	655	12729	-167	1.1	9.5
RP644	644	12647	-165	0.7	10.0
RP639	639	12610	-165	0.2	10.0
RP634	634	12572	-152	0.2	13.2
RP629	629	12535	-158	2.0	11.8
RP625	625	12505	-159	2.0	11.5
RP614	614	12423	-168	2.0	9.3
RP609	609	12386	-163	2.0	10.6
RP604	604	12349	-171	2.0	8.7
RP599	599	12312	-162	2.0	10.7

RP595	595	12282	-164	2.0	10.4
RP589	589	12237	-166	0.7	9.9
RP579	579	12163	-154	1.2	12.6
RP576	576	12141	-158	0.1	11.8
RP569	569	12088	-169	1.1	9.1
RP565	565	12059	-160	0.1	11.2
RP560	560	12021	-164	1.2	10.2
RP556	556	11992	-166	1.4	9.8
RP545	545	11910	-163	1.5	10.5
RP540	540	11873	-150	1.3	13.6
RP535	535	11835	-155	2.0	12.5
RP530	530	11798	-145	2.0	14.7
RP526	526	11768	-141	1.1	15.6
RP520	520	11724	-163	1.0	10.5
RP510	510	11649	-155	1.0	12.4
RP505	505	11612	-159	1.0	11.6
RP500	500	11575	-156	1.0	12.2
RP496	496	11545	-162	1.1	10.8
RP490	490	11500	-145	1.8	14.7
RP480	480	11426	-159	1.0	11.6
RP477	477	11403	-148	2.0	14.0
RP470	470	11351	-154	2.0	12.6
RP466	466	11322	-143	1.5	15.3
RP461	461	11284	-132	2.0	17.8
RP457	457	11255	-127	2.0	18.8
RP446	446	11173	-126	1.2	19.2
RP441	441	11135	-140	1.1	16.0
RP436	436	11098	-130	2.0	18.1
RP431	431	11061	-137	2.0	16.5
RP427	427	11031	-138	1.5	16.3

RP421	421	10987	-136	2.0	16.9
RP411	411	10912	-133	1.5	17.4
RP406	406	10875	-138	1.7	16.4
RP401	401	10838	-143	1.4	15.2
RP397	397	10808	-140	1.1	15.9
RP391	391	10763	-142	0.9	15.5
RP381	381	10689	-136	1.5	16.9
RP371	371	10578	-143	1.3	15.2
RP367	367	10520	-136	2.0	16.9
RP362	362	10446	-127	1.2	19.0
RP359	359	10402	-130	2.0	18.1
RP356	356	10358	-134	2.0	17.4
RP353	353	10314	-136	2.0	16.8

Table 2. Hydrogen isotope of sediment bound C_{16} *n*-acid and inferred temperature records from Blood Pond, northeastern North America.

Sample I.D.	Depth (cm)	Age (yr BP)	C_{16} *n*-acid δD (‰, VSMOW)	C_{16} *n*-acid δD Standard Deviation of three measurements ‰, VSMOW)	Temperature inferred from C_{16} δD (°C)
RP1049	1049	14447	-157	0.2	13.5
RP1043	1043	14420	-151	1.8	15.3
RP1038	1038	14396	-157	0.4	13.6
RP1033	1033	14373	-158	1.1	13.2
RP1028	1028	14350	-153	0.6	14.9
RP1023	1023	14327	-160	1.1	12.7
RP1019	1019	14308	-165	2.0	9.6
RP1013	1013	14280	-156	1.2	14.1
RP1008	1008	14257	-155	1.3	14.3
RP1003	1003	14233	-151	1.5	15.5
RP998	998	14210	-157	1.2	13.5
RP993	993	14187	-165	1.5	11.2
RP989	989	14168	-151	0.2	15.5
RP983	983	14140	-168	2.0	10.4
RP978	978	14117	-167	1.0	10.5
RP973	973	14094	-159	1.1	13.2
RP970	970	14080	-152	0.4	15.2
RP963	963	14047	-151	1.0	15.4
RP958	958	14024	-151	1.0	15.6
RP954	954	14005	-146	1.6	17.0
RP948	948	13978	-150	0.9	15.8

RP943	943	13954	-157	1.4	13.6
RP938	938	13931	-154	1.3	14.5
RP933	933	13908	-150	0.9	15.7
RP928	928	13885	-145	0.9	17.4
RP924	924	13866	-149	0.8	16.0
RP918	918	13838	-149	0.2	16.2
RP913	913	13815	-154	0.5	14.6
RP908	908	13791	-155	1.7	14.4
RP903	903	13768	-156	0.9	13.8
RP898	898	13745	-152	1.3	15.1
RP894	894	13726	-156	1.9	13.9
RP888	888	13698	-156	0.5	13.8
RP883	883	13675	-161	0.8	12.3
RP878	878	13652	-155	1.0	14.3
RP875	875	13638	-155	1.1	14.2
RP868	868	13608	-155	1.2	14.2
RP863	863	13589	-160	1.3	12.8
RP859	859	13574	-167	1.7	10.6
RP856	856	13563	-168	0.5	10.3
RP850	850	13540	-167	0.8	10.7
RP845	845	13521	-164	1.0	11.6
RP840	840	13503	-168	0.9	10.2
RP835	835	13484	-155	0.2	14.1
RP830	830	13465	-161	1.5	12.4
RP826	826	13450	-160	0.2	12.6
RP820	820	13427	-168	0.4	10.3
RP815	815	13409	-157	1.2	13.5
RP810	810	13390	-163	0.2	11.7

RP805	805	13371	-159	0.9	13.1
RP800	800	13352	-159	0.6	13.0
RP796	796	13337	-168	1.0	10.4
RP790	790	13315	-156	1.6	14.0
RP785	785	13296	-154	0.7	14.5
RP780	780	13277	-150	0.1	15.7
RP777	777	13266	-152	1.3	15.0
RP770	770	13240	-145	1.3	17.2
RP765	765	13221	-155	1.9	14.2
RP764	764	13217	-164	1.2	11.4
RP760	760	13202	-155	0.5	14.2
RP754	754	13180	-159	1.9	13.0
RP749	749	13161	-165	1.5	11.3
RP744	744	13142	-164	1.2	11.5
RP739	739	13123	-158	1.0	13.5
RP734	734	13105	-149	1.6	16.0
RP730	730	13090	-164	0.9	11.5
RP724	724	13067	-166	0.7	11.0
RP719	719	13048	-159	1.4	13.1
RP714	714	13030	-150	0.1	15.7
RP709	709	13011	-166	1.8	11.0
RP704	704	12992	-154	0.6	14.6
RP700	700	12977	-153	0.3	14.9
RP694	694	12954	-170	0.1	9.6
RP689	689	12936	-164	2.0	11.5
RP684	684	12917	-180	2.4	6.6
RP681	681	12906	-165	1.8	11.2
RP674	674	12877	-165	0.9	11.1

RP670	670	12857	-173	2.0	8.9
RP668	668	12847	-168	1.8	10.2
RP662	662	12816	-171	1.4	9.4
RP658	658	12796	-176	1.5	7.8
RP652	652	12765	-171	1.2	9.3
RP647	647	12740	-167	2.0	10.6
RP642	642	12715	-167	0.8	10.6
RP637	637	12689	-169	1.8	10.0
RP632	632	12664	-168	1.5	10.4
RP628	628	12643	-167	0.4	10.7
RP622	622	12613	-171	1.2	9.4
RP617	617	12588	-177	1.9	7.5
RP612	612	12562	-171	1.8	9.3
RP607	607	12537	-166	2.0	10.9
RP602	602	12511	-174	1.4	8.4
RP598	598	12491	-175	0.8	8.3
RP592	592	12461	-181	1.7	6.3
RP587	587	12435	-170	2.0	9.8
RP582	582	12410	-167	1.1	10.5
RP579	579	12394	-170	0.9	9.8
RP572	572	12359	-165	1.4	11.3
RP568	568	12339	-166	1.4	10.9
RP563	563	12313	-167	1.3	10.5
RP559	559	12293	-174	1.5	8.5
RP553	553	12262	-171	1.4	9.3
RP548	548	12237	-174	1.1	8.4
RP543	543	12211	-169	0.5	10.1
RP538	538	12186	-170	0.3	9.7

RP533	533	12161	-170	0.2	9.6
RP529	529	12140	-175	1.4	8.3
RP523	523	12110	-189	1.6	3.9
RP518	518	12084	-173	0.2	8.7
RP513	513	12059	-168	1.0	10.4
RP508	508	12034	-181	0.2	6.2
RP503	503	12008	-166	0.5	11.0
RP499	499	11979	-170	1.7	9.5
RP493	493	11914	-165	0.4	14.3
RP488	488	11860	-159	1.3	13.0
RP483	483	11806	-156	0.6	13.9
RP480	480	11773	-161	1.1	12.6
RP473	473	11697	-153	0.1	14.8
RP468	468	11643	-164	0.3	13.0
RP464	464	11600	-168	1.4	11.8
RP460	460	11557	-167	0.5	12.2
RP454	454	11492	-158	1.8	14.4
RP449	449	11437	-161	0.2	11.6
RP444	444	11383	-165	1.8	10.4
RP439	439	11329	-160	1.4	11.9
RP434	434	11275	-156	0.7	14.1
RP430	430	11231	-158	2.0	13.5
RP424	424	11166	-154	1.9	14.5
RP419	419	11112	-154	1.2	14.5
RP414	414	11058	-153	1.2	14.9
RP409	409	11004	-150	1.9	15.6
RP404	404	10950	-149	0.2	16.2
RP400	400	10906	-150	1.5	15.8